WADC TECHNICAL REPORT 54-33
PART 2

PRELIMINARY MICROSCOPIC STUDIES OF CERMETS AT HIGH TEMPERATURES

THOMAS S. SHEVLIN
HERBERT W. NEWKIRK
E. GEORGE STEVENS
HAROLD M. GREENHOUSE

THE OHIO STATE UNIVERSITY
RESEARCH FOUNDATION

FEBRUARY 1956

MATERIALS LABORATORY
CONTRACT No. AF 33(038)-16911
PROJECT No. 7350
TASK No. 73500

WRIGHT AIR DEVELOPMENT CENTER
AIR RESEARCH AND DEVELOPMENT COMMAND
UNITED STATES AIR FORCE
WRIGHT-PATTERSON AIR FORCE BASE, OHIO

Carpenter Litho & Prtg. Co., Springfield, O.
300 - April 1956

FOREWORD

This report was prepared by The Ohio State University Research Foundation under USAF Contract No. AF 33(038)-16911. This contract was initiated under Project No. 7350, "Ceramic and Cermet Materials", Task No. 73500, "Ceramic and Cermet Materials Development", formerly RDO No. 615-17, "Ceramic Materials", and was administered under the direction of the Materials Laboratory, Directorate of Research, Wright Air Development Center, with Mr. L. D. Richardson acting as project engineer.

This report covers period of work from 1 March 1953 to 30 September 1954.

ABSTRACT

SECTION 1 - CHANGES IN THE MICROSTRUCTURE OF SOME TiC BASE CERMETS, WITH TIME, AT HIGH TEMPERATURES

The effect of heat treatment in a vacuum or inert-gas atmosphere at 2000°F on the microstructure of Kentanium samples K-151-A and K-152-B is discussed. Equipment and techniques employed in carrying out the research are discussed in detail. The effects of a solution-reprecipitation mechanism are discussed and a tentative theory is advanced relating the observed changes in microstructure to the steep slope of the stress-rupture curves for these cermets.

SECTION 2 - STUDY OF SOME TiC BASE CERMETS BY MEANS OF HIGH TEMPERATURE X-RAY DIFFRACTION TECHNIQUES

High temperature x-ray diffraction studies on phases stable at 2000°F in samples K-151-A and K-152-B and evidence for the solid solubility of TiC in Ni at this temperature are presented. In addition, the thermal expansion data of Ni from room temperature to 2000°F has been determined by high temperature x-ray techniques. The equipment used and the techniques employed in this research are discussed in detail. Evidence is presented which indicates that a solution-precipitation mechanism is responsible for the microstructure changes observed and reported in Section 1.

SECTION 3 - ELECTRON MICROSCOPY OF SOME TiC BASE CERMETS

A new electron microscopy replication technique is presented and its application in resolving the microstructure of sample K-152-B is discussed. The colloidal dispersion present in the Ni phase of this cermet have been resolved and found to be small particles of TiC. The origin of this precipitate and its effects on the high temperature strength of TiC-Ni cermets are discussed.

SECTION 4 - COEFFICIENT OF EXPANSION STUDIES ON HIGH TEMPERATURE ALLOYS

The relationship between thermal shock resistance and the linear thermal expansion of the phases composing a cermet is discussed. Techniques and apparatus for fabricating and testing alloys having thermal expansion characteristics similar to titanium carbide are presented. Thermal expansion data for the systems Fe-Co-Ni, Fe-Co-Ni-Cr, Cr-Mo-Ni, TiC+Fe-Co-Ni and TiC+Fe-Co-Ni-Cr are listed.

SECTION 5 - PREPARATION OF HIGH Ni-LOW TiC CERMETS FOR IMPACT AND THERMAL SHOCK STUDIES

Techniques and apparatus for the fabrication of TiC-Ni cermets suitable for impact and thermal shock studies and containing 73.1% Ni, 80.9% Ni, 87.9% Ni and 94.2% Ni by weight are given.

Modulus of rupture values are listed for these compositions and data are given on impact strengths.

SECTION 6 - INVESTIGATION OF TiB_2 AND $MoSi_2$ AS THE CERAMIC COMPONENT OF A CERMET

The possibility of using a mixture of TiB_2 and $MoSi_2$ as components of a new high temperature cermet is discussed.

SECTION 7 - STUDY OF THE EFFECT OF HEAT TREATMENT ON IMPACT STRENGTH OF K-151-A and K-151-B

The effect of heat treatment on the impact strength of Kentanium samples K-151-A and K-151-B is discussed. Apparatus and techniques employed in this research are discussed in detail.

PUBLICATION REVIEW

This report has been reviewed and is approved.

FOR THE COMMANDER:

M. R. WHITMORE
Technical Director
Materials Laboratory
Directorate of Research

TABLE OF CONTENTS

Table of Contents (Cont.)

Table of Contents (Cont.)

LIST OF TABLES

List of Tables (Cont.)

LIST OF ILLUSTRATIONS

List of Illustrations (Cont.)

List of Illustrations (Cont.)

PAGE

List of Illustrations (Cont.)

PAGE

SECTION 1

CHANGES IN THE MICROSTRUCTURE OF SOME TiC BASE CERMETS, WITH TIME, AT HIGH TEMPERATURES

INTRODUCTION

Since World War II, the rapid development of jet and rocket engines of increased thrust and efficiency has accelerated the search for new and better-high-temperature materials. The trend in current and future power plant designing demands operating temperatures well beyond the region where known metals are useful. For this reason, ceramics are currently receiving much attention in high-temperature research. In particular, it has been found that a combination of a ceramic material and a metal, commonly called a cermet, is potentially useful.

Years of research, in many laboratories around the world, have brought these materials from the laboratory bench to commercial production and application. For example, the Metallwerk Plansee in Austria is manufacturing, under the trade name of "WZ Alloys", turbine blades and parts composed of titanium carbide (TiC) with Co-Cr, Ni-Cr or Co-Ni-Cr as the binder metal. Metro-Cutanit, Ltd., England, is manufacturing "Elmet-H" alloys closely related to the "WZ" alloys.

Hard Metal Tools, Ltd., is currently producing parts composed of chromium carbide (Cr_3C_2) or TiC with cobalt (Co) or nickel (Ni) as the auxiliary metal. Recently the General Electric Company has developed the "Series 600 Carboloy Chrome Carbide" compositions.

One of the best high-temperature materials developed to date is composed of titanium carbide, a small percentage of a solid solution of titanium, tantalum, and niobium carbides, and 20 to 30 percent nickel as the primary auxiliary metal. A cermet of this type manufactured under the trade name of Kentanium by Kennametal, Inc., Latrobe, Pennsylvania, has been extensively tested for many years in the form of valves, valve seats, nozzle blades, and rotor blades. This material meets most of the requirements for a blading material; for example, it has high oxidation and thermal shock resistance, a low density, a high level of hot strength. The compositions, however, are brittle and their high-temperature strength decreases rapidly with time. This decrease is clearly seen in Figure 1, which shows several stress-rupture curves for Kentanium grade samples, K-151-A and K-152-B, at different temperatures, as well as curves for a cermet designated III-B, which was developed in The Ohio State University laboratories, and a typical superalloy currently used as turbine blading for jet engines. The data used to plot this graph are given in Table I. Examination of the graph reveals that:

1. For a given alloy, the higher the temperature the lower the stress-rupture strength.

2. At the same temperature, increasing the metal content of the Kentanium samples decreases the stress-rupture strength and leads to a more rapid decrease in high-temperature strength with time, i.e., K-152-B has a steeper stress-rupture curve than K-151-A.

3. At the same temperature, TiC cermets containing 20% Ni by weight possessed a much higher stress-rupture strength than either the superalloy or the TiC cermet containing 30% Ni by weight. K-152-B appears to be superior to the superalloy up to 100 hours.

4. Cermet III-B has a higher stress-rupture strength for a longer period of time than any of the compositions tested. It is to be noted that this material does not contain a pure metal as the auxiliary phase.

5. The short-time tensile strengths of the Kentanium samples at 1600°F and 1800°F are much higher than those of the superalloy at the same temperatures. However, a rapid decrease in strength with time occurs as is indicated by the steep slopes of the stress-rupture curves for these materials. As a result, K-152-B has about the same high temperature strength as the superalloy after 100 hours and very little strength after 1000 hours.

It is felt that this rapid decrease in strength with time at high temperatures is more than should have to be tolerated in these samples. It is further believed that some additional physical or chemical changes are occurring in these materials, beyond those normally taking place with time at high temperature in the superalloys or oxide base cermets. Certainly there is little doubt that the factors accounting for the high-temperature strength of cermet III-B are not present in the Kentanium samples or superalloys.

Research in recent years on metal carbide cermets has indicated that the auxiliary metal phase, with its ability to take carbide into solid solution, has a profound influence on the physical properties of these bodies, particularly their high-temperature strength. It is believed that the presence of carbide in solid solution in these bodies has a detrimental effect on the high-temperature strength for the following reasons:

1. It provides material for transport (by diffusion) through the metallic phase.

2. Since, at a given temperature, a solute dissolved in a saturated solution is in equilibrium with undissolved solute, a constant interchange (by diffusion mechanisms) of dissolved solute, reprecipitating, and undissolved solute, dissolving, is occurring.

3. The result of this solution-reprecipitation phenomenon can be observed in the greater degree of coalescence of carbide areas in annealed cermets as compared to assintered bodies. The coalescence of carbide areas results in a decrease in the carbide-metal interfacial area and decreases the total surface energy of the carbide. This results in an increase in the proportion of metal-to-metal bonds. The metal-to-metal bond is very weak at

TABLE I

STRESS-RUPTURE DATA OF K-151-A, K-152-B, III-B AND A SUPERALLOY

Alloy	Composition, weight %	Stress-rupture strength, psi					Reference
		Temp		Time in hours			
		°F	°C	10	100	1000	
K-151-A	65TiC+15(Ti,Ta,Nb)C+20Ni	1600	871	27,700	23,500	19,300	Metal Progress April, 1952
		1800	980	15,300	11,800	7,000	
K-152-B	62TiC+8(Ti,Ta,Nb)C+30Ni	1600	871	21,000	15,300	9,400	Metal Progress April, 1952
		1800	980	10,500	5,100	0	
Super Alloy	Co+Cr+Ni	1600	871	19,500	15,000	10,400	Kennametal Inc. Bulletin 1052
		1800	980	7,700	5,100	2,300	
III-B	55.4TiC+17.9TiB_2+ 10.0Si+16.7Co	1800	980	27,700	26,700	26,000	O.S.U.-W.A.D.C. Laboratory Data

high temperatures as is evidenced by the steep stress-rupture curve for metals. The structure formed by the coalescing of carbide areas at 2000°F, for example, is not nearly as strong as that formed at the sintering temperature of the cermet (2500 - 3000°F), because of the incomplete bonding (lack of an appreciable number of strong TiC-TiC bonds) at this relatively low temperature.

It should be possible, therefore, to manufacture a carbide base cermet possessing good high temperature strength by decreasing the amount of carbide material in transport, i.e., using an auxiliary metal which is a poorer solvent for the carbide in question. This can be accomplished either by alloying the existing metal phase present in the body, substituting another carbide or other refractory phase, for the one presently used, substituting a different metal for the metallic phase or elimination of it entirely as in III-B.

Since it was felt that considerable TiC would be in solid solution in Ni in cermets K-151-A and K-152-B and that, with time at high temperatures, this material would be in transport, producing the results discussed above, considerable improvement in the high-temperature strength of these bodies could be achieved by modifying the metal binder phase.

A research program was started to investigate whether or not this phenomenon does take place in Kentanium samples K-151-A and K-152-B and to prove or disprove the occurrence of carbide structural changes according to the solution-reprecipitation mechanism.

Initially it was decided to anneal one K-151-A and one K-152-B sample at 2000°F in a vacuum or in an inert gas atmosphere, photographing and observing the same area before and after treatment. However, it was found that after 25 hours the polished surface was oxidized or roughened by surface diffusion. Therefore, it was decided to anneal many samples at 2000°F, quenching each one separately in oil after a specified time, in order to freeze any high-temperature phases or transformations that may have occurred. Although the samples possessed excellent oxidation resistance, they were heated in a vacuum or inert gas atmosphere in order to eliminate entirely any competing oxidation mechanism. A temperature of 2000°F was chosen because no eutectics or unstable phases exist at this temperature and because this is the maximum temperature at which these compositions would be expected to serve. This upper-limit of temperature, moreover, would accelerate any chemical or physical changes that might be taking place. The changes in the micro and crystal structures would then be studied as functions of time by means of light and electron metallographic techniques and room-temperature x-ray diffraction procedures.

The solid solubility of TiC in Ni at 2000°F would be determined by high temperature x-ray diffraction procedures. In addition, experiments would be devised to observe the diffusion of TiC in Ni by moving boundary method. This technique would involve the pressing of a polished Ni surface against the polished surface of a cermet and observing the Ni-cermet interface after various periods of heat treatment. The pressing and holding of the "sandwich" would be accomplished by using a Ni crucible with a screw cap.

LITERATURE SURVEY

In recent years several investigators have provided considerable data for supporting the phenomenon discussed above. Wyman and Kelley[1] have shown that solution of tungsten carbide (WC) in Co occurs at high temperatures. They report that isolated carbide grains grew in size, showing that the material necessary for growth must diffuse through the bonding metal. They say that the mechanism for growth appears to depend on the diffusion of carbide through the Co. It was found that the smaller particles disappeared, thus supplying material for the growth of the larger grains. A solution-precipitation mechanism is thus indicated. As grain growth proceeded at high temperatures, with time, the physical properties of their materials deteriorated.

G. A. Meerson et al.[2], report the growth of TiC grains with time at the temperature of molten Co. They further state that this growth must take place by means of a solution of the smaller TiC grains in the molten metal and subsequent recrystallization onto larger carbide grains. They also report the same behavior for a TiC-WC solid solution.

F. Skaupy[3,4] found that grain growth of WC took place in his samples at the temperature of molten Co. He also believes that the growth is due to a solution of small WC particles in molten Co and reprecipitation of WC on larger carbide grains on cooling.

Takeda[5] arrived at the conclusion that Co is much better than Ni or iron (Fe) as a binder metal for WC, because Ni and Fe retain in solid solution much more carbide than does Co in the finished and cooled material. This gives rise to embrittlement of the Ni and Fe, and hence these metals are no longer able to provide even limited stress relief leading to a relatively brittle body. In contrast, Co separates out the largest portion of the WC during the cooling cycle, while the carbide grains that have remained undissolved, are enlarged. The Co is still brittle by reason of triaxial constraint, but is not so brittle as when this condition plus carbide solution prevails. Hence, the solubility of the carbide in the metal exerts a considerable influence on the final product.

W. Dawihl and J. Hinnueber[6] prepared specimens of WC with 11% Co by weight and found that a rapid decrease in rupture strength occurred with increasing sintering temperature above 2910°F. They attributed this to the intensified processes of diffusion and solution of the carbide. They conclude that the ability of the metallic phase to take carbide material into solid solution greatly influences the physical properties of the body. H. Franssen[7] also noted in WC cermets at the sintering temperature that particle size continues to increase and that the cemented carbide alloys are in a metastable state physically.

C. C. McBride[8] found that grain growth of TiC took place in Co and Ni-bonded cermets, and H. S. Cannon and F. V. Lenel[9] considered the mechanism for grain growth in cermets as occurring through a solution-reprecipitation mechanism.

J. Gurland[10] reports that carbide grain size increases can be attributed to (1) a solution and reprecipitation of the carbide phase in and from the binder during heating and cooling cycles, (2) transfer of carbide from small to large grains by diffusion through the binder at the sintering temperature, and (3) coalescence of adjacent carbide grains. The last theory was advanced to account for the occasional appearance of very large grains in localized areas of the microstructure. A survey of grain growth of WC during sintering was undertaken, and it was reported that the grains take on characteristic angular shapes. A plot of the frequency of occurrence of each angular measurement on the polished surface has a decided maximum at 90°, indicating that the grains tend toward rectangular shapes.

Through E. R. Stover's research[11], we learn that the mechanical properties of cermets are influenced by size, shape, and distribution of the grains. Small, rounded, uniformly distributed carbide grains have been associated with higher strengths than the larger, angular grains resulting from sintering at high temperatures. Stover further reports that grain growth by solution and reprecipitation through the liquid metallic phase results in a large volume of liquid around each carbide grain at the higher sintering temperatures. Rapid cooling from such temperatures causes larger, more angular grains to form in the cermet microstructure.

Recently Knudsen et al.[12], reported that examination of a Kentanium sample K-162-B*, stressed for 1,073 hours at 1850°F, revealed a coalescence of the carbide grains. They reported that the smaller grains were cohering and also growing into larger carbide areas.

MATERIALS AND COMPOSITIONS

Cermets

The compositions discussed are listed in Table II. The weight percent values are given by Kennametal, Inc., and the volume percentages have been calculated from the densities, based on the assumption of a mechanical mixture and a density of 8.9 g/cm^3 for Ni, 5.35 g/cm^3 for the carbide phase in cermet K-151-A, and 5.16 g/cm^3 for the carbide phase in K-152-B. In K-151-A the carbide phase was assumed to contain 66.32% Ti, 9.38% Nb, 6.10% Ta, and 18.20%C by weight. In K-152-B the carbide phase was assumed to contain 71.66% Ti, 5.72% Nb, 3.72% Ta, and 18.90% C by weight. These compositions were calculated from the data supplied by Kennametal, Inc., on the compositions of the cermets involved, and from the data in the paper by Redmond and Smith[13] which gives the compositions of the added ternary carbide solid solution as 50.0% Nb, 32.5% Ta, 7.0% Ti, and 10.5% C by weight. The densities were determined from x-ray data, using a_o=4.34Å for the carbide phases in both cermets, and from the weighted average of the volumes occupied by the various components.

---

* K-162-B contains by weight 30% Ni, 5% Mo, and 8% solid solution of (Nb, Ta, Ti)C, plus 57% TiC.

TABLE II

Batch Compositions of K-151-A and K-152-B

Designation	Component	Weight %	Volume %
K-151-A	SS*(TiC, NbC, TaC)	80.0	86.92
	Ni	20.0	13.08
K-152-B	SS*(TiC, NbC, TaC)	70.0	80.10
	Ni	30.0	19.90

SS* - Solid Solution

Using the weighted average of the volumes, a density of 8.78 g/cm^3 was calculated for the added solid solution of ternary carbides. The volume percentages calculated using this value for the solid solution of ternary carbides, 4.9 g/cm^3 for TiC, and 8.9 g/cm^3 for Ni in the various carbides, gave identically the same results as those calculated by the first method.

Ni-TiC Diffusion

Ni-Electrolytic 99.9%, 2.0 inches x 2.0 inches x 0.50 inch blocks, International Nickel Co., Bayonne, N.J.

K-151-A and K-152-B compositions given in Table II.

PREPARATION

Cermets

The specimens were obtained from Kennametal, Inc. in the form of 0.38 inch diameter by 0.75 inch long slugs. Small samples 0.38 inch in diameter and 0.13 inch long were cut from these slugs using a diamond cutoff wheel. After marking the samples for identification purposes by notching the edges with the diamond wheel, they were washed in benzene and then dried in an oven at 230°F. Finally, the samples were washed with acetone and again dried in an oven at 230°F. After being weighed, each sample was provided with a bail of 0.010 inch tungsten (W) wire having a small loop at the top for hanging.

Ni-TiC Diffusion

Small discs, 0.13 inches in diameter and 0.13 inches long, of K-152-B, K-151-A and Ni were machined from the slugs of cermet and blocks of Ni respectively. The faces of these small discs were polished and made as flat as possible.

Quench Furnace

A furnace was designed and built to permit the heating and quenching of samples either in a vacuum or in an inert gas atmosphere. Figure 2 shows the vacuum quench furnace and accessories. It consists essentially of furnace, heating chamber, quenching system, vacuum system, and temperature control system. The completely assembled system is shown in Figure 4.

The vertical, split-type furnace contains a 4.5 x 4.5 x 6.0 inch firing zone appropriately insulated and designed for service to 2500°F. It is resistance-heated by four standard Globar elements in series. The split feature was incorporated to facilitate loading; this makes the specimen support assembly and the heating chamber removable as a unit.

The heating chamber is a McDanel refractory porcelain tube, which is sealed to the sample support assembly at the top and to the vacuum pumping system at the bottom through the use of "O" rings. The convenient removal and replacement of the tube necessary in the loading of samples, is thus provided for.

The quenching system is shown in detail in Figure 2. It consists of a quenching receptacle and a sample support release device, shown in Figure 3. The quenching receptacle is a drilled copper (Cu) block resting on a water-cooled support, and may or may not be filled with a liquid quench medium. Common practice is to use Octoil S, high vacuum pump oil within the receptacle. One to four samples may be supported in the furnace at one time, and they can be dropped into the receptacle independently. Each sample, provided with a bail, is supported by threading the bail over 0.010 inch W wire stretched between the common lead and one of the four electrically insulated leads located around the common lead. These leads are 0.050 inch molybdenum (Mo) wire. The electrically insulated wires are contained in fine alumina tubes from the end in the hot zone of the chamber to near the end which emerges from the fixture at the top of the chamber. A vacuum seal is effected by embedding the ends of these tubes and the protruding wires in "Apiezon W" wax at the point where they emerge from the fixture. The common lead is uninsulated, and is connected to the fixture built up from a standard wrought-copper tee. It is positioned in the hot zone by reason of attachment to a two-hole thermocouple insulating tube which is centrally located. The wires of the supporting system are positioned relative to one another by their manner of mounting in the Cu tee fixture at the top of the McDanel tube.

Any one sample can be dropped by fusing the wire over which the bail is hung. This is done by passing a sufficiently heavy current through the supporting W wire. In some cases where not many samples are to be dropped, the 0.010 inch W sample support wires are strung between two 0.050 inch Mo wires and the sample dropped by passing a current through this pair of wires.

The vacuum system is made up of vacuum pumps, gauges, and the heating chamber. The pumping system consists of a Distillation Products Industries (now Consolidated Vacuum Corporation) MC-275 oil diffusion pump backed by a Welch 1403B mechanical pump. Three different vacuum gauges are used. A McLeod gauge is used for intermittent measurement of the pressure in the forearm of the diffusion pump, a National Research Corporation thermocouple gauge is used to follow the pressure changes near the throat of the diffusion pump during boiler heat up, and a D.P.I. Model 273 Phillips gauge is used to measure the pressure at the Cu tee fixture on the top of the heating chamber during operation at low pressure. This location of the Phillips gauge was selected so that the pressure measured during operation would be the highest permanent gas pressure in the system. The gauge is mounted in the tabulation seal attached to the Cu tee fixture. This fixture, in conjunction with the heating chamber, completes the closed vacuum system.

Titanium (Ti) chips used as getters are located in the hot zone of the tube which serves as the heating chamber for the samples. These getters are for the permanent gases oxygen (O_2) and nitrogen (N_2) which may be present in small amounts. In one sense they may be considered as part of the pumping system.

The temperature control system consists of the power transformer, a bank of resistors, sensing thermocouple, and a Foxboro control-point controller. Manual setting or adjustment of the three-power-regulating components allows any desired temperature up to approximately 2500°F to be maintained for long periods of time. To establish and maintain a given temperature, the desired temperature is set on the control-point controller. Power is increased manually over a period of time by advancing the setting of the power transformer until slightly more power is supplied than is required to maintain the control temperature with the furnace at equilibrium. At this time the sensing couple signals the control instrument which activates a switch placing power-dissipating resistors in series with the transformer and the furnace. These can be adjusted to dissipate approximately 10% of the power supplied by the transformer. When the furnace temperature falls below the control point, the instrument, signaled by the sensing couple, again activates the switch and shunts the series-connected resistors so that all the power available from the transformer is applied to heat the furnace. This temperature control system might appear to require anticipators to smooth out the fluctuations accompanying signalling and response. However, the specific heat and insulating effects of the tube, and the vacuum within the tube used as the heating chamber, are so effective in stabilizing the temperature of the samples that a check thermocouple with its junction in the midst of these samples indicates no temperature fluctuations.

Metallograph

The metallograph used to observe the samples in this research was a Reichert Universal Camera Microscope Model "MeF."

Room Temperature X-Ray Diffraction

All room temperature x-ray photographs were taken with 114.6 mm Debye-Scherrer powder cameras, mounted on a Philips Metallix Model 5100

Type 12043-14044 x-ray diffraction unit containing a Co target x-ray tube. Films were measured on a Norelco illuminator and measuring device capable of reading to ±0.05 mm.

Ni Crucibles

Several small Ni crucibles, designed to hold the Ni-cermet "sandwiches" together, were made from Ni blocks. The crucibles were 0.38 inches in diameter and 1.0 inches long and contained a threaded hole, 0.19 inches in diameter and 0.88 inches deep. A small threaded plug 1.0 inch long screwed into the hole.

PROCEDURES

Firing

In vacuum operation, four or fewer samples, provided with bails as described above, are supported on 0.010 inch W wires stretched between the common lead and the surrounding leads.

The system is assembled, the gauges are mounted, and the vacuum pumps started. After a vacuum of 2×10^{-5} mm Hg has been attained, the furnace is slowly brought to temperature and allowed to equilibrate at the control point, which has been 2000°F or 1700°F. After a time lapse, usually 24 hours or longer, one or more samples are dropped by fusing the support wire using a Variac set at 50 volts and delivering less than 8 amperes. For this operation the grounded support fixture serves as the terminal for the common lead, and the appropriate independently insulated lead serves as the other terminal. The sample drops into the cold quenching oil in the Cu receptacle.

In operation under a helium (He) atmosphere the same general procedure is followed except that after a vacuum of 2×10^{-5} mm Hg is obtained, the diffusion bump is shut off and cold water is circulated through the coils surrounding the boiler. After a period of 3 or 4 minutes the forepump is disconnected from the system by closing a large screw clamp. A small screw clamp, located on a rubber hose which connects the purification train to the throat of the forepump, is opened and He gas is admitted to the system. The He gas, purified by passing it through a trap containing activated charcoal cooled to the temperature of liquid air, is flushed vigorously through the system for one minute. The small screw clamp is then closed, the large screw clamp opened, and the system pumped down again using the diffusion pump to attain a high vacuum. This evacuation and flushing operation is repeated six times. At the end of the final operation, the large screw clamp is then closed, the large forepump is shut off, and the small screw clamp left wide open. The valve on the He tank is cracked just sufficiently for gas to be supplied if the pressure should drop in the furnace. A small pressure-regulating device, located in the gas line between the tank and the cold charcoal trap, keeps the system under a practically static He atmosphere, 2.0 inches Hg above atmospheric pressure.

As pointed out earlier, the selected operating temperature is usually 2000°F or 1700°F, and this can be controlled very closely in the vicinity of the samples. Fluctuations, so small as to be undetectable with the ordinary portable laboratory potentiometer, are believed to be less than 1°F.

All quenched samples are reweighed and then cut into semicircular halves. One half is taken for x-ray analysis and the other half for metallographic examination.

Ni-TiC Diffusion

One Ni disc and one cermet disc, either K-151-A or K-152-B, are placed with their polished faces together at the bottom of one of the Ni crucibles previously described. In all experiments the Ni disc is the bottom half of the sandwich. The screw is inserted and tightened down onto the sandwich. The whole assembly is provided with a bail of 0.010 inch W wire having a small loop for hanging. The crucible is mounted on the sample and quenching device as previously described. After a prescribed length of time at 2000°F in vacuum the support wire is fused, the specimen quenched and the furnace cooled to room temperature. The crucible is then cut in half along the long axis, mounted in Bakelite, and polished, so that the interface between the Ni and cermet may be examined by metallographic techniques. Usually only one crucible is fired during any one experiment.

Metallography

All samples to be polished are mounted in green Precisionite thermosetting mounting powder using a Buehler AB-1315 mounting press. The samples are mechanically polished by first rough grinding on No. 380 Behr-Manning silicon carbide paper, followed by intermediate grinding on No. 400 paper and final grinding on No. 500 paper. The final polishing operation utilizes AB Miracloth mounted on a flat brass lap 4.0 inches in diameter, rotating at a speed of 1725 rpm, using iron oxide (jeweler's rouge) as the abrasive. All excess rouge is removed from the surface of the sample by polishing on a clean Miracloth flooded with double distilled water.

In some cases it is necessary to etch the specimens in order to bring out the structure more clearly. The etching is electrolytic, at 6 volts for approximately 3 seconds in 10% by weight oxalic acid solution, using the sample as the anode. The etching apparatus used is shown in Figure 5.

The above etching procedure does not bring out the TiC grain boundaries. Numerous etchants and techniques were tried, but any which attacked the TiC grain boundaries also dissolved away the Ni phase. Etch staining techniques also failed to isolate any of the phases or grain boundaries present. A heat tinting technique, involving a 1-second electrolytic etch in 5% by weight chromic acid solution and then heat treatment of the sample at 900°F for 5 minutes, was successful. All polished samples were stored in a desiccator filled with indicating Drierite.

All photomicrographs shown in this report were taken with reflected light, bright field illumination, at a magnification of 1500 times, using

a 12X plane eyepiece, a dry Fluorite semiapochromatic objective having an initial magnification of 85:1 and numerical aperture 0.85. Pictures are recorded on Kodak "M" plates, 9 x 12 cm, using an exposure time of 3 seconds with aperture iris diaphragm set at the No. 2 position. The negatives were developed at 68°F in Kodak D-76 solution for 20 minutes, washed for 30 seconds, then fixed for 10 minutes in Kokak F-5 solution. After being washed for one hour, the negatives were sponged clean, placed on a suitable rack and air dried.

Area photographs were taken by isolating the given area with diamond scratches and then photographing, being careful to overlap successive photographs.

X-Ray Diffraction

Eight-hour exposures were usually taken, employing Co radiation filtered through Fe foil. Films were developed at 68°F in Kodak D-19 solution for 4 minutes, then washed for 30 seconds, fixed in Kodak F-5 solution, washed for an additional hour, and then hung up to dry. All lattice constants were determined with precision by using the Straumanis[14] reflection a_o values as a function of $F(\theta)=1/2\ \frac{\cos^2\theta}{\sin\theta} + \frac{\cos^2\theta}{\theta}$ and extrapolating linearly to $\theta = 90°$; $F(\theta) = 0.15$.

The samples to be x-rayed were crushed in a hardened steel mortar of the Plattner "diamond" type until the crystallites pass through a 325-mesh screen. The resulting powder was mixed with "Duco" cement until a thick paste was obtained. Thin fibers are formed by extruding the paste through a small spinnerette in the head of the extruding apparatus shown in Figures 6 and 7. After drying under a heat lamp for 2 hours these samples are ready to be mounted in the x-ray camera.

RESULTS AND DISCUSSION

Quench Studies

All samples heat-treated showed little change in weight.

Since no difference in microstructure appeared to exist between the samples heated in a vacuum and in a He atmosphere only one series of photomicrographs is illustrated. Figures 10 through 21 show the microstructures of samples heated at 2000°F in a He atmosphere for the length of time indicated. Figures 8 and 9 show the microstructure of the as-sintered specimens.

All photomicrographs show clearly that the dark grey carbide phase is the continuous phase and the light Ni phase discontinuous. Observations of samples under oblique illumination reveal that the Ni phase is depressed and that the carbide phase is elevated.

In the K-151-A as-sintered sample, it will be noted that completely cubic carbide grains or Ni skeletal crystals are numerous. In addition it appears that these skeletal crystals are not oriented. Note the colloidal dispersion present in the Ni phase.

The K-152-B as-sintered sample reveals that, because of the larger amount of Ni or alloy present, Ni diffusion and replacement of TiC has advanced to a greater extent. This causes the carbide grains or Ni skeletal crystals to be more nearly cubic. These crystals again are not oriented. The Ni phase also contains a colloidal dispersion. In general, the pattern of the Ni phase indicates that not only does a grain boundary replacement relationship between Ni and TiC appear to exist, but there is evidence supporting the view that the Ni has diffused into the carbide structure in such a way as to permit the cubic crystal structure of the carbide to control the shape of the Ni phase. In rare instances, diffusion of the carbide into the Ni phase appears to have taken place.

The dark grey phase, circled in the photomicrographs, appears to be present in all samples. This phase appears to vary in color from a reddish-pink to dark grey. Its morphology appears to be controlled by the cubic lattice structure of the carbide. Grains of this phase become larger and more numerous as the Ni content of the cermet increases. A similar effect was observed by McBride[16] in studying the impregnation of porous TiC rods with Ni. He reported discrete grey TiC particles with a dark grey phase present in the material. He interpreted the darker regions of the particles as corresponding to the formation of a new phase similar to the phase precipitated in the Ni.

The black areas within the squares on all the photomicrographs, and present in the Ni phase, have been found to be voids.

The orientation and size increase of the carbide grains or cubic Ni skeletal crystals in this series of photographs appears to indicate that, with time at 2000°F, the carbide grains or Ni skeletal crystals decrease in number and increase in size. In addition, the interface between the Ni and the carbide phase appears to be rounding off. This is most pronounced at the corners.

After prolonged study it became apparent that a single photograph of the microstructure was not giving a clear picture of a representative area of the sample. This suggested that a truer picture of the microstructure might be obtained by photographing one large area. Samples K-151-A and K-152-B as sintered, and K-151-A and K-152-B heat treated for 100, 200, 300 and 500 hours at 2000°F in a He atmosphere, were rephotographed and an area 16 x 12 inches successfully obtained.

Examination of these areas reveals that:

1. In all cases a representative area of the sample is obtained because a repeating unit pattern is observed.

2. The carbide grains or Ni skeletal crystals are larger in the 500-hour samples than in the as-sintered specimens.
3. In the as-sintered specimens clusters of small carbide grains are observed. These have disappeared almost entirely in the 500-hour samples.
4. The Ni-TiC interfacial boundaries in the 500-hour K-152-B sample appears to be more rounded and not as angular as they are in the as-sintered sample.
5. The dark grey areas, circled in the photographs, are larger and more numerous in the 500-hour K-152-B sample than in the as-sintered sample. This effect is not as pronounced in the pair of K-151-A samples.
6. The black areas, within the squares in the picture, appear to be more numerous in the 500-hour samples. This increase in the number of black areas appears to correlate with the presence of less Ni in the 500-hour samples.

The heat tinting technique provided additional information. By this method each phase develops a thickness of oxide layer dependent upon its composition. The variation in thickness of the oxide layers influences the absorption of visible radiation and causes the phases to appear in different colors. This affords a means of distinguising between the components solely on the basis of differences in color of the oxide layers.[17]

This technique clearly reveals the larger carbide grains or Ni-skeletal crystals in the 500-hour samples when compared to the as-sintered specimens, and shows that the dark grey phase, spoken of earlier in this report, has a composition different from the surrounding carbide phase.

X-ray powder patterns taken of all the specimens treated revealed no change in crystal structure when compared with powder patterns of as-sintered specimens. In Tables III to X are tabulated the "d" spacings and lattice constants for the various components in the cermets K-151-A and K-152-B as sintered and for the same set of samples after 500 and 1000 hours at 2000°F in a He atmosphere. These are compared with the same data for the pure materials.

Comparison of the Ni lines in these patterns with the lines of pure Ni metal reveal that not only is the unit cell size of Ni in the sample enlarged but also the intensities of some lines have changed, particularly the lines due to the 311, and 222 planes which are broad and diffuse. The first phenomenon observed indicates some solid solubility of TiC in the Ni metal while the second indicates that some phenomenon is present which is disrupting the periodicity of the Ni atoms in the Ni crystal lattice. A stress-strain phenomenon or the solid solubility of TiC in Ni could account for this observed condition.

No definite change in the intensities of the TiC lines in the Kennametal samples is noted on comparison of the x-ray powder patterns with that for

TABLE III

Room Temperature X-ray Data of K-151-A
As Sintered

Line	hkl	d in Å	$\frac{I}{I_o}$	Remarks
1	111	2.48	6	TiC
2	200	2.15	10	TiC
3	111	2.03	5	Ni
4	200	1.76	3	Ni
5	220	1.53	9	TiC
6	311	1.30	8	TiC Broad
7	220	1.250	7	Ni
8	222	1.250	7	TiC Broad
9	400	1.082	4	TiC Broad
10	311	1.065	3	Ni Broad & Diffuse
11	222	1.020	2	Ni Broad & Diffuse
12	331	0.99406	9	TiC Ka 1
13	331	0.99454	3	TiC Ka 2
14	420	0.96906	10	TiC Ka 1
15	420	0.96885	7	TiC Ka 2

Extrapolated Ni $a_o = 3.53_5$ Å

Extrapolated TiC $a_o = 4.335_0$ Å

TABLE IV

Room Temperature X-Ray Data of K-151-A
500 Hours at 2000°F. He Atmosphere. Quenched in Oil.

Line	hkl	d in Å	$\frac{I}{I_o}$	Remarks
1	111	2.49	8	TiC
2	200	2.16	9	TiC
3	111	2.03	4	Ni
4	200	1.77	2	Ni
5	220	1.56	9	TiC
6	311	1.31	8	TiC Broad
7	220	1.250	6	Ni
8	222	1.250	6	TiC Broad
9	400	1.084	3	TiC Broad
10	311	1.067	2	Ni Broad & Diffuse
11	222	1.022	1	Ni Broad & Diffuse
12	331	0.99441	6	TiC Ka 1
13	331	0.99441	4	TiC Ka 2
14	420	0.96913	10	TiC Ka 1
15	420	0.96920	6	TiC Ka 2

Extrapolated Ni a_o = 3.54_4 Å

Extrapolated TiC a_o = 4.335_2 Å

TABLE V

Room Temperature X-Ray Data of K-151-A
1000 Hours at 2000°F. He Atmosphere. Quenched in Oil.

Line	hkl	d in Å	$\frac{I}{I_o}$	Remarks
1	111	2.49	8	TiC
2	200	2.16	10	TiC
3	111	2.03	4	Ni
4	200	1.77	3	Ni
5	220	1.53	7	TiC
6	311	1.31	6	TiC Broad
7	220	1.250	5	Ni
8	222	1.250	5	TiC Broad
9	400	1.082	3	TiC Broad
10	311	1.067	1	Ni Broad & Diffuse
11	222	1.021	1	Ni Broad & Diffuse
12	331	0.99358	4	TiC Ka 1
13	331	0.99364	2	TiC Ka 2
14	420	0.96880	9	TiC Ka 1
15	420	0.96863	5	TiC Ka 2

Extrapolated Ni a_o = 3.53_9 Å
Extrapolated TiC a_o = 4.333_5 Å

TABLE VI

Room Temperature X-Ray Data of K-152-B
As Sintered

Line	hkl	d in Å	$\frac{I}{I_o}$	Remarks
1	111	2.49	8	TiC
2	200	2.16	10	TiC
3	111	2.04	7	Ni
4	200	1.77	3	Ni
5	220	1.53	9	TiC
6	311	1.30	7	TiC Broad
7	220	1.249	7	Ni
8	222	1.249	7	TiC Broad
9	400	1.083	2	TiC Broad
10	311	1.068	3	Ni Broad & Diffuse
11	222	1.022	2	Ni Broad & Diffuse
12	331	0.99391	7	TiC Ka 1
13	331	0.99391	6	TiC Ka 2
14	420	0.96898	9	TiC Ka 1
15	420	0.96899	6	TiC Ka 2

Extrapolated Ni a_o = 3.547 Å

Extrapolated TiC a_o = 4.335$_0$ Å

TABLE VII

Room Temperature X-Ray Data of K-152-B
500 Hours at 2000°F. He Atmosphere. Quenched in Oil.

Line	hkl	d in Å	$\frac{I}{I_o}$	Remarks
1	111	2.49	8	TiC
2	200	2.16	10	TiC
3	111	2.03	8	Ni
4	200	1.76	2	Ni
5	220	1.53	9	TiC
6	311	1.31	7	TiC Broad
7	220	1.249	5	Ni
8	222	1.249	5	TiC Broad
9	400	1.083	2	TiC Broad
10	311	1.065	3	Ni Broad & Diffuse
11	222	1.021	1	Ni Broad & Diffuse
12	331	0.00341	8	TiC Ka 1
13	331	0.99368	6	TiC Ka 2
14	420	0.96848	9	TiC Ka 1
15	420	0.96901	8	TiC Ka 2

Extrapolated Ni a_o = 3.54_8 Å

Extrapolated TiC a_o = 4.335_4 Å

TABLE VIII

Room Temperature X-Ray Data of K-152-B
1000 Hours at 2000°F. He Atmosphere. Quenched in Oil.

Line	hkl	d in Å	$\frac{I}{I_o}$	Remarks
1	111	2.49	8	TiC
2	200	2.16	10	TiC
3	111	2.04	7	Ni
4	200	1.77	4	Ni
5	220	1.53	8	TiC
6	311	1.30	5	TiC Broad
7	220	1.249	5	Ni
8	222	1.249	5	TiC Broad
9	400	1.082	3	TiC Broad
10	311	1.067	2	Ni Broad & Diffuse
11	222	1.021	1	Ni Broad & Diffuse
12	331	0.99322	5	TiC Ka 1
13	331	0.99321	4	TiC Ka 2
14	420	0.96848	9	TiC Ka 1
15	420	0.96935	4	TiC Ka 2

Extrapolated Ni a_o = 3.54_2 Å

Extrapolated TiC a_o = 4.334_0 Å

TABLE IX

Room Temperature X-Ray Data of Pure Ni

Line	hkl	d in Å	$\frac{I}{I_o}$	Remarks
1	111	2.03	10	
2	200	1.76	10	
3	220	1.246	10	
4	311	1.0626	10	Ka_1
5	311	1.0626	8	Ka_2
6	222	1.0177	5	Ka_1
7	222	1.0175	4	Ka_2

Extrapolated $a_o = 3.524_8$ Å

TABLE X

Room Temperature X-Ray Data of Norton TiC

Line	hkl	d in Å	$\frac{I}{I_o}$	Remarks
1	111	2.45	8	
2	200	2.15	10	
3	220	1.52	9	
4	311	1.300	4	
5	222	1.246	2	
6	400	1.0797	3	Ka_1
7	400	1.0797	3	Ka_2
8	331	0.99196	4	Ka_1
9	331	0.99182	3	Ka_2
10	420	0.96695	10	Ka_1
11	420	0.96699	8	Ka_2

Extrapolated $a_o = 4.326_3$ Å

pure TiC. The lines caused by the reflections from 311, 222 and 400 planes of TiC in the Kennametal samples appear much broader, and a slightly larger unit cell size is indicated. The first effect may again be caused by a stress-strain phenomenon, while the second effect is caused by the solid solution of TaC and NbC in the TiC lattice.

Another similar series of quenching experiments was conducted in He atmosphere at a temperature of 1700°F. Not enough research time was available to study the results of this work.

Ni-TiC Diffusion

Several experiments were tried using both K-151-A and K-152-B discs. A cut and polished sample is shown in Figure 22. These experiments showed that while no diffusion of TiC into the Ni disc occurred, diffusion between the Ni disc and the Ni in the cermet did take place. Failure to observe any TiC on the Ni side of the Ni-cermet boundary might be due to several reasons. First, the solid solubility of any TiC which did diffuse past the boundary allows the TiC to remain in solid solution upon quenching. Second, a colloidal dispersion may be present but, because of the small size of the grains, is not resolved by the optical microscope.

CONCLUSIONS

On the basis of the results obtained to date we can conclude that in samples K-151-A and K-152-B:

1. Grain coalescence takes place with time at 2000°F. Small clusters of TiC grains coalesce to form larger masses of TiC. This indicates that the cermets are in a metastable state and that with time at temperature, the system is trying to approach a state of equilibrium. The coalescence and rounding of the TiC grains is the approach toward the attainment of this state. This coalescence results in a decrease in high temperature strength as we have theorized in paragraph 3, page 4 of this section.

2. No change in crystal structure takes place with time at 2000°F. No new phases are formed and the solid solubility relationships at this temperature do not appear to be time dependent. Hence, the Ni binder phase is saturated with TiC and the TiC in solid solutions is in equilibrium with undissolved TiC.

3. Carbide Ni interfacial boundaries appear to be rounding. The grains are trying to develop a minimum surface to volume ratio by becoming spheroidal. Thermodynamically this is the most stable condition for these particles.

4. The carbide phase is not a homogeneous solid solution but displays composition variation within grains. Since TiC is known to lose carbon at higher temperatures[18] to form a carbon-deficient defect lattice similar to TiO, perhaps this phase is TiC possessing a carbon deficiency.

5. Since the results of a solution-reprecipitation mechanism have been observed one must conclude that it is operating in this system.

6. It should be possible to produce a cermet possessing improved high temperature strength by reducing the solubility of TiC in the auxiliary metal phase. This could be done most easily by alloying the existing Ni phase in cermets K-151-A and K-152-B. The Ni-Cr-Mo alloy discussed in Section 4 might yield the best results.

7. Valuable information relevant to the above conclusions could be obtained by studying the relationship between the solubility of refractory phases in auxiliary metal or alloy phases of cermets and the high temperature strength properties of these bodies by means of high temperature x-ray diffraction techniques.

SECTION 2

STUDY OF SOME TiC BASE CERMETS BY MEANS OF HIGH TEMPERATURE X-RAY DIFFRACTION TECHNIQUES

INTRODUCTION

If carbide grain coalescence is occurring at 2000°F through the solution-precipitation mechanism discussed in Section 1 of this report, TiC must have an appreciable solid solubility in Ni at this temperature.

In the past, several investigators have tried to measure this solubility. Honeycombe[19] reports that Sarubin[20,21] determined the solubility of TiC in Ni and Co. Unfortunately no data are given on the temperature at which these experiments were conducted. The Russian investigator found that TiC was insoluble in Ni and that Co dissolved up to 5 percent TiC by weight. Ni is reported to dissolve up to 20 percent TaC, 12 percent Mo_2C, 8 percent Cr_3C_2, and 15-30 percent WC by weight.

Polikarpova[22] studied the interaction between TiC and Co. He concluded that TiC forms with Co a solid solution in which titanium atoms replace the cobalt atoms. The solubility of TiC in Co attains 7-10 percent by weight at 2100-2280°F.

Germany[23] found that Co dissolves in TiC and Kieffer[24] has stated that solid solutions of Group IV carbides with Group VI carbides (WC dissolved in TiC, for example) can dissolve 3-5 percent by weight Ni or Co at room temperature. However, Metcalf[25] found "no evidence from either x-ray diffraction data or spectroscopic data (analysis of carbides extracted from sintered products to suggest that WC, TiC, or their solid solutions dissolve Co. Stover[11] found that Ni dissolved up to 4 atomic percent TiC at 2192°F and 5 atomic percent at 2354°F. He found that Ni was nearly insoluble in TiC within this range of temperature.

Recently R. Edwards and T. Raine[26] found that TiC is soluble up to 5 weight percent in Ni at 2282°F, up to 10 percent by weight in Co and less than 0.5 percent by weight in Fe.

In general, the agreement of values at any particular temperature is poor and no data are available for the solubility at 2000°F. One can estimate, however, that the solubility of TiC in Ni at 2000°F must lie within the range 0.5 to 4.0% by weight.

All of the determinations to date have been made by standard metallographic techniques. These would involve the mixing of the components in

the required amounts, the forming of a green compact by pressing in a die, and the heat-treating of this compact in either an arc furnace or induction furnace under a vacuum or inert gas atmosphere. Finally the sample is annealed at the required temperature and quenched, and the structure observed under the metallograph or by means of room temperature x-ray diffraction techniques.

It is felt, however, that this procedure very seriously contaminates and alters the compositions of the samples involved. A better method would be to study the solubility of the components at the specified temperature, in a vacuum or inert gas atmosphere, by means of high temperature x-ray technique. In addition, this technique permits the study of high temperature reactions and phase transitions at high turbine operating temperatures. It also affords a method of obtaining stress-strain and thermal expansion data.

It was decided therefore to construct a high temperature x-ray diffraction camera and with this instrument determine:

1. The solid solubility of TiC in Ni at 2000°F.

2. Whether any new phases or transformations occurred up to or at 2000°F in the samples K-151-A and K-152-B.

3. Evaluate the thermal expansion characteristics of the samples K-151-A and K-152-B and the pure components, and investigate the stress-strain phenomena involved.

APPARATUS

High Temperature X-Ray Camera

Many high temperature x-ray cameras have been described in the literature in the past and an effort was made to incorporate their best features.

Figure 2-23 (Drawing No. 441-4) is the assembly drawing of the camera. It is essentially a 114.6 mm powder camera and consists of three major parts: the body, the top cover, and the film cassette. The top cover is sealed to the body of the camera by means of an "O" ring and the film cassette slides over the top cover into its correct position. The camera is water cooled with coils mounted into both the body and the top cover of the camera. A band of beryllium (Be) foil, mounted in the top cover, allows the deffracted x-ray beam to pass out of the camera and strike the x-ray film. The camera can be operated under a vacuum or with an inert gas atmosphere.

The assembled brass shell of the camera is shown in Detail No. 27, Figure 24. The body of the camera, Figure 25, contains the lower of two identical Pt-20% Rh wound furnaces, the specimen holder rotating device, cooling coils, a tube for connection to the vacuum pumps and a set of vacuum gauges. It is mounted on a base, Figure 26, which slides along the tract mounted on the Philips x-ray unit. Screw clamps on the right side of the

base lock the camera into position on the track. The top cover, Figure 27, contains the slit system for collimating the x-rays, the upper of the two identical furnaces, cooling coils and a thin band of Be readily penetrable by x-rays. Electrical connections are made through the glass-to-metal seals mounted in the top and bottom of the camera.

The furnace, Detail No. 1C, Figure 28 and shown in Figures 25 and 27, A and B, consists of two opposing alumina cores, wound with No. 25 gauge Pt-20% Rh wire. It is capable of heating a specimen to 2732°F. A thin coating of alumina, 0.13 inch in thickness, covers the outside of the heaters and supports the wire on the cores. The two furnaces are connected in series outside the camera. An x-ray gap of 0.13 inch is left between the furnace sections.

The collimator, Detail No. 29, Figure 28, and also Figure 27, C, is of the circular pinhole type. The x-rays pass through an 0.030 inch diameter hole drilled through the lead-filled end of a stainless steel tube and emerge through an 0.018 inch diameter hole drilled through a lead plug which has been inserted into the opposite end of the tube. The beam and fluorescent screen, Detail No. 28, Figure 28, is simpler than the usual type in that it does not extend inward to the sample. Exposure times vary with specimens, types of film and x-ray source; however, as an example, exposures at 15 ma, using CoKa radiation are of the order of 4 hours. A thin cellophane film mounted on the front of the entrance aperture of the collimator completes the vacuum seal.

The cassette frame, Detail No. 11, Figure 31 and the film cassette disassembled in Figure 32, slide over the outside of the camera. The cassette is entirely independent of the vacuum chamber and may be removed and reloaded without interference with the vacuum, heating, or water-cooling systems and without upsetting alignment with the source of x-rays. The film, cut to shape by means of the template B and razor blade, is inserted into the brass band film holder, Detail No. 14, Figure 31, between the brass sheet and a piece of black photographic paper mounted on the sheet C in Figure 32. This unit is assembled in the cassette frame A and held there tightly by means of the pin D. Although a light-tight seal is usually made, the brass band stray-light shield E, insures against any light exposing the film.

The specimen is mounted on a sapphire rod and held there by means of alumina cement. A small screw mounted in the base provides a means for centering the specimen. Rotation of the sample is accomplished by means of a gear and chain assembly which rotates the specimen at approximately 3 rpm. See D, Figure 33.

The vacuum is obtained with an H-2-P National Research Corporation three-stage oil diffusion pump (G in Figure 34) backed by a 1403 Welch mechanical pump (A in Figure 35). The vacuum is measured using a National Research Corporation 501 thermocouple gauge and a National Research Corporation 507 ionization gauge. A single NRC combination thermocouple and ionization gauge control panel Type 710 is used with these gauges (E in Figure 36).

A Pt, Pt-10% Rh thermocouple, Reference No. 34, Figure 23, is built into the section of the furnace mounted in the top cover and is used to measure the temperature of the specimen. This thermocouple was calibrated against the known melting point of pure Cu and was found to agree within ± 1°F.

The power source for the furnaces and pumps consists of one 0-100 volt Powerstat, mounted in the control panel, F, Figure 36, with its output connected to the input of a 135 volt Variac C in Figure 35. The Powerstat regulates the voltage to the furnace and the Variac, which is set at 50 volts, serves as a step-down transformer. The two transformers are fed by a 1 KVA Sola constant voltage transformer, D, Figure 35. A maximum power of 240 watts is used at 2000°F. See Figure 29. Since there is no temperature-sensing controller in the system, constant temperature is maintained by supplying constant power to the heaters. Several minutes are allowed to let the system come to equilibrium after power is applied, even though the heaters come to operating temperatures almost immediately. The temperature of the furnace can be controlled to within ±5°F by this method.

Arc Furnace

While mixing and extrusion of the pure powdered materials in the required proportions would produce the best stoichiometric samples, the actual melting of the materials to form a small ingot would produce a denser sample in which the components were already in a more advanced state of diffusion. Both techniques were used, to learn something about the relative merits as well as to obtain good x-ray samples.

An arc furnace was chosen in preference to other types of heating units (induction furnaces, Globar type, etc.) mainly for the following reasons:

1. Little or no crucible contamination of sample.

2. Ease of producing an O_2-free atmosphere.

3. Unit is of the right capacity for fabricating samples.

The arc furnace, shown in Figures 37 and 38, was originally designed by Donald McPherson[27] and reassembled by this project with some changes. It consists of a crucible B (see figure 39), made of solid Cu, with a small Ni crucible approximately 1.C inch OD x 0.75 inch ID x 0.50 inch high and 0.38 inch deep inside, inserted into a cavity drilled into the original Cu stock. Two other holes near the edge of the Cu stock contain pieces of Ti rod, protruding about 0.50 inch above the surface of the stock. These rods serve as strikers for the arc, and when the arc is stuck they serve as a getter for O_2 and N_2.

This crucible is placed in the bottom of a Cu container, which is 2.5 inches in diameter, 5.3 inches deep, with tapered walls 0.063 inch thick. This assembly is surrounded at the bottom by a Cu water jacket 3.0 inches ID and at the top by a 5.0 inch OD brass cooling jacket. The top ring of this upper cooling jacket has an annular inset, which contains a rubber gasket. A depressed ring-groove in the crucible flange fits against this gasket, providing a watertight seal. The container also contacts the brass assembly at this point, placing the entire bottom unit at ground potential. This part of the furnace is fastened to the table top by three set-screws spaced at 120°. Insulating washers separate the table from the electrical circuit. The 5.0 inch OD brass furnace head is insulated from the container assembly by means of a 0.50 inch thick Synthane ring. Seals are provided between the container and insulating ring and between the head and insulating ring using Neopreme "O" rings, 4.4 inches in diameter. The entire head assembly is cooled by a water jacket. A water-cooled, TiC + Ni tipped electrode passes through a 1.0 inch Cu bellows, having a 4.0 inch free length soldered to a brass ring which threads into the center of the head. A Teflon gasket provides the seal at this point. The electrode height is adjustable and can be rotated 360° within the furnace. A brass ring in the head prevents the electrode from approaching closer to the container side wall than 0.50 inch. The furnace head is provided with a 0.75 inch sight tube containing a 0.25 inch thick gasketed pyrex sight glass.

A 0.75 inch Cu tube provides the outlet to the vacuum pump from the furnace chamber. The entire head assembly is secured to the crucible unit during operation by means of four clamps which are anchored to, but insulated from, the table top. The clamps pivot at the lower connection and can be swung free for dismantling the furnace. For runs involving an inert atmosphere, such as He, the gas enters just below the sight tube and exits through a tube in the furnace head. This tube is fitted with a tee, one section leading to a McLeod gauge and the other downward to a Hg seal designed to maintain a gas pressure in the furnace of 2.0 inches of Hg above atmospheric. This line contains a stopcock which is closed off when vacuum operation is desired.

A Welch Duo-Seal Model 1405 H mechanical pump is employed to evacuate the furnace.

Power for melting the samples is supplied by a Wilson Hornet 300 ampere, DC welding generator.

PROCEDURES

Firing-High Temperature X-Ray Camera

In operation, the sample is mounted and aligned as described, the top cover is placed in position and the film holder is slid into place. Water is allowed to pass through the cooling coils and the vacuum pumps are started. The furnace is slowly brought up to temperature by advancing the variable transformer mounted on the control panel.

When the unit is to be cooled down, the furnace may be shut off manually or, with the relay switches set to "dependent-water", the camera and diffusion pump will be shut off when the x-ray exposure has been completed.

As a safety precaution against sudden pressure changes, the relay switch is turned to the "dependent-vacuum" position. Any sudden rise in pressure will immediately shut off the x-ray unit, camera, and diffusion pump.

The furnace has been run for over 1000 hours and shows no signs of burning out. Starting from room temperature and increasing the voltage slowly, it is possible to reach constancy of temperature at 2000°F within one hour. As an example of the rate of thermal response, using a Ni wire specimen, and raising the voltage from 50 volts to 55 volts, corresponding to a current increase of 0.6 amps, the temperature of the furnace increased from 1500°F to 1700°F in 12 minutes.

Figure 29 shows a typical temperature versus power curve, which is highly reproducible.

The curve in Figure 30 shows the rapid cooling of the camera with the normal water flow of approximately 1 gallon per minute. Typical cooling rates are: from 2000°F to 200°F, 30 minutes; from 2000°F to 85°F, 60 minutes. When the temperature of the specimen is 2000°F, the outside surfaces of the brass case remain slightly below room temperature.

Firing-Arc Furnace

In operation the sample to be melted was placed in the bottom of the Ni crucible, the furnace assembled, and the system evacuated to approximately 0.1 mm Hg for about one minute. The vacuum pump was shut off and He was admitted to the system. The He gas was purified by passing it first through a tower of activated alumina, which removed the moisture; then through a tower of Ti metal heated to 1382°F, which removes any O_2 or N_2 that may be present. The He was then flushed vigorously through the system for one minute. This evacuation and flushing operation was repeated six times. At the end of the final operation the valve was cracked just sufficiently for gas to be supplied if the pressure dropped in the furnace. The furnace was now under a practically static He atmosphere, 2.0 inches Hg above atmospheric pressure.

The cooling water was now turned on. Flow was adjusted to 2.5 to 3.0 gallons per minute around the crucible and 1.5 gallons per minute through the electrode. The welding generators were started. An arc was struck on the Ti striker and transferred to the charge. Approximately 125 amperes was used and the arc length was about 0.50 inch.

After approximately five seconds, during which time the electrode was rotated vigorously, the electrode was withdrawn and the power shut off. The sample was first allowed to cool, then the water and He were shut off and the furnace was opened. The charge was turned over and the entire operation repeated until the sample was completely melted.

Different evacuation and melting procedures were tried. The amperage and voltage were varied and different arc lengths were investigated. The above procedure, however, was found most satisfactory.

In all cases the welding generator was operated on straight polarity with the electrode, the cathode, and the melt and crucible, the anode.

A chemical analysis was made on several of the compositions melted. In general, all melted compositions analyzed twice as high in TiC than was originally present. This increase in TiC concentration can be attributed to volatization of Ni metal during melting.

Spectroscopic analysis of the samples revealed only the elements that were present before arc melting; hence, no specimen contamination occurred during arc melting.

SOLID SOLUBILITY STUDIES

Materials and Composition

The following materials were used in compositions covered in this section:

Ni - Mond Ni powder, 4 microns in size, 99.7% minimum Ni content, International Nickel Co., Bayonne, N. J.

TiC - Stoichiometric TiC analyzing 0.1% free C, minus 325 mesh, Norton Co., Worchester, Mass.

The compositions discussed in this section are given in Table XI.

TABLE XI

Batch Compositions of Ni + TiC for High Temperature X-Ray Studies

Material	Compositions in weight %							
	1	2	3	4	5	6	7	8
Ni	90.0	95.0	96.0	97.0	98.0	99.0	99.5	100.0
TiC	10.0	5.0	4.0	3.0	2.0	1.0	0.5	-----

Preparation of Batch

Ten-gram batches of the above compositions were weighed and mechanically mixed. One series of samples was extruded using the techniques discussed

in Section 1 of this report. Another series was made by pressing the powder into small cylinders, and then arc melting them by the techniques discussed above. Figure 39 shows before and after arc melted samples. These samples were reweighed and then cut into 3 parts. One section was taken for x-ray examination, another for quench studies and metallographic examination, and the last for chemical analysis.

The sample taken for x-ray analysis was machined to a small fiber 0.25 inch long and 0.0060 inch thick.

All the samples were stored in a desiccator filled with indicating Drierite until ready for use.

Results and Discussion

Sufficient research time was available to investigate the 0.5% TiC by weight extruded sample. Room temperature photographs were taken both before and after heating. One 8-hour photograph was taken of the material after it had been at 2000°F for 3-1/2 hours. Another 8-hour exposure was made after 19-1/2 hours at this temperature. A final pattern was taken after 50 hours at 2000°F.

Lines due to TiC are still visible in the 19-27 hour photograph. They have disappeared entirely in the 50-58 hour exposure. The room temperature photograph of this sample reveals an increase in lattice constant and confirms the solid solubility of 0.5% TiC in Ni metal at 2000°F. These values are given in Tables XII to XVI.

TABLE XII

Room Temperature X-Ray Data of Ni + 0.5% TiC As Mixed

Line	hkl	d in Å	I/I_o	Remarks
1	111	2.23	1	TiC
2	111	2.03	10	Ni
3	200	1.94	1	TiC
4	220	1.88	2	TiC
5	200	1.76	10	Ni
6	220	1.245	9	Ni
7	311	1.0621	9	Ni
8	222	1.0176	8	Ni Ka 1
9	222	1.0169	7	Ni Ka 2

Ni Extrapolated a_o = 3.522$_8$Å.

TiC Extrapolated a_o = No back reflection lines.

TABLE XIII

X-Ray Data of Ni + 0.5% TiC at 2000°F
3 1/2-11 1/2 Hours

Line	hkl	d in Å	I/I_o	Remarks
1	111	2.44	2	TiC
2	200	2.12	3	TiC
3	111	2.07	10	Ni
4	200	1.79	8	Ni
5	220	1.50	3	TiC
6	220	1.266	7	Ni
7	311	1.0812	6	Ni Ka 1
8	311	1.0806	6	Ni Ka 2
9	222	1.0350	4	Ni Ka 1
10	222	1.0346	4	Ni Ka 2
11	331	0.97304	1	TiC
12	420	0.94726	1	TiC Ka 1
13	420	0.94760	1	TiC Ka 2

Ni Extrapolated $a_o = 3.587_3$ Å

TiC Extrapolated $a_o = 4.237_6$ Å

TABLE XIV

X-Ray Data of Ni + 0.5% TiC at 2000°F
19 1/2-27 1/2 Hours

Line	hkl	d in Å	I/I_o	Remarks
1	111	2.45	2	TiC
2	200	2.11	3	TiC
3	111	2.07	10	Ni
4	200	1.79	9	Ni
5	220	1.50	2	TiC
6	220	1.267	6	Ni
7	311	1.0811	8	Ni
8	222	1.0356	5	Ni Ka 1
9	222	1.0352	5	Ni Ka 2
10	331	0.97222	1	TiC
11	420	0.94763	1	TiC Ka 1
12	420	0.94754	1	TiC Ka 2

Ni Extrapolated $a_o = 3.587_3$ Å

TiC Extrapolated $a_o = 4.2376$ Å

TABLE XV

X-Ray Data of Ni + 0.5% TiC at 2000°F
50-58 Hours

Line	hkl	d in Å	I/I_o	Remarks
1	111	2.07	10	Ni
2	200	1.79	7	Ni
3	220	1.268	6	Ni
4	311	1.0824	8	Ni Kal
5	311	1.0825	4	Ni Ka2
6	222	1.0365	3	Ni Kal
7	222	1.0361	1	Ni Ka2

Extrapolated a_o = 3.590 Å

TABLE XVI

Room Temperature X-Ray Data of Ni + 0.5% TiC
After Heating for 58 Hours at 2000°F

Line	hkl	d in Å	I/I_o	Remarks
1	111	2.03	9	Ni
2	200	1.76	7	Ni
3	220	1.245	8	Ni
4	311	1.0626	10	Ni Kal
5	311	1.0626	5	Ni Ka2
6	222	1.0174	6	Ni Kal
7	222	1.0175	4	Ni Ka2

Extrapolated $a_o = 3.525_5$ Å

Comparison of this lattice constant with that for Ni in the K-151-A and K-152-B samples shows the latter to be much larger, indicating considerably more TiC solid solubility than we have measured thus far. It is interesting to note that upon cooling to room temperature the carbide remained in solid solution and did not reprecipitate.

The solid solubility of TiC in Ni appears to be at least 0.5% by weight at 2000°F and may be larger.

It will be noted that the extrapolated lattice constant for TiC in these mixtures is smaller than the extrapolated value for pure TiC at room temperature. This effect is also noticed in the calculated "d" spacings.

Photographs taken of untreated mixtures containing 0.5, 1.0, 2.0, 3.0, 4.0, 5.0 and 10.0, % TiC by weight at room temperatures in Philips 114.6 mm Debye-Shearer cameras also show the same phenomenon. The exact cause for this shift in the diffraction lines of TiC in these mixtures is unknown at the present time. It may possibly be due to an absorption phenomenon occurring in the samples or it may be due to the diffraction by the sample of Fe Ka radiation emanating from the Fe filter.

HIGH TEMPERATURE PHASE STUDIES

Materials and Compositions

The materials and compositions used in this section are the same as those listed in Table II, of this report.

Preparation of Batch

The samples to be x-rayed were crushed in a hardened-steel mortar of the Plattner "diamond" type until the small particles passed through a 325-mesh screen.

The samples were then extruded by the methods already described in Section 1 of this report.

Results and Discussion

Kentanium samples K-151-A and K-152-B showed no phase transformations on heating up to 2000°F and developed no new phases after heating the samples for 75 hours at this temperature. A longer period of time resulted in oxidation of the cermets to TiO_2 (rutile) and NiO.

THERMAL EXPANSION STUDIES

Materials and Compositions

The materials and compositions used in this section are the same as those listed in Table II, Section 1, of this report, in the case of Kentanium samples K-151-A and K-152-B.

Ni-pure wire, 0.0060 inch diameter, Driver-Harris, Co., Harrison, N.J.

TiC - Stoichiometric TiC analyzing 0.1 free C, minus 325 mesh, Norton Co., Worcester, Mass.

Preparation of Batch

The Kentanium samples and the TiC powder to be x-rayed were prepared by the usual extrusion technique.

In addition several Kentanium samples K-151-A and K-152-B were machined down to thin fibers 0.0060 inch in diameter.

Results and Discussion

Research time available permitted investigation of the thermal expansion behavior of pure Ni. These data are given in Table XVII and the expansion is shown graphically in Figure 40. Here are plotted the percent linear expansion values of the metal versus temperature. This graph also shows a comparison between the curve obtained by x-ray diffraction and that obtained by dilatometric measurements.

TABLE XVII

Linear Thermal Expansion of Ni

Linear expansion in %	Temperature, °F
0.0000	85
0.1558	240
0.2551	350
0.6943	783
0.9494	1064
1.091	1210
1.219	1330
1.489	1607
1.686	1800
1.899	2000

CONCLUSIONS

No new phases or transformations develop on heating Kentanium samples K-151-A and K-152-B up to 2000°F and none appear to develop after heating the sample for 75 hours at this temperature. These results are in complete agreement with our quench studies which also showed that no new phases developed under the same conditions.

The thermal expansion of Ni metal has been extended to higher temperatures by this research. Up to 1400°F, the slopes of the expansion curves obtained by x-ray diffraction procedures and dilatometry measurements are similar. A comparison of either of these two curves with the thermal expansion curve for TiC (Figure 55) shows at once the differences in expansion behavior. It is obvious that internal body strains will exist in any cermet made from these two materials.

These internal strains are probably the cause for the broad, diffuse reflections obtained from the 311 and 222 planes of Ni and the 311, 222 and 400 planes of the carbide phase in K-151-A and K-152-B. It is believed that

the presence of these strains causes the cermet to have a level of brittleness, which might be lowered if an improved thermal expansion match between the phases could be effected. It is for this reason that a program was initiated in order to obtain a binder metal which would have a coefficient of expansion equal to or slightly greater than that of the ceramic component. A more detailed discussion of this topic can be found in Section 4 of this report.

TiC has been found to be soluble in Ni metal at 2000°F at least to the extent of 0.5% by weight. It is possible that the solubility is even greater.

Since the sizes of the Ni and Ti atoms differ by less than 15%, substitutional solid solution can readily occur between these two atoms to fit in the octahedral holes of the Ni face-centered cubic crystal lattice. It appears that the conditions necessary for transport of TiC through the Ni phase of these cermets, by substitutional replacement of Ti atoms for Ni atoms and C diffusion interstitially, are present in this system.

In addition, it is believed that the colloidal dispersion present in the Ni phase and unresolved in our optical photomicrographs, but resolved by the electron microscope (See Section 3), is TiC which was in transport and precipitated from the saturated Ni phase on cooling.

No carbide was observed to precipitate from the sample containing 0.5% TiC by weight upon cooling from 2000°F, because either this concentration of TiC is soluble in Ni at room temperature or the solution is supersaturated with respect to TiC.

Evidence obtained to date indicates that the mechanism responsible for the coalescence of small TiC grains on heat-treating samples K-151-A and K-152-B at 2000°F is solution-reprecipitation. The same process would be expected at lower temperatures at a slower rate.

SECTION 3

THE ELECTRON MICROSCOPY OF SOME TiC BASE CERMETS

INTRODUCTION

In Sections 1 and 2 of this report mention was made of the colloidal dispersion present in the Ni phase. Since these particles are less than 2000 Å in diameter, they are incapable of being resolved even by the best optical microscope. On the other hand, they are about the right size to diffract ordinary white light; hence, they show up as small black spots or blurs on the optical photomicrographs. If one wishes to study this dispersion he must take advantage of the higher magnification and resolution offered by the electron microscope.

The question is raised as to the nature of these small particles. In particular, are they small particles of TiC? If they are, one can postulate that these particles may be TiC which has diffused through the Ni lattice and precipitated from the saturated solid solution on cooling. It was important, therefore, from the standpoint of the solution-precipitation mechanism, to resolve this finely divided phase.

Since electrons are readily absorbed by thick metallic specimens, replicas must be made of their surface structures. While many excellent techniques have been described in the past for making replicas of metallic surfaces, most either suffer from the limitation of quality and reproducibility or tend to be involved and time consuming. A new method was sought, therefore, which would combine both speed in the production of the replicas and accuracy in the reproduction of the metal microstructure.

Calbick[29] has shown that metal atoms tend to stick where they strike on thermal evaporation, moving only a very short distance before they nucleate to form small crystallites. Oxides such as silica (SiO_2) and silicon monoxide, tend to form amorphous films and migrate large distances, 5,000 Å or more, before finally condensing. In addition SiO_2 films tend to "roll up" in the washing solution, are dimensionally unstable, and are time consuming to prepare. The desirability of using metals for the preparation of replicas is thus indicated.

Calbick also states that with replicas possessing an average mass thickness of 10 μg per sq cm the resolution of the replica films are inversely proportional to their density. Recently Hibi and Yada[30] have shown that the higher the heat of sublimation of the metal forming the film the better the resolution. The desirability of using a metal of high density and possessing a large heat of sublimation is thus indicated.

While osmium, iridium and platinum (Pt) are the most dense metals in the periodic table, the first two can be excluded because of their scarcity and cost. Pt possesses a very high density, 21.7, and a very high heat of

sublimation, approximately 128 Kcal per mole. Calbick[31] reports a calculated intrinsic resolution of around 46 Å for replicas made of this material. Its drawbacks, which prevented its use to date, are its high cost and the ease with which it alloys with most other elements. Some investigators[32] also have reported the need of a good vacuum (10^{-5} mm of Hg or lower) in order to evaporate sufficient material.

A research program was initiated in order to develop a better technique for making replica films and to utilize this technique for investigating the colloidal dispersion present in the Ni phase of our cermet compositions K-151-A and K-152-B.

MATERIALS AND COMPOSITIONS

All samples used in this section were the heat treated samples discussed in Section 1 of this report. Their compositions are listed in Table II.

Pt - CP wire, 0.010 inch diameter, Baker and Co. Inc., Newark, N. J.

W - CP wire, 0.040 inch diameter, Callite Tungsten Corp., Union City, N. J.

EQUIPMENT

Evaporation Unit

The apparatus employed for all vaporizations is shown in operation in Figure 41 and with the bell jar removed in Figure 42.

The vacuum is obtained by using a horizontal Distillation Products Inc. diffusion pump MF-250 backed by a water cooled Cenco Hypervac "20" forepump powered by a 1/2 HP motor. This equipment is mounted under the table and enclosed in plywood and an acoustical blanket. Pressures are read by using a DPM-36 ionization gauge control panel equipped with a VG-1A Ionization gauge tube for taking readings below 10^{-3} mm of Hg and two-station DPC-236 Pirani Gauge control panel equipped with PR-1110 Pirani tubes for reading from 0.75 to 10^{-3} mm of Hg. All this equipment, plus a Type 20 Powerstat is mounted in the panel on top of the table.

The inlet of air and the regulation of the forepump and diffusion pump evacuations are controlled by a series of mechanical valves, the handles of which can be seen at the side of the unit in Figures 41 and 42.

Electron Microscope

The electron microscope used in an RCA model EMU-2C employing electrons accelerated by a potential of 50KV.

Electron Metallography

Before replicas can be made which reproduce metal structures accurately, the specimen must be prepared in such a manner that the true structure of the material is revealed. In general, the surface of the specimen should be free from disturbed metal and scratches. While electropolishing would be the most satisfactory, no one has yet developed a method for electropolishing these carbide cermets. A mechanical polishing technique was thus employed in full realization of its inherent limitations.

The specimen was polished by the methods discussed in Section 1 of this report, the only change being that the sample was wiped clean with a paste of MgO on cotton for 5 minutes prior to forming the replica.

After mechanical polishing, the specimens were etched without delay in order to prevent surface passivation. An electrolytic etch was used, involving the use of a 10% by weight oxalic acid solution and using the sample as the anode at six volts. Samples were etched for 1, 2, 4, and 8 seconds, a replica being made after each etching.

The mounted specimen to be replicated was placed, with its polished side up, at the bottom of the molding die which is part of the No. 1315 AB mounting press described in Section 1 of this report. Lucite* powder was then poured on top of the specimen to a height of about 0.50 inch. This is sufficient material to produce a sample 0.25 inch in thickness. The top plunger was slid into place and the mold brought up to a temperature of 284°F, under a constant pressure of 2,000 psi. A pressure of 7,000 psi was then applied and left on for 1 minute, keeping the temperature constant. The die was then cooled, keeping the pressure at 7,000 psi until room temperature was reached.

The mold was taken apart and the mounted sample and Lucite replica separated by mechanical means. The replicated metallic structure can be studied by observing the Lucite surface under a conventional optical microscope.

After the plastic replica had been mounted on a small brass platform which in turn was mounted on a post in the vacuum evaporation unit, Pt was vaporized, first perpendicular to the replicated surface and then at an angle of 15°.

A 40 mil W filament bent to form a V, and containing approximately 25 mg of Pt at the apex of the V, is mounted in the heater assembly. The Lucite replica is mounted on the horizontal brass plate allowing a 2.0 inch specimen-to-filament distance. The bell jar is placed over the entire assembly and a vacuum of 10^{-5} mm of Hg is obtained. The Powerstat is advanced rapidly to 20 volts at which potential the Pt melts. As the

---

* Lucite was used instead of polystyrene because the latter tends to "craze."

potential is slowly increased to 30 volts the Pt begins to vaporize. The Powerstat is then raised to 40 volts over a period of 30 seconds. The entire evaporation requires about 60 seconds. When the unit has cooled, air is allowed into the system and the bell jar is removed. The entire operation is repeated once more with the specimen at an angle of 15° to a perpendicular drawn through the W filament.

After evaporation the excess Pt was removed with a cotton swab moistened with acetone and the surface was scored with a razor blade into 0.13 inch squares.

The Lucite was dissolved by immersing the sample in a solution of ethyl bromide containing 10% benzene. The films freed themselves from the Lucite 1 to 5 minutes after immersion. The undissolved Lucite was removed from the solution and most of the solution removed by suction. A fresh washing solution was recharged. After two hours, this solution was removed by suction and a fresh wash solution again added. After 2 more hours the films were picked up on 400 mesh stainless steel screens, placed on filter paper, covered with a Petri dish and allowed to dry under the heat from a light bulb. After drying, the specimens are ready to be mounted in the electron microscope.

The standard techniques were used in operating the electron microscope and in the processing of all film. All photographs reproduced in this report were photographed originally on Kodak Lantern Slide medium plates at a magnification of 6,500X and then enlarged to 13,000 diameters.

RESULTS AND DISCUSSION

While it is impractical to reproduce all the photographs taken, a few illustrating important results are shown in Figures 43 to 54.

These photographs illustrate very nicely the applicability of the method. In addition, they provide us with considerable evidence for believing the colloidal dispersion in the Ni phase is a dispersion of small particles of TiC. The minute grains are circled in the photomicrographs and can easily be seen to possess the general morphology and surface structure of the larger TiC grains. In addition, there is considerable evidence of disturbed Ni metal, indicating the necessity for a better method of specimen preparation.

The region within the square in Figure 53 is the dark grey phase within the circles in the photomicrographs in Section 1 of this report. Note that it is depressed below the surface of the surrounding carbide phase.

CONCLUSIONS

The two-step positive Pt replica method described in this report has been found to be rapid in its preparation and accurate in its portrayal of the original cermet microstructure. Improvements such as electropolishing the specimen and constructing an evaporation apparatus which would allow for the simultaneous evaporation of several specimens at different angles would improve the method considerably.

The colloidal dispersion in the Ni phase has been found to consist of finely divided particles of TiC. Worked Ni metal also contributes to the optical phenomenon observed.

One can theorize that the TiC was at one time in transport (diffusing through the Ni crystal lattice at high temperatures) and upon cooling precipitated out of the Ni-TiC saturated solution.

These results confirm the findings reported in Sections 1 and 2 of this report. As mentioned in these sections, a TiC cermet of improved high temperature strength could be fabricated by incorporating in the body a metallic phase which would be a poorer solvent for TiC. This would result in a marked decrease in grain coalescence and, as has been suggested, improved high temperature strength.

SECTION 4

COEFFICIENT OF EXPANSION STUDIES ON HIGH TEMPERATURE ALLOYS

INTRODUCTION

As mentioned in Section 2, the match between the thermal expansion curves for Ni and TiC is quite poor. This is shown in Figure 55. This suggests that the internal body strains in TiC-base cermets must be high, and that possibilities of altering this relationship favorably may exist. It is suspected that such improvement has been advantageously effected in the case of alumina-base cermets because the replacement of Cr with a Cr-Mo alloy as the metal phase has brought about physical property changes which could reasonably be attributed to a lower thermal expansion of the Cr-Mo alloy employed, relative to that of Cr. It is also thought that the Ni in a TiC-base cermet would be stressed in tension when cooled from the maturing temperature of the cermet because of the greater contraction of the Ni phase relative to the carbide phase. This condition of stress and apparent constraint indicates that a level of brittleness exists which might be lowered if an improved thermal expansion match between the phases can be effected. Although the resistance of carbide-base cermets to thermal shock is considered to be good, even if at times erratic, it presumably could be improved or made more consistent by improving the match between the thermal expansion curves for the two phases.

To attain the highest and most consistent resistance to thermal shock, it appears that the ideal binder metal in a cermet body should be one which has a coefficient of expansion (and contraction) equal to or slightly greater than that of the ceramic component. It should be stable throughout the range of use temperature anticipated, and be insensitive to the effects of interaction with the ceramic phase. This would seem to mean high bond strength between metal atoms and indicate the use of hard refractory metals or solid-solution alloys containing such metals in significant amounts. Multiple-phase alloys would seem incapable of improving the two-phase relationship in present carbide-base cermets for it would appear to amount to substituting one mismatch for another.

In many of the present low expansion alloys it is noted that a low expansion range exists from room temperature to a few hundred degrees above room temperature. Thereafter the expansion increases and the rate approximately parallels that for such metals as Fe, Ni, and Co. The temperature at which a rather abrupt change in the slope of the thermal expansion curve occurs, does not coincide with an inversion and, as a matter of fact, many low expanding alloys of this type are known to be solid solution alloys and to undergo no phase changes. Such behavior is described in general terms as being caused by metastability at low temperatures. Certain bond alteration, but not crystallographic alteration, is believed to coincide with the temperature of inflection which appears on thermal expansion curves.

MATERIALS

The following materials were used in the compositions covered in this section:

TiC - 325 mesh, free carbon 0.05% max, Norton Company, Worchester, Mass.

Fe - plastic Fe, Plastic Metals Co., Johnstown, Pa.

Ni - 98.0% + Ni, Charles Hardy, Inc., New York, N. Y.

Co - 98.0% + Co, Charles Hardy, Inc., New York, N. Y.

Cr - 99.0% + Cr, Charles Hardy, Inc., New York, N. Y.

Mo - C.P. Hydrogen Reduced, Charles Hardy, Inc., New York, N. Y.

COMPOSITIONS

The compositions discussed in this section are given, with their designation, in the following table:

TABLE XVIII

Batch Compositions of High Temperature Alloys

Designation	Component	Weight %
Fernico	Fe	54.0
	Ni	28.0
	Co	18.0
Fernichrome	Fe	37.0
	Ni	30.0
	Co	25.0
	Cr	8.0
T-420-G	TiC	70.0
	Fernico	30.0
T-520-G	TiC	70.0
	Fernichrome	30.0
T-1320-G	TiC	70.0
	Ni	10.0
	Cr	10.0
	Mo	10.0

Twelve alloy compositions in the Ni-Cr-Mo ternary system were prepared at 25% intervals (by weight) for thermal expansion studies.

PREPARATION OF BATCH

The compositions T-520-G, T-420-G, and T-1320-G were prepared in 500 gram batches by milling in one-quart steel mills. Co bonded WC slugs were used as grinding balls. Approximately 12 pounds of assorted slugs were used in each charge. Methanol was used as the vehicle and the milling time was 50 hours per batch.

After milling, the batches were air dried and granulated through a 42 mesh screen to prepare them for forming.

Fernichrome and Fernico compositions and the alloy compositions of the Ni-Cr-Mo ternary system were prepared by first dry blending the metal powders in porcelain mills using No. 2 solid rubber bottle stoppers as the ball charge. The batches were mixed for 16 hours. Five percent by weight of Carbowax was thoroughly mixed into the compositions as a binder and lubricant in the forming operation. The Carbowax was mixed into the compositions by first melting the wax at approximately 194°F and then hot mixing the powdered compositions with the liquid Carbowax. These mixtures were then granulated through a 42 mesh screen to prepare them for forming.

FORMING

Specimen Types

Specimens of the compositions T-420-G, T-520-G and T-1320-G were formed as bars 4.5 inches x 0.50 inch x 0.15 inch. Solid turbine nozzle diaphragm blades having the external shape of the J-35-A-13 blade were formed with compositions T-520-G and T-1320-G. Rods were formed, approximately 12.0 inches long and 0.50 inches in diameter, of the Ni-Cr-Mo ternary alloy system compositions and Fernichrome and Fernico alloys.

Operations

The bar specimens were formed by pressing between two punches, both being free to move with respect to a stripcase steel die. The die cavity of 4.5 inches x 0.50 inch controlled two of the dimensions of the bar. The thickness was controlled by the volume of the charge. Pressures ranged from 17,600 psi to 22,000 psi as determined by the highest useful pressures which would provide sufficient strength for handling without pressure cracks.

After the above preliminary forming the bars were placed in rubber envelopes, the envelopes evacuated to approximately one mm of Hg, and the bars repressed hydrostatically to 35,000 psi.

Turbine nozzle diaphragm blades were formed by hydrostatically pressing the cermet powders contained in a rubber envelope. The forming of the rough blanks was accomplished by (1) filling the rubber envelopes, held in a mold which conforms to the shape of the blade, (2) sealing the envelope with a rubber stopper through which a hypodermic needle was inserted, and (3) evacuating the envelopes through the hypodermic needle with a mechanical

pump. This evacuation gives the powder charge enough rigidity to retain its shape in handling.

Hydrostatic pressing at 35,000 psi produces a dense, machinable blank. The ends of the blank are cut square and mounted in the jig, "A", of the sanding drum assembly shown in Figure 56. The jig, "A", is essentially a clamp with faces having the shape of the airfoil section. With the blank in position, the sanding drum, "B", driven by a flexible shaft attached to the motor, "C", is guided by hand along the ends of the clamp, which serve as templates. The final forming of the blade is accomplished by moving the rotating sanding drum manually over the blank until it conforms to the airfoil templates. Compensation for shrinkage is accomplished by making the blade oversize.

The Ni-Cr-Mo alloys and Fernichrome and Fernico alloys were formed into rough rods by pressing hydrostatically the metal powders contained in a rubber envelope. The rough rods were pressed at 35,000 psi. The resultant rods were densely packed and had excellent green strength with the Carbowax binder. The rods were then dewaxed using a 48 hour schedule from room temperature to 275°F.

FIRING

Furnaces

The specimens containing TiC were fired in a vacuum induction furnace, Figure 57. The Ni-Cr-Mo alloys were fired in a Mo-wound gas-tight furnace. The furnace has a 2.0 inch ID and is described fully in ASTIA Report No. ATI 7516 dated May 15, 1947.

Atmosphere

The TiC specimens were fired in the induction furnace in a vacuum atmosphere on the order of 0.2-0.4 mm of Hg at the maturing temperature. This low vacuum was necessitated by the rapid firing schedule used in sintering the specimens.

The metal alloys were fired in the Mo resistance furnace in a purified hydrogen (H_2) atmosphere. The H_2 was passed through Cu turnings at 1000°F, through a tower of activated alumina and over calcium chips at 600°F. Titanium hydride (TiH_2) was used in the firing chamber as a source of Ti to serve as a getter. At red heat the hydride dissociates leaving finely divided Ti which has a great affinity for O_2.

Temperature

The firing temperatures for the T-420-G and T-520-G compositions were found to be essentially the same on the basis of the modulus of rupture tests at room temperature. The modulus of rupture determinations were made on bars sintered at 2700°F, 2800°F, and 2900°F. On the basis of the results shown in Tables XX and XXI, 2700°F is considered to be the optimum firing temperature for both compositions.

Although strength differences are small for the firing temperatures in the range 2700°F to 2900°F, indicating a wide sintering range, 2700°F was selected as the best of the three temperatures studied, because, other things being equal, a desirable minimum of grain growth would be expected at the lowest temperature.

Preliminary firings of the T-1320-G compositions were made but the firing temperature was not determined owing to the fact that the induction furnace was being used for another investigation phase of this project and was not available.

The alloys of the Ni-Cr-Mo ternary were fired to the various temperatures shown in the table below. The Fernichrome and Fernico alloy rods were fired to 2750°F.

TABLE XIX

Temperatures Used to Sinter Various Alloys of Ni-Cr-Mo Ternary

Designation	Composition, weight %	Temperature, °F	Remarks
1	25Cr-75Ni	2720	Fired above melt point
2	75Ni-25Mo	2660	" " " "
3	50Cr-50Ni	2720	" " " "
4	50Ni-50Mo	2560	" " " "
5	25Cr-50Ni-25Mo	2390	Sintered dense
6	75Cr-25Ni	2400	Slightly porous
7	25Ni-75Mo	2400	Sintered dense
8	50Cr-25Ni-25Mo	2400	" "
9	25Cr-25Ni-50Mo	2400	Slightly porous
10	50Cr-50Mo	3050	Sintered dense
11	75Cr-25Mo	3050	Sintered dense
12	25Cr-75Mo	3050	" "

Compositions 1, 2, 3, and 4 were fired above their melting points in suitably shaped refractory boats. This was necessary because the extremely short sintering range of the specimens prevented sintering a dense body without complete deformation of the specimen.

TESTING

Firing Shrinkage

Linear firing shrinkage was determined as the ratio of the length decrease to the green length expressed in percent. The firing shrinkages for compositions T-420-G and T-520-G are 14.0% and 13.0% respectively.

Thermal Expansion

ASTIA Report No. ATI 55703 dated December 15, 1948.
OSU Report No. 50, December 15, 1948.

The thermal expansion of TiC is shown in Figure 55. The equipment consists of a Globar-heated horizontal tube furnace with apertures through which observation of reference marks on the specimen can be made with a pair of filar-head microscopes. These are joined by a fixture of negligible thermal expansion at ordinary temperatures. Pt wires fixed in slots cut into the specimen are used as references for measurement of length changes as the furnace temperature changes. Apertures in the back of the furnace permit back illumination for visibility at low temperatures.

The thermal expansions of the laboratory prepared Fernichrome and Fernico alloy rods were measured using the same telescopic equipment as above, but using a furnace modification wherein a slotted bottom permitted weighted Pt wires attached to the specimen to hang below the furnace and serve as references for the measurement of expansion using the filar-heat telescopes. This modification, shown in Figure 58, is an improvement over the practice of putting the reference marks directly on the specimen in the furnace. The thermal expansion results for Fernico are shown in Figure 59 and for Fernichrome in Figure 60.

The thermal expansions of the T-420-G and T-520-G compositions and the Ni-Cr-Mo alloys were measured from room temperature to 1400°F. A fused quartz tube and dilatometer apparatus placed in a nichrome resistance furnace with a vertical firing chamber were used for these expansion determinations.

The thermal expansion curves for compositions T-420-G and T-520-G are shown in Figure 61. These curves are approximately the same as for TiC alone (also shown in Figure 61).

Figure 62 is a graphical representation of thermal expansion curves for Ni, TiC, and all the Ni-Cr-Mo alloys studied. It should be noted that the graph does not represent the actual difference in the magnitude of expansion of the alloys; only the order of magnitude of thermal expansion is shown. To eliminate the need for numerous graphs, complete curves from 75°F to 1400°F are not shown. The portions of the curves not shown on the graph do not indicate any inversions by reason of inflection points.

Figure 63 is a triaxial graph of the Ni-Cr-Mo ternary. The straight lines show the compositions of the various alloys. The contour lines show the thermal expansions from 75°F to 1400°F of the alloys studied. One graph is plotted on the composition basis of weight percent and the other on the basis of atomic percent. These graphs permit prediction of the thermal expansions of alloys in the ternary and, thereby, aid in selecting an alloy expansion of the TiC phase in a cermet.

Modulus of Rupture

Modulus of rupture was determined on T-420-G and T-520-G bar specimens at room temperature and at 2000°F. At room temperature the modulus of rupture of the specimens was determined using two ball supports on 3 inch

centers near the ends of the bar in order to eliminate torsion effects. A center load was applied through a clevis attached to a beam located below the supports, the coupling being effected through a universal linkage. A clevis pin applies a line load to the specimen. At 2000°F a Globar-heated furnace containing parallel silicon carbide (SiC) knife-edge supports located on 2.5 inch centers was used. These supports are 12.0 inches long and a number of specimens can be located on them. At the center of span between these supports, a SiC rod protruding through the top of the furnace is attached to a lever loading mechanism. The hot end of the rod has a rounded knife-edge contacting the specimen during loading. Lead shot loading and automatic shutoff devices are provided. The long lower supports facilitate alignment and permit one specimen after another to be positioned under the loading rod and broken during a single furnace heat. The modulus of rupture values are shown in the following tables.

TABLE XX

Modulus of Rupture Values
of Composition T-420-G

Firing Temperature, °F	Temperature of test, °F	Modulus of Rupture, psi
2700	75	103,300
2700	75	95,200
2800	75	93,300
2800	75	99,000
2900	75	97,300
2900	75	89,800
2700	2000	15,000
2700	2000	16,000
2700	2000	17,800

TABLE XXI

Modulus of Rupture Values
of Composition T-520-G

Firing Temperature, °F	Temperature of test, °F	Modulus of Rupture, psi
2700	75	105,000
2700	75	92,000
2800	75	97,000
2800	75	98,600
2900	75	88,000
2900	75	89,800
2700	2000	34,400
2700	2000	25,200
2700	2000	32,600

Oxidation Resistance

Oxidation behavior at 2000°F was evaluated to determine the suitability of T-420-G and T-520-G for high temperature use. Data are presented in Table XXII in terms of mg/cm^2 of weight gain due to the oxidation reaction. A value of K was determined for the expression $G^2=Kt$, where G is the weight gain in mg per cm^2, t is time in minutes, and K is a proportionality constant furnishing a measure of oxidation resistance. It should be noted that the expression applies to "parabolic oxidation" and presupposes that the rate at any instant is inversely proportional to the thickness of oxide, or the amount of oxide, G, coating the surface at time t. Curves of G^2 versus t are nearly straight lines, the small departure being attributable to decrease in the cermet-oxide interfacial area which is assumed to be constant in the above expression. The value of K is approximately 3.8 $mg^2/(cm^4 \times min.)$ for both T-420-G and T-520-G. This is quite high and indicates a low level of oxidation resistance. By way of comparison, K for TiC alone under the same oxidation conditions is 1.15.

TABLE XXII

Oxidation of 70 TiC-30 Fernico
and of 70 TiC-30 Fernichrome at 2000°F

Composition	Specimen Number	Weight gain, mg/cm^2		
		25 hrs	50 hrs	109.5 hrs
70 TiC-30 Fernico				
	2	80	120	160
	5	84	130	170
	6	84	130	170
70 TiC-30 Fernichrome				
	4	73	109	147
	5	79	119	160
	6	75	114	151

RESULTS AND DISCUSSION

The T-420-G and T-520-G cermets exhibited thermal expansion curves which approach the expansion of TiC. The modulus of rupture at 2000°F for these materials indicated a useful level of strength for stationary components. However, the oxidation resistance of these materials is low and for this reason further investigation and evaluation of the compositions was deemed unprofitable. In spite of this, two nozzle diaphragm blades of composition T-520-G (this composition exhibited approximately twice as much hot strength at 2000°F as did T-420-G) were fabricated to check the thermal shock resistance of a cermet with a relatively close expansion match of the hard and soft phases. However, lack of time prevented the firing of these blades and consequently thermal shock resistance data are not available for evaluation.

Composition T-1320-G, 70 TiC-10 Mo-10 Ni-10 Cr, was selected for further study on the basis of the thermal expansion studies of the Ni-Cr-Mo ternary system and an estimate of the alloys suitability as a binder phase for TiC (i.e., oxidation resistance, wettability, etc). Bar specimens and two nozzle diaphragm blades of this composition were prepared. Only preliminary firings of the bars were made along with specimens from another phase of this contract work. No data which could be evaluated were obtained from these firings. This work was discontinued in favor of the high Ni-TiC firing behavior study which required the vacuum induction furnace equipment. The contract terminated before the induction furnace could be made available for study of the firing behavior of the T-1320-G compositions.

SECTION 5

PREPARATION OF HIGH Ni-LOW TiC CERMETS FOR IMPACT AND THERMAL SHOCK STUDIES

INTRODUCTION

TiC-Ni cermet compositions containing 60 to 90% Ni by volume were to be investigated and evaluated for impact strength and thermal shock resistance. It was anticipated that high temperature strength, which is low in Ni, would be improved by addition of small percentages of a hard phase, TiC. Thermal shock resistance and impact resistance was also expected to be improved by the high Ni content. The following section describes the work that has been accomplished to date in testing and evaluating these high-Ni compositions.

MATERIALS

The materials used for this phase of the investigation were:

TiC - minus 325 mesh powder, free carbon 0.05% max, Norton Company, Worchester, Mass.

Ni - 98.0% + Ni, minus 325 mesh powder, Charles Hardy Inc., New York, N.Y.

COMPOSITIONS

The compositions discussed in this section are given, with their designations, in Table XXIII.

PREPARATION OF BATCH

All the compositions were prepared in approximately 500 gram batches by milling in quart capacity steel mills. The milling time was 50 hours. Co bonded WC slugs of various sizes, 0.75 inch x 0.75 inch, 1.0 inch, and 1.5 inch in length, were used as grinding balls. Approximately 12 pounds of slugs were used in each charge. Methanol was used as the vehicle.

After milling, the batches were air dried and granulated through a 42 mesh screen. Preliminary pressing tests indicated that a binder would be necessary.

Approximately 3 percent camphor was used as the binder. A solution of camphor and ether was prepared and the batch materials were thoroughly mixed into the solution. The mixture was stirred until the ether had completely volatilized. The material was then granulated through a 42 mesh screen in preparation for forming.

TABLE XXIII

Batch Compositions of High Ni-Low TiC Cermets

Designation	Components	Weight %	Volume %
T-46.3-G	TiC	26.9	40.0
	Ni	73.1	60.0
T-47.1-G	TiC	19.1	30.0
	Ni	80.9	70.0
T-47.8-G	TiC	12.1	20.0
	Ni	87.9	80.0
T-48.4-G	TiC	5.8	10.0
	Ni	94.2	90.0

FORMING

Specimen Types

Specimens were formed as bars, 4.5 inches by 0.50 inch by 0.15 and 0.22 inch thick, and as turbine nozzle-diaphragm blades which are solid and have an external shape of the J-35-A13 type blade.

Operations

Bar specimens were formed by pressing between two punches, both being free to move with respect to a strip case steel die. The die cavity of 4.5 inches by 0.50 inch controlled two dimension of the bar. The thickness was controlled by the volume of the charge. Pressure used was approximately 22,000 psi which provided good handling strength without pressure cracks.

After this initial forming, the bars were placed in rubber envelopes evacuated to approximately 1 mm of Hg and repressed hydrostatically to 35,000 psi. The resultant specimens are dense and have good handling strength. The binder, camphor, was removed by heating the bars to 240°F for approximately 8 hours in a small drier.

Turbine nozzle-blades were roughly formed by direct hydrostatic pressing of powder contained in a rubber envelope. The blank was formed by (1) filling the rubber envelopes held in a mold which conforms to the shape of the blade, (2) sealing the envelope with a rubber stopper through which a hypodermic needle was inserted and (3) evacuating the envelopes with a mechanical pump through the hypodermic needle. This evacuation gives the blank sufficient rigidity to retain its shape in handling.

Hydrostatic pressing at 35,000 psi produces a binder-free, dense, machineable blank. The ends of the blank are cut square and mounted into the jig, "A", of the sanding drum assembly shown in Figure 56. The jig, "A", is essentially a clamp with faces having the shape of the air foil section. With the blank in position, the sanding drum, "B", driven by a flexible shaft attached to the motor, "C", is guided by hand along the ends of the clamp, which serve as templates. The final forming of the blade is accomplished by moving the rotating sanding drum manually over the blank until it conforms to the airfoil template. Compensation for shrinkage is accomplished by making the blade oversize.

FIRING

Furnace

The induction furnace consists of a 14 inch induction coil which is energized by a 50 KW generator. The specimens are placed on a graphite pallet inside a graphite crucible which has a 7-inch ID, 8-inch OD and is 14 inches in height. The crucible is insulated with lamp black, which is retained in the coil cavity with a sheet of mica inside of the coil and a sheet of thin asbestos next to the mica.

The coil and the crucible are encased in a gas-tight water-cooled brass case.

An optical pyrometer is used to measure temperature through a glass-covered sight hole in the brass-case cover and a sight tube in the graphite crucible cover. Temperature control is accomplished manually by adjusting the power input to the induction coil.

At room temperature a vacuum of 3×10^{-5} mm of Hg is attained by using a mechanical forepump in conjunction with an oil diffusion pump. Using an 8 hour firing cycle to 2400°F the vacuum can be held at less than 25×10^{-3} mm of Hg.

Atmosphere

The firing atmosphere employed in the firing of all specimens was a vacuum below 0.1 mm of Hg.

Temperatures

The optimum firing temperatures of the various compositions were found to be in the range of 2330°F to 2360°F. However, the sintering ranges of the compositions are extremely short, from 5°F to 10°F. The firing temperature was not determined for each composition, owing to the extremely short sintering range coupled with the high reactivity of the compositions with the setting refractories.

Discussion

In the preliminary firings temperatures from 2400°F to 2600°F were tried. Most of the specimens formed low melting eutectic liquids by reaction with the setting refractories and were destroyed. This problem of maintaining shape when the metal undergoes incipient fusion is a common one in the firing of cermets having high metal contents and low contents of primary refractory grain to maintain shape.

Various materials were used in an attempt to eliminate these reactions. The first of the materials was TiH_2. A slip of TiH_2 was applied in a thin layer on a graphite pallet. This pallet was then fired to 2700°F in a vacuum. Upon firing, the TiH_2 dissociates and the Ti metal reacts with the graphite pallet leaving a thin layer of TiC as the setting surface. When this pallet was used to fire specimens to 2400°F, the Ni in the specimens diffused into the porous TiC shell, forming a eutectic melt with the underlying graphite and destroying the specimens.

Using thin pressed TiC strips as the setting refractory looked promising at 2400°F as no reaction was noted after the first firing. However, these initial specimens were porous. Subsequent firings at and above 2400°F yielded specimens in which metallic Ni migrated to the surface of the specimen bars and diffused into the TiC setting strips. These specimens exhibited porosities which varied from one end of the bar to the other. This porosity is believed to be caused by oxidation of the TiC in the specimens, due to a poor vacuum caused by the outgassing of absorbed gases during heating. This oxidation reaction caused the formation of titanium oxides which increased the refractoriness of the specimens and reduced the wettability of the TiC by the Ni. This is believed to facilitate Ni migration to the surface of the specimens and its diffusion into the setting media.

Granular graphite formed a low melting eutectic liquid with Ni when fired to 2400°F. The specimens were destroyed and on the basis of this test the material was deemed unsuitable.

Other materials, which proved to be unsuitable owing to their reactivity with the Ni phase, were boron carbide (B_4C), titanium diboride (TiB_2), SiC and Ti metal. These materials were tested at temperatures between 2300°F and 2600°F.

As the firings continued it became evident that the vacuum atmosphere must be kept below 25 microns to insure that the desirable eutectics between the Ni and TiC in the specimens are not precluded by the oxidation of the TiC phase. This was expected to lower the sintering temperatures for densification which were indicated in the preliminary firings.

In the more recent firings, during which more emphasis was placed on the maintenance of high vacuum, it was decided to test high purity electrically fused alumina as a setting medium because Ni does not readily wet this compound. This, however, was done reluctantly because past experience with alumina had shown that this material reduces in a high vacuum in contact with graphite. To eliminate contact of the alumina grains with the graphite

a small pan of Mo was fabricated to hold the alumina grains and the cermet specimens were in turn placed on the grains. Using this technique no difficulty due to the reduction of the alumina was encountered. However, a slight reaction between the alumina grains is noted on specimens fired above 2325°F. This reaction was not destructive and can be tolerated. At temperatures in the order of 2365°F and above, the specimens were over-fired and destroyed.

TESTING

Firing Shrinkage

Linear firing shrinkage was determined as the ratio of the length decrease to the green length expressed in percent. Firing shrinkages at the various temperatures are shown in Tables XXIV to XXVII.

Porosity

Porosity of the specimens was determined by first weighing the bars dry, boiling the specimens in water for five hours or more, and obtaining suspended weights and saturated weights. The percent porosity calculated from these data is shown in Tables XXIV to XXVII.

Modulus of Rupture

Modulus of rupture determinations were made at room temperature and at 1800°F. This was accomplished at room temperature using two ball supports on 3 inch centers near the ends of the bar to eliminate torsion effects. A center load was applied through a clevis which is attached to a beam below the loading supports with a universal linkage. At 1800°F a Globar-heated furnace containing parallel SiC knife-edge supports located on 2.5 inch centers was used. These lower supports are 12 inches long and a number of specimens can be located on them. At the center of span between the supports, A SiC rod protruding through the top of the furnace is attached to a lever loading mechanism. The hot end of the rod has a rounded knife edge which contacts the specimen during loading. Shot loading and automatic shutoff are provided. The use of the long lower knife edges facilitates alignment and permits one specimen after another to be positioned under the loading rod and broken during a single furnace heat. See Figure 64. Modulus of rupture values for the various compositions are given in Table XXIV to XXVII.

TABLE XXIV

Physical Data of Composition T-46.3-G

Specimen Number	Firing Temperature °F	Soak, Hours	Linear Firing Shrinkage, o/o	Apparent Porosity, o/o	Modulus of Rupture, psi
1	2330	1.0	14.3	0.1	188,000
2	2330	1.0	14.0	0.1	199,000
3	2340	1.0	8.8	14.2	91,000
4	2340	1.0	9.2	12.6	93,000
5	2340	1.0	9.3	17.7	65,000
6	2325	1.5	9.9	8.4	23,000*
7	2325	1.5	9.7	8.8	24,000*
8	2325	1.5	9.7	13.8	93,000
9	2310	1.0	7.9	17.8	80,000
10	2325	1.5	9.3	13.7	87,000
12	2345	1.0	12.1	0.8	24,000*
13	2345	1.0	12.2	1.1	25,000*
14	2345	1.0	12.2	1.4	143,000
15	2310	1.0	8.0	17.9	79,000
16	2345	1.0	11.6	0.5	153,000
17	2350	1.0	9.6	13.5	113,000
18	2350	1.0	9.3	12.1	20,000*
19	2350	1.0	9.8	11.6	21,000
20	2310	1.0	8.0	17.3	84,000
21	2340	1.0	10.3	8.8	124,000
22	2340	1.0	10.1	6.0	134,000
23	2340	1.0	10.2	5.2	140,000
24	2340	1.0	10.5	0.7	149,000
26	2340	1.0	10.6	0.3	169,000
27	2340	1.0	10.6	0.7	164,000

* Modulus of rupture at 1800°F

TABLE XXV

Physical Data of Composition T-47.1-G

Specimen Number	Firing Temperature, °F	Soak, Hours	Linear Firing Shrinkage, o/o	Apparent Porosity, o/o	Modulus of Rupture, psi
1	2330	1.0	10.2	7.0	135,000
2	2330	1.0	10.3	6.8	143,000
3	2310	1.0	9.2	15.8	105,000
4	2340	1.0	8.4	15.8	86,000
5	2340	1.0	8.6	15.6	82,000
6	2340	1.0	8.4	15.9	82,000
7	2325	1.5	8.6	15.2	88,000
8	2310	1.0	6.7	19.8	77,000
9	2325	1.5	8.9	12.0	17,000*
10	2325	1.5	8.9	14.1	100,000
11	2325	1.0	8.8	10.5	18,000*
12	2345	1.0	11.5	1.3	22,000*
13	2310	1.0	7.0	19.2	78,000
14	2345	1.0	11.5	0.3	24,000*
15	2345	1.0	11.8	0.9	143,000
16	2345	1.0	11.5	0.8	135,000
17	2350	1.0	8.5	13.3	17,000*
18	2350	1.0	8.6	14.2	17,000*
19	2350	1.0	8.6	15.7	88,000
20	2350	1.0	8.6	16.4	84,000
21	2340	1.0	10.5	12.4	149,500
22	2340	1.0	10.7	7.8	135,000

* Modulus of rupture at 1800°F

TABLE XXVI

Physical Data of Composition T-47.8-G

Specimen Number	Firing Temperature °F	Soak, Hours	Linear Firing Shrinkage, o/o	Apparent Porosity, o/o	Modulus of Rupture, psi
1	2330	1.0	9.8	0.1	102,000
2	2330	1.0	8.6	0.7	87,000
3	2340	1.0	8.9	0.2	121,000
4	2340	1.0	8.6	1.6	72,000
5	2340	1.0	9.3	0.4	86,000
6	2325	1.5	11.4	11.8	17,000*
7	2325	1.5	9.5	0.4	85,000
8	2325	1.5	10.6	3.5	17,000*
10	2310	1.0	8.2	8.7	90,000
11	2310	1.0	6.9	25.7	83,000
12	2310	1.0	7.8	13.0	86,000
13	2325	1.5	8.1	13.6	89,000
14	2345	1.0	10.4	1.1	18,000*
15	2345	1.0	11.0	0.5	20,000*
16	2345	1.0	10.7	0.5	113,000
17	2350	1.0	8.6	11.9	17,000*
18	2350	1.0	8.1	12.2	15,000*
19	2350	1.0	8.4	12.7	151,000
20	2350	1.0	8.7	10.9	93,000
23	2340	1.0	7.0	18.6	85,000
24	2340	1.0	7.0	18.3	80,500
27	2340	1.0	6.8	19.2	79,700
28	2340	1.0	7.0	19.1	74,000

* Modulus of rupture at 1800°F

TABLE XXVII

Physical Data of Composition T-48.4-G

Specimen Number	Firing Temperature, °F	Soak, Hours	Linear Firing Shrinkage, o/o	Apparent Porosity, o/o	Modulus of Rupture, psi
2	2330	1.0	6.7	16.1	51,000
3	2330	1.0	6.7	16.2	60,000
6	2310	1.0	5.3	17.2	61,000
7	2310	1.0	5.5	17.6	52,000
10	2310	1.0	5.0	18.7	51,000
11	2340	1.0	6.5	14.6	56,000
12	2340	1.0	7.1	13.9	53,000
13	2340	1.0	6.4	13.7	66,000
14	2325	1.5	6.1	15.6	9,000*
16	2325	1.5	6.3	14.3	10,000*
17	2325	1.5	6.3	16.6	50,000
18	2325	1.5	8.7	4.1	59,000
19	2345	1.0	10.9	0.7	19,000*
20	2345	1.0	10.5	0.3	17,000
21	2345	1.0	11.0	0.2	86,000
22	2350	1.0	6.4	14.3	12,000*
23	2350	1.0	6.7	13.6	20,000*
25	2350	1.0	6.8	15.2	56,000
26	2350	1.0	6.3	16.7	51,000

* Modulus of rupture at 1800°F

Impact Strength

A limited amount of impact strength testing was accomplished. However, the difficulties encountered in the firing of specimens prevented the production of entirely satisfactory impact specimens. An impact tester, Figure 65, similar to the NACA design was used. The tester consists mainly of a specimen holder, an impact hammer, an electromagnet to position and hold the hammer, and a device to adjust the height of the electromagnet and hammer in order to deliver various desired impact loads to the specimens. The values obtained are in inch-pounds to break a 1 inch cantilever specimen struck 0.88 inch from the supported end.

Composition T-46.3-G, specimen Nos. 1 and 2, gave a mean impact strength value of 10.4 inch-pounds. Composition T-47.1-G, specimen Nos. 1, 2, and 3 gave a mean value of 7.5 inch-pounds. Composition T-47.8-G, specimen Nos. 13, 15 and 16, gave a mean value of 10.2 inch-pounds. Composition T-48.4-G is too ductile to be tested for impact on this type of apparatus. Reliability of these data is doubtful and they are given only as an indication of the impact strength values of these compositions.

Thermal Shock

Thermal shock testing was to be carried out at WADC laboratories with turbine nozzle diaphragm blades under similar conditions. These blades were pressed but difficulties encountered in determining the optimum sintering temperatures of the compositions prevented the sintering and finishing of the blades for testing before the termination of the contract.

RESULTS AND DISCUSSION

Firing behavior tests are incomplete and therefore results of the experimentation are inconclusive. Preliminary firings presented a contact refractory problem which destroyed most of the specimens. There was not sufficient time for completion of experiments to evaluate fully the properties of the high Ni compositions.

The data obtained indicate that the T-46.3-G composition, sintered completely dense, should have a modulus of rupture value in the order of 200,000 psi at room temperature and in the order of 25,000 to 30,000 psi at 1800°F. Impact resistance, also with completely dense specimens, at room temperature on the modified NACA design impact apparatus should be approximately 14.0 inch-pounds. However, these are only indications based on data obtained from specimens which were not sintered dense, and more experimentation would be required to substantiate these indications. Indications based on the physical data obtained for the other compositions show modulus of rupture values in the order of 170,000 psi for modulus of rupture values in the order of 170,000 psi for T-47.1-T, 150,000 psi for T-47.8-G, and 100,000 psi for T-48.4-G, at room temperature. At 1800°F the modulus of rupture may be expected to approximate 25,000 psi for T-47.1-G, 20,000 psi for T-47.8-G, and 18,000 psi for T-48.4-G. Impact strength for all the compositions should be excellent. It should be remembered that more work is required to support the above interpretation of limited data.

SECTION 6

INVESTIGATION OF TiB_2 AND $MoSi_2$ AS THE CERAMIC COMPONENT OF A CERMET

INTRODUCTION

A new high-temperature[33] material with excellent stress-sustaining characteristics at 1800°F and designated composition III-B, has been discussed in detail in WADC Technical Report 53-287. It was mentioned in this report that the material was very brittle because of the absence of a ductile metallic phase. Continued research was therefore directed toward the development of a new high temperature material possessing the desired properties.

The information obtained from the research and development of cermet III-B was utilized. This information was two-fold, viz:

1. Oxidation resistance can be achieved by introducing boron (B) and silicon (Si) in the cermet body in such proportions that upon oxidation of the cermet an impervious borosilicate surface layer will be produced.

2. The reason for the excellent flat stress-rupture curve of cermet III-B (see Figure 1) is not definitely known; however, based on the microstructures of samples heated for 2700 hours at 1800°F it is believed that there is no chemical or physical change taking place with time within this cermet, although it contains TiC and Co, and Co is believed to have a greater solubility for TiC than Ni. This, of course, is in marked contrast with TiC base cermets bonded with pure metals. As a consequence, TiC bonded with a pure metal will not produce a flat stress rupture curve. Although it may be possible to alter this situation by using alloys or intermetallic compounds to bond TiC, the resultant material would be considerably more brittle than TiC bonded with pure metals and would be similar to cermet III-B in this respect. We therefore, planned to change the refractory phase partially or entirely. TiB_2 and $MoSi_2$ were the first to be considered for the new refractory phase.

On the assumption that B and Si must be introduced into the cermet to provide oxidation resistance, experimentation was first initiated to study the effect of B and Si on the binder metal. Because of the high chemical and thermal stability of TiB_2, this compound was chosen as the agent to introduce B into the cermet. Si was introduced in the elemental form, or as $MoSi_2$.

MATERIALS

The following materials were used in compositions in this section:

Cr - Electrolytic process, minus 325 mesh, 99% minimum Cr content, Charles Hardy, Inc., New York, N.Y.

Co - 98.0% + Co, Charles Hardy, Inc., New York, N. Y.

Ni - Minus 300 mesh, 98% + Ni, Charles Hardy, Inc., New York, N. Y.

Fe - Plastic Fe, Plastic Metals Co., Johnstown, Penn.

Si - Minus 300 mesh, 97% Si, Charles Hardy, Inc., New York, N. Y.

$MoSi_2$ - Minus 100 mesh containing 63.44% Mo, 36.45% Si, 0.17% impurities, Electro Metallurgical Division of Union Carbide and Carbon Corporation.

TiB_2 - Minus 20 mesh containing 66.51% Ti, 31.1% B, 1.7% total C, 0.69% minor impurities (1.2% estimated free C), Norton Company, Worchester, Mass.

COMPOSITIONS

The following compositions discussed in this section are given in Table XXVIII.

PREPARATION OF BATCH

The compositions were prepared by milling 500 gram batches in one-quart capacity steel mills. Co bonded WC slugs were used as the grinding medium. Benzene was used as the vehicle.

After milling, the batches were dried in an oven and granulated through a 65 mesh screen to prepare them for forming.

FORMING

Bar specimens were formed by pressing between two punches, both being free to move with respect to a stropcase steel die. The die cavity of 4.5 inches by 0.50 inches controlled two dimensions of the bar. Pressures ranged between 10,000 psi and 14,000 psi.

After this initial forming the bars were placed in rubber envelopes, evacuated to approximately 1mm of Hg and re-pressed hydrostatically to 35,000 psi.

FIRING

The bars were fired under a purified He atmosphere in a furnace consisting of a gastight refractory procelain tube heated within a tubular Globar element surrounded by suitable insulating refractories[34]. They were heated at the rate of approximately 400°F per hour to the soaking temperature, and this temperature was maintained for one hour.

TABLE XXVIII

Batch Compositions of TiB_2 and $MoSi_2$ Cermets

Designation	Component	Weight %
1	Fe	71.5
	Ni	15.1
	TiB_2	8.6
	Si	4.8
2	Fe	76.5
	Ni	10.1
	TiB_2	8.6
	Si	4.8
3	Fe	95.0
	$MoSi_2$	5.0
4	Fe	70.0
	$MoSi_2$	30.0
5	Fe	50.0
	$MoSi_2$	50.0
6	Fe	80.1
	Ni	15.1
	Si	4.8
7	Fe	85.0
	Ni	10.1
	Si	4.8
8	Fe	85.1
	Si	48.0
	Co	10.1
9	Fe	95.0
	Si	5.0
10	Fe	90.0
	Si	10.0
11	Fe	86.6
	TiB_2	8.6
	Si	4.8
12	TiB_2	65.0
	Fe	33.2
	Si	1.8

TABLE XXVIII (continued)

Designation	Component	Weight %
13	TiB_2	75.0
	Fe	25.0
14	Fe	75.0
	TiB_2	25.0
15	III-B	50.0
	Co	50.0
16	III-B	80.0
	Co	20.0
17	III-B	80.0
	Ni	20.0
18	(95 TiB_2 + 5 $MoSi_2$)	70.0
	Fe	30.0
19	Co	70.0
	(95 TiB_2 + 5 $MoSi_2$)	30.0
20	(95 TiB_2 + 5 $MoSi_2$)	70.0
	Ni	30.0
21	(95 TiB_2 + 5 $MoSi_2$)	60.0
	Ni	40.0
22	(95 TiB_2 + 5 $MoSi_2$)	70.0
	Co	30.0
23	(95 TiB_2 + 5 $MoSi_2$)	70.0
	Cr	30.0

TESTING

Modulus of Rupture

The apparatus is described and the necessary calculations to be performed are given in Section 4 of this report.

Oxidation Resistance

The oxidation resistance of samples was determined using a small bar specimen. The weight gain calculated in grams per square centimeter for a 24 hour exposure to air in an electrically heated laboratory furnace held at 2000°F was used as the parameter for evaluating the data.

RESULTS AND DISCUSSION

The results of the firings and various tests are listed below:

Number	Result
1	Weak porous structures with a considerable amount of the composition sweating out at 2450°F.
2	Same as Composition 1.
3	Strong and very ductile, a bar may be bent almost in half without breaking. 2450°F is just below fusion of this composition. Poor oxidation resistance.
4	Completely fused at 2450°F.
5	Porous and weak at 2500°F.
6	Strong but porous. Fired to 2450°F.
7	Strong, porous and ductile. Fired to 2450°F. Poor oxidation resistance.
8	Same as Composition 5.
9	Same as Composition 5.
10	Brittle; metal sweating out at 2450°F.
11	Same as Composition 1. Poor oxidation resistance.
12	Sweated out at 2450°F.

Number	Result
13	Porous and weak; underfired at 2450°F.
14	Porous and weak with metal sweating out at 2200°F.
15	Sweated out at 2200°F.
16	Sweated out at 2700°F but underfired at 2600°F.
17	Sweated out at 2200°F.
18	Very brittle. Slightly porous at 2700°F. Oxidation resistance fair at 2000°F. Room temperature modulus of rupture = 36,000 psi.
19	Sweated out at 2200°F.
20	Dense at 2850°F and 3000°F. Very brittle but good oxidation resistance. Modulus of rupture at room temperature = 45,000 psi. Fired to 2850°F. Modulus of rupture at room temperature = 33,000 psi. Fired to 3000°F.
21	Dense and considerably less brittle than No. 20 and 22. Modulus of rupture at room temperature = 38,000 psi. Fired to 2600°F.
22	Dense but very brittle. Good oxidation resistance. Modulus of rupture at room temperature = 42,000 psi. Fired to 2850°F. Modulus of rupture at room temperature = 30,000 psi. Fired to 3000°F.
23	Underfired at 2850°F. Underfired at 3000°F.

The results indicate that 5% Si can be added to Fe or high Fe-Ni-Co alloy to produce a strong ductile alloy. A content of 10% Si will embrittle Fe, and more than a 5% addition of $MoSi_2$ will lower the melting temperature of Fe below 2450°F. The sweating out of metal in the compositions containing small amounts of TiB_2 substantiate the low melting eutectic of 1174°C (2145°F) as indicated in the B-Fe phase diagram in the Metals Handbook[35]. Although this diagram is incomplete, application of the available data to a TiB_2-Fe diagram indicates that greater than 38% Fe with TiB_2 will result in this low temperature eutectic.

Using the entire composition of III-B as a base, we have tried adding additional Co in an effort to get some ductile metal into the sintered product and thus improve its resistance to heat shock. This does appear promising. With 20% additional Co the composition is still underfired at 2600°F and Co begins to sweat out at 2700°F. If it can be fired dense at all, the sintering range will be very narrow. Sample No. 16 indicates that with additions of Co greater than 20%, sweating out will occur at as low a temperature as 2200°F.

The refractory base 95% TiB_2 + 5.0% $MoSi_2$ can be metal bonded with 30% of Fe, Ni, or Co. The oxidation resistance is fair in the case of Fe and good with Ni or Co. Sample No. 21 with 40% of Ni by weight looks more promising. It sinters dense at 2600°F, it is quite oxidation resistant, the modulus of rupture is fair, and it is considerably less brittle than the other compositions.

CONCLUSIONS

While it is indicated from the above results that a cermet of composition 50% (95 TiB_2 + 5 $MoSi_2$) plus 50% Ni might offer good oxidation resistance, have reasonably good high temperature strength, and be less brittle than cermet III-B, the bodies containing silicides are still more brittle than can be tolerated at the present time.

Therefore, it was recommended that research on the above phase of this project be discontinued.

SECTION 7

STUDY OF THE EFFECT OF HEAT TREATMENT ON IMPACT STRENGTH OF K-151-A AND K-151-B

INTRODUCTION

Heat treatment of some cermets may have an effect on certain properties such as rupture strength, thermal shock resistance, and impact strength by inducing changes in the microstructure. This section is concerned with the heat treatment effect on the impact strength of Kennametal compositions K-151-A and K-151-B. It is realized that these materials are deficient in impact strength but it was hoped that an insight into the effect of treatment on this property might result from limited study.

No effort was made to study changes in microstructure of the specimens before and after heat treatment.

MATERIALS AND COMPOSITIONS

The specimens are commercial compositions obtained from Kennametal Inc., Latrobe, Pennsylvania. These compositions are listed in Table XXIX.

TABLE XXIX

Batch Compositions of K-151-A and K-151-B

Designation	Component	Weight %
K-151-A	TiC	65.0
	SS*(TiC,NbC,TaC)	15.0
	Ni	20.0
K-151-B	TiC	72.0
	SS*(TiC,NbC,TaC)	8.0
	Ni	20.0

SS* - Solid Solution

The specimens for testing measured 0.19 inch x 0.19 inch x 1.5 inches.

EQUIPMENT AND PROCEDURE

Furnaces

The furnaces used for the heat treatment were both of the electric Globar type with automatic temperature regulation. One furnace consisted of a firing chamber containing an impervious porcelain tube, 3.0 inches ID with a 0.38 inch wall. This tube furnace was used to heat treat specimens in a flowing He atmosphere. The furnace used to treat specimens in air was also a Globar-heated type.

Heat Treatment

All bars which were to be heat treated were weighed and marked. Six specimens of each composition were charged into the atmosphere furnace. The furnace was evacuated with a mechanical vacuum pump to 0.3 mm of Hg and then flooded with He. This procedure was repeated twice and then a continuous stream of He was allowed to flow into the firing chamber during the heating cycle. Heat treatment in this atmosphere was for 140 hours at 1700°F, after which the furnace and specimens were allowed to cool to room temperature.

Six weighed specimens of each composition were charged into the Globar furnace without the atmosphere control. These specimens were treated in air for 140 hours at 1700°F and were then allowed te cool to room temperature while in the furnace.

TESTING

Oxidation

Oxidation is shown as the ratio of the weight gain in heating to the original specimen weight shown in percent. This is shown in Tables XXX and XXXI.

Impact

Impact testing was accomplished on an impact testing apparatus, Figure 65, built in this laboratory and similar to the National Advisory Committee for Aeronautics design. The apparatus consists primarily of a specimen holder, a 0.4 pound impact hammer, an electromagnet to hold and position the hammer, an arrangement to adjust the height of drop of the hammer, and a scale to show the height of drop.

Impact strength is shown in inch-pounds. The data can be found in Tables XXX and XXXI.

TABLE XXX

Impact Strength Data of K-151-A Specimens Heat-Treated and Untreated and Oxidation Weight Gain

Specimen Number	Impact Strength, Inch-lbs			Oxidation Weight gain, %
	Untreated	Treated in air	Treated in He	
1	3.7			
2	3.6			
3	3.4			
4	3.6			
5	3.4			
6	3.4			
7	3.5			
8	4.2			
9	4.2			
10		2.6		0.76
11		2.4		0.67
12		2.2		0.68
13		2.3		0.75
14		2.4		0.72
15		2.6		0.74
16			2.1	0.32
17			2.3	0.39
18			2.8	0.41
19			2.0	0.41
20			2.3	0.44
21			2.3	0.38

TABLE XXXI

Impact Strength Data of K-151-B Specimens Heat-Treated and Untreated and Oxidation Weight Gain

Specimen Number	Impact Strength, Inch-lbs.			Oxidation Weight Gain, %
	Untreated	Treated in Air	Treated in He	
1	5.6			
2	5.4			
3	5.2			
4	3.8			
5	4.0			
6	4.6			
7	5.0			
8	5.6			
9	5.8			
10		2.0		1.10
11		2.0		1.03
12		1.9		1.11
13		2.0		1.11
14		1.9		1.12
15		2.0		1.08
16			1.8	0.73
17			1.9	0.73
18			1.7	0.74
19			1.5	0.79
20			1.6	0.67
21			2.1	0.84

RESULTS AND DISCUSSION

In the case of both compositions K-151-A and K-151-B, heat treatment does have a detrimental effect on impact strength. This loss of impact strength may be attributed to the effect of oxidation on the specimens and/or the effect of the heat treatment on the microstructure.

Some of the oxidation effects may be summarized as follows:

1. Thickness and the physical and compositional character of the oxide layer.

2. Preferential oxidation of phases which may or may not be correlated with partial pressures of O_2. (For example, reduced partial pressure of the O_2 may facilitate oxidation of carbide phases rather than of the Ni phase.)

3. Oxidation along grain boundaries of the cermet structure.

Any of these oxidation phenomena can result in the formation of stress risers on the surface of the cermets and thereby reduce impact strength. As an example of category number "1", a relatively dense adherent oxide coating with voids at the metal: oxide interface may result in stress risers. An example of categories number "2" and "3" is the formation of small surface notches, stress risers, due to preferential or grain boundary oxidation. Another consideration of the effect of oxidation on the impact strength of the specimen is the reduction of the effective cross-sectional area which can resist impact stresses.

In comparing the loss of impact strength of the two compositions, approximately 65% for K-151-B compared to 36% for K-151-A, would indicate that the extent of oxidation is the factor in explaining the strength decrement, since the K-151-B displayed the greater extent of oxidation and is known to be more oxidation sensitive. However, comparing oxidation extent to impact strength loss of the specimens of both compositions individually, the specimens which were heat treated in He exhibited a slightly greater decrement of strength than the specimens which were heat treated in air. This would indicate that the type of oxidation, rather than the extent of oxidation, or the heat treatment effect on the microstructure, may be important factors which should be considered in this decrement of impact strength.

In considering the effect of microstructure changes due to the treatment at 1700°F for 140 hours, reference should be made to Section 1 of this report. The data from this microstructure study show that no detectable changes in microstructure could be found in this type of cermet after heat treatment at 2000°F for time periods up to and including 300 hours. Therefore, it would seem safe to assume that the loss of impact strength is due to one or more oxidation effects and not to microstructure changes.

CONCLUSION

Heat treatment of Kentanium compositions K-151-A and K-151-B at 1700°F for 140 hours in atmospheres which permit oxidation of the order encountered in these tests is detrimental to the impact strength of these cermets.

REFERENCES

1. Wyman, L. L. and Kelley, F. D. Cemented Tungsten Carbide; A Study of the Action of the Cementing Materials. Australian Society of Mining and Metallurgical Engineers. Volume 93, 1931, p 208.

2. Meerson, G. A., Zverev, G. L. and Osinovskaya, B.Ye. Investigation of the Behavior of Titanium Carbide in Cemented Carbide Alloys. Zhurnal Prikladnoi Khimil. Volume 13, No. 1, 1940, pp 66-75. Translated by Henry Brutcher, Inc., Altadena, California.

3. Skaupy, F. Cemented Carbides, Considered from the Viewpoint of Dispersoid Chemistry. Communication No. 1, Kolloid Zeitschrift, Volume 98, 1942, pp 92-95. Translated by Henry Brutcher, Inc., Altadena, California.

4. Skaupy, F. Communication No. 2, Kolloid Zeitschrift. Volume 102, 1943, pp 269-271.

5. Takeda. Metallographic Study of the Action of the Cementing Materials on Tungsten Carbide. Science Reports, Tohaku Imperial University. Volume 1, 1936, pp 864-871.

6. Dawihl, W. and Hinnueber, J. On the Structure of Cemented Hard Metal Compositions. Kolloid Zeitschrift. Volume 104, 1943, Nos. 2-3, pp 233-236. Translated by Henry Brutcher, Inc., Altadena, California.

7. Franssen, H. Structure of Cemented Carbide Compositions, Archiv fur das Eisenhuttenwesen. Volume 19, 1948, pp 79-84. Translated by Henry Brutcher, Inc., Altadena, California.

8. McBride, C. C. TiC Base Cermets. Master of Science Thesis. The Ohio State University, 1950.

9. Cannon, H. S. and Lenel, F. V. Some Observations on the Mechanism of Liquid Phase Sintering. Plansee Proceedings. 1952, p 106.

10. Gurland, J. A Study of the Effect of Carbon Content on the Structure and Properties of Sintered WC-Co Alloys. Journal of Metals. Volume 6, 1954 p 285.

11. Stover, E. R. The Binder Phase in Titanium Carbide-Nickel Cermets. Master of Science Thesis. Massachusetts Institute of Technology, 1952.

12. Knudsen, F. P., Moreland, R. E. and Geller, R. F. Physical Properties of Titanium Carbide Base Cermets at Elevated Temperatures. Final Summary Report, National Bureau of Standards, January, 1954, pp 20,30.

13. Redmond J. and Smith, E. Cemented Titanium Carbide. Metals Transactions. Volume 185, 1949, p 988.

14. Straumanis, M. Journal Applied Physics, 1949, pp 20, 726.

15. Henry, N. F. M., Lipson, H. and Wooster, W. A. The Interpretation of X-ray Diffraction Photographs. D. Van Nostrand Co. Inc., 1951, p 193.

16. McBride, C. Report No. 6, 1950. The Ohio State University Research Foundation Contract No. AF 33(038)-6841.

17. Kehl, L., The Principles of Metallographic Laboratory Practice. 3rd Edition, McGraw Hill Co. New York, p 77-79.

18. Mauer, Floyd A. and Boly, Leonard H., National Bureau of Standards Report No. 3445. February 14, 1954.

19. Honeycombe, R. W. K. The Preparation and Properties of Cemented Carbides. Australian Institute of Mining and Metallurgy, Volume 128, 1942, p 227.

20. Sarubin, N. M. and Molkor, L. P. Abstract Chemical Zentrablatt. Volume 1, 1936, p 2196.

21. Sarubin, N. M. and Molkor, L. P. Alloys of Cobalt With Molybdenum, Titanium and Tantalum Carbides. Metallurgical Abstracts. 1935, p 148.

22. Polikarpova. X-ray Laboratory, Electrozavod. Extract of paper submitted to obtain degree of Certified Engineer. M.G.U., 1937.

23. Germany. Determination of the Solid Solubility of Cobalt and Iron in Refractory Carbides. Metal Powder Report. 1948. p 142.

24. Kieffer, R. Theoretical Aspects of Sintering of Carbides. Physics of Powder Metallurgy, edited by W. E. Kingston, McGraw Hill, 1951, pp 278-29.

25. Metcalfe, A. G. The Mutual Solid Solubility of WC and TiC. Journal of the Institute of Metals. Volume 73, 1947, p 591.

26. Edwards, R. and Raine, T. The Solubility of Some Stable Carbides in Cobalt, Nickel and Iron at 1250°C. Plansee Proceedings. Volume 1, 1952 p 232.

27. McPherson, D. J. The Preparation and Properties of Titanium-Chromium Binary Alloys. Ph.D. Dissertation. The Ohio State University, 1949.

28. Barret, C. S. Structure of Metals. McGraw Hill Book Co., New York, 1952, p 220.

29. Calbick, C. H. Bell System Technical Journal. 1952, pp 798-824.

30. Hibi, Tadotosi and Yada Keiji High Resolution Replicas and Their Application. Journal of Applied Physics. Volume 25, 1954, pp 712.

31. Calbick, C. J. Inorganic Replication: Interpretation of Electron Micrographs. Symposium on Techniques for Electron Metallography. American Society for Testing Materials, Special Technical Publication No. 155, 1953, p 42.

32. O'Bryan, H. M. Evaporation Technique for Highly Refractory Substances. Review of Scientific Instruments. Volume 5, 1934, p 125.

33. Greenhouse, H. M., Stoops, R. F., and T. S. Shevlin A New Carbide-Base Cermet Containing TiC, TiB_2, and CoSi. Journal of the American Ceramic Society. Volume 37, No. 5, May 1954, p 203.

34. Blackburn, A. R., Shevlin, T. S. and Lawers, H. R. Fundamental Study and Equipment for Sintering and Testing of Cermet Bodies: II. Furnace Equipment for Cermet Fabrication. Journal of the American Ceramic Society. Volume 32, 1949, No. 3, pp 89-93.

35. Metals Handbook, American Society for Metals. 1948 Edition p 1175.

36. Pauling, L. Nature of the Chemical Bond. Cornell University Press. 2nd Edition, Ithaca, N.Y., 1940.

37. Schwarzkopf, P. and Kieffer, R. Refractory Hard Metals. MacMillan Company. New York, 1953.

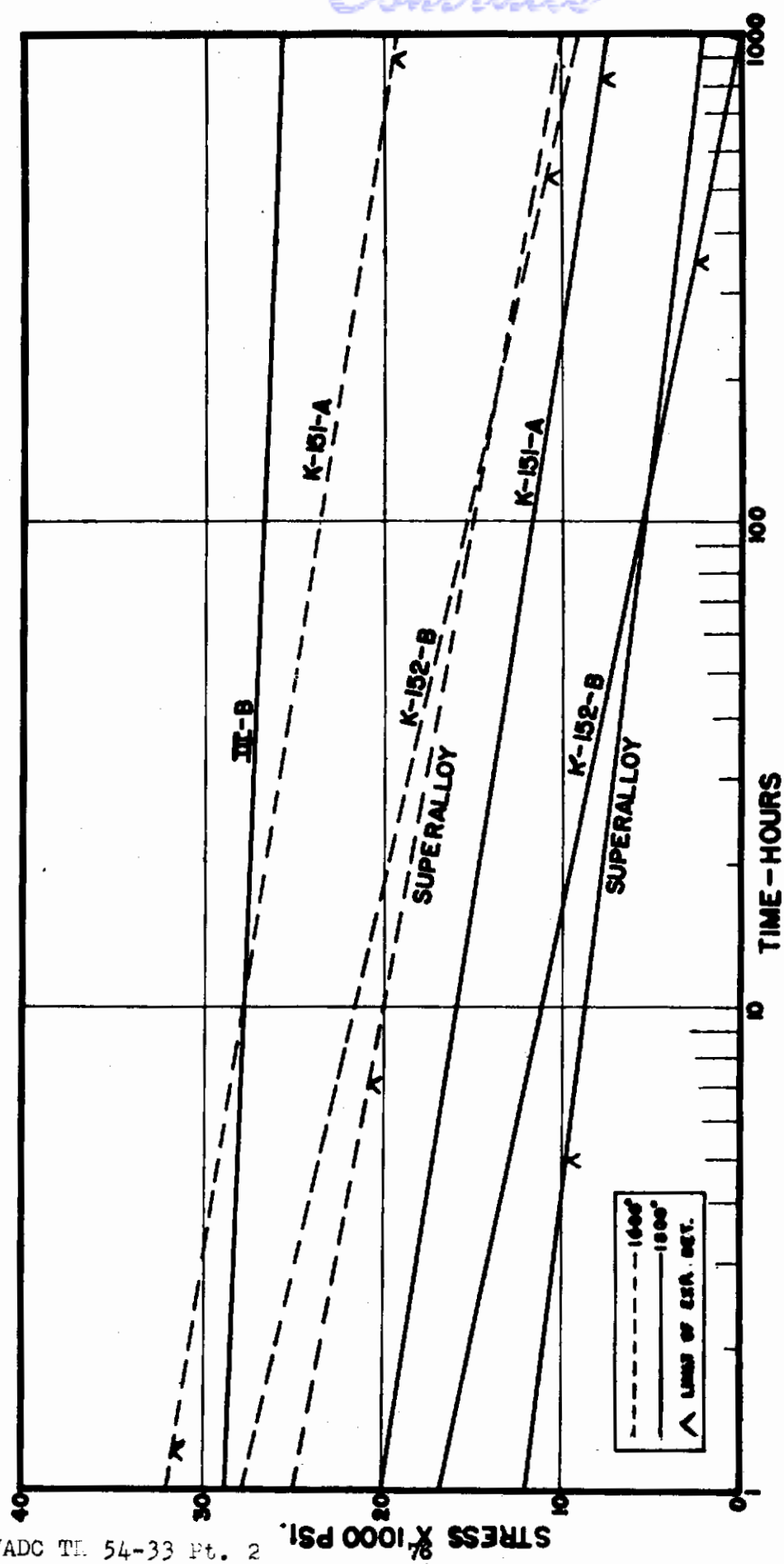

Figure 1. Stress-rupture in tension curves for samples K-151-A, K-152-B, cermet III-B and a superalloy at 1600°F and 1800°F.

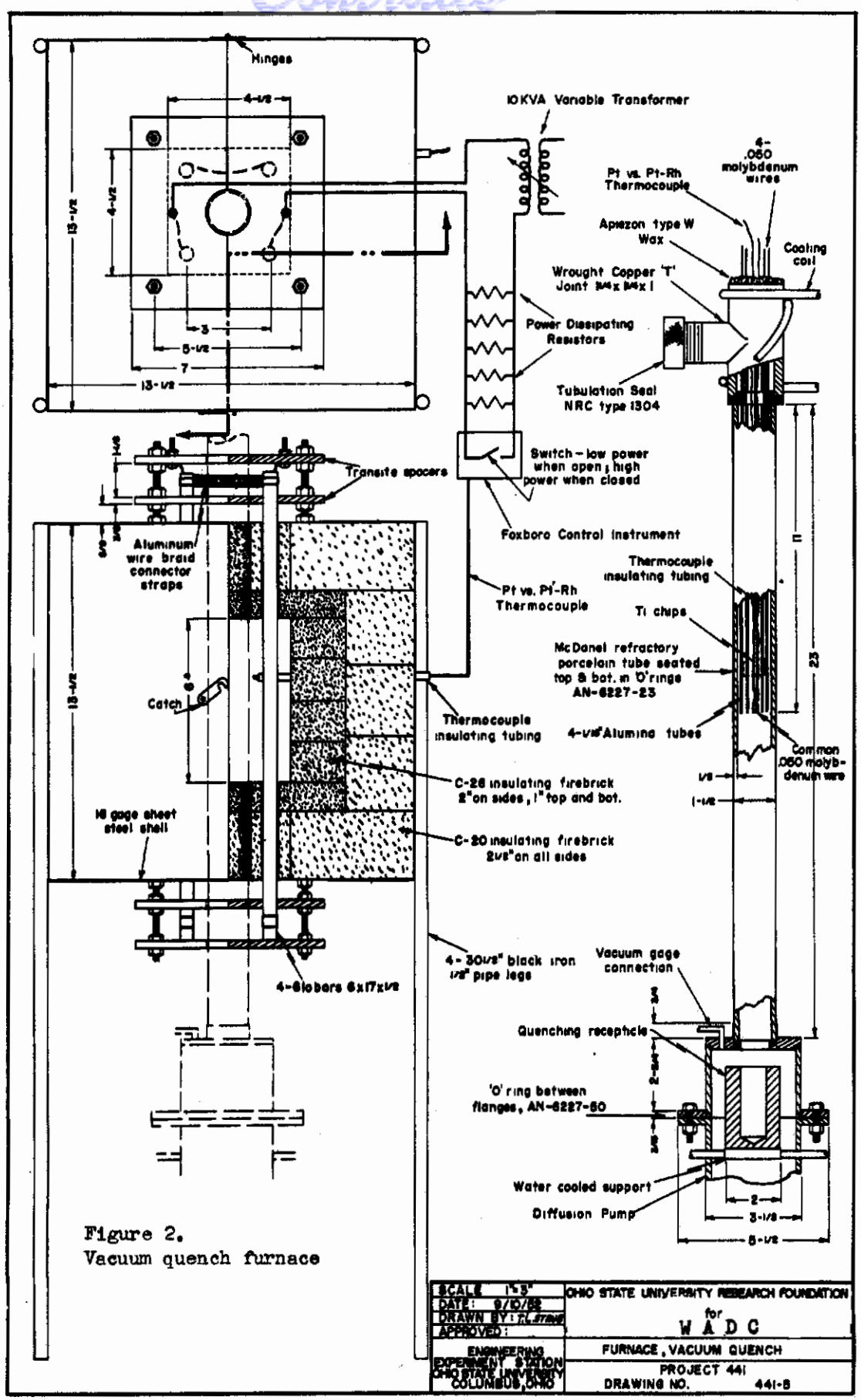

SCALE 1"=5"	OHIO STATE UNIVERSITY RESEARCH FOUNDATION
DATE: 9/10/52	for
DRAWN BY: R.L. STRAUB	W A D C
APPROVED:	
ENGINEERING EXPERIMENT STATION OHIO STATE UNIVERSITY COLUMBUS, OHIO	FURNACE, VACUUM QUENCH
	PROJECT 441
	DRAWING NO. 441-S

Figure 2.
Vacuum quench furnace

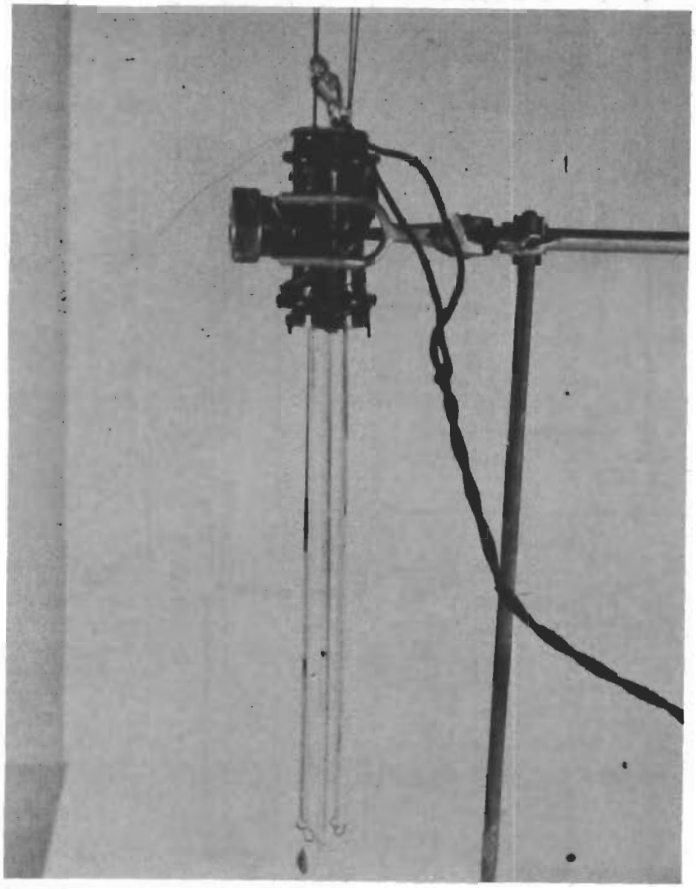

Figure 3. Sample supporting and dropping apparatus. Note specimen in dropping position.

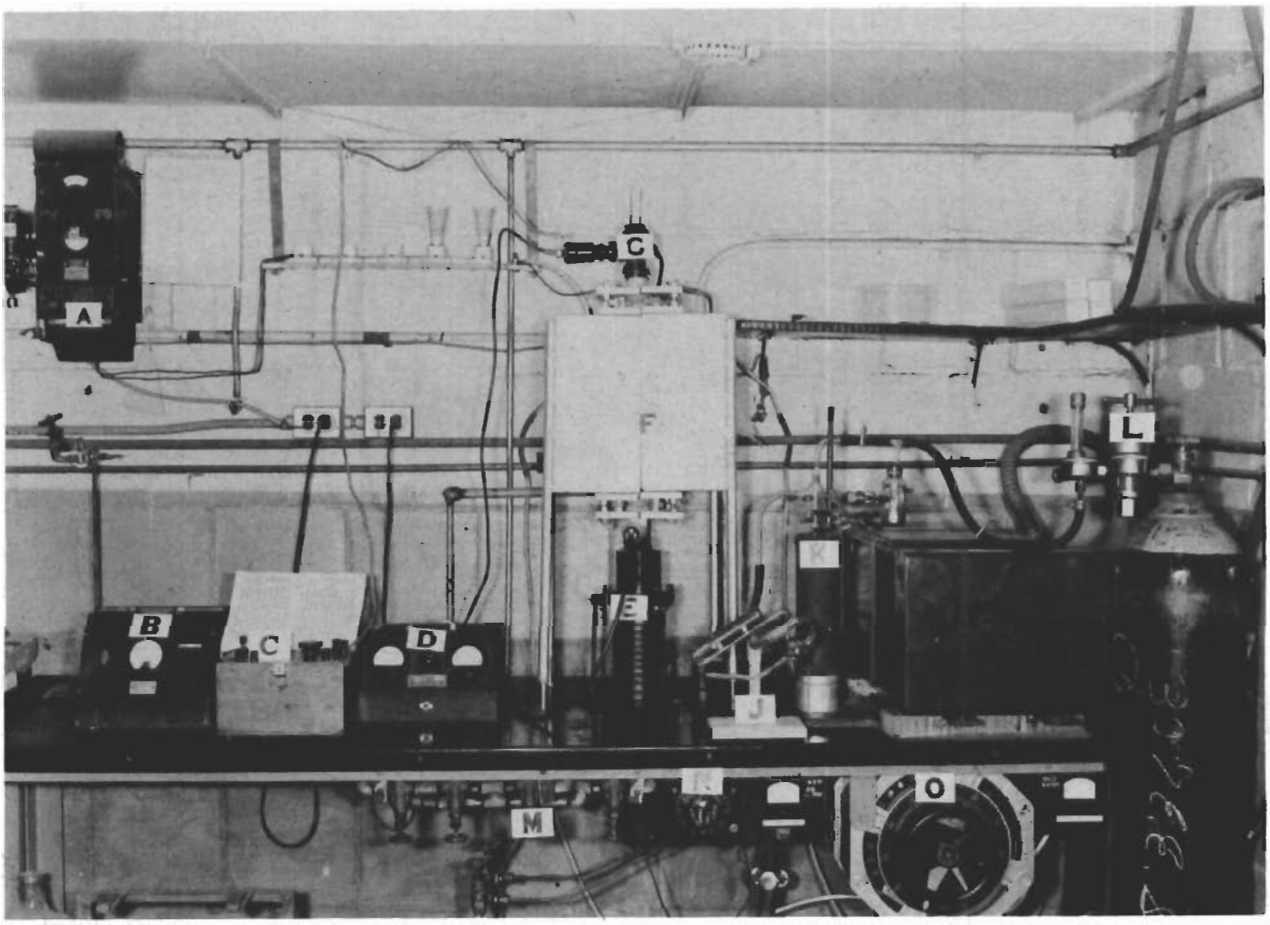

Figure 4. Assembled quenching system.

A. Foxboro potentiometer controller.
B. Phillips gauge control panel.
C. Leeds and Northrup potentiometer.
D. Thermocouple gauge control panel.
E. Diffusion pump.
F. Furnace.
G. Cu tee fixture and Phillips gauge.
J. McLeod gauge.
K. Gas purification unit.
L. Tank of He gas.
M. Cooling water controls.
N. Powerstat for diffusion pump heater.
O. Powerstat for controlling power to furnace.

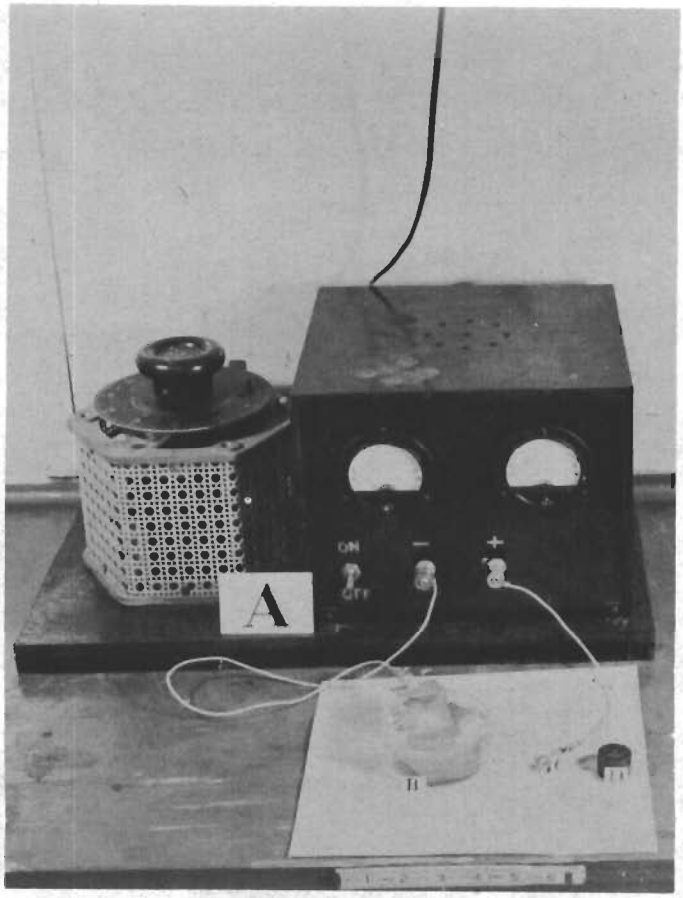

Figure 5. Electrolytic etching apparatus.

A. Powerstat and rectifier assembly.
B. Etching solution.
C. Anode specimen holder.
D. Sample mounted in Bakelite.

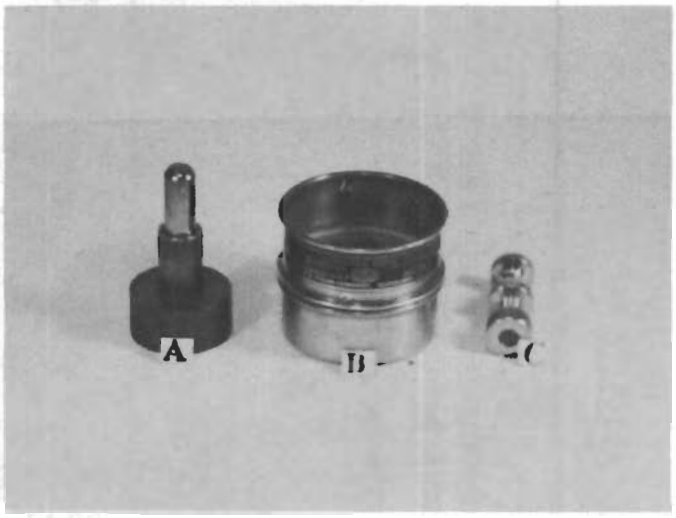

Figure 6. X-ray specimen preparation equipment - assembled.

A. Plattner hardened steel mortar and pestle.
B. 325 mesh seive.
C. Extruding apparatus.

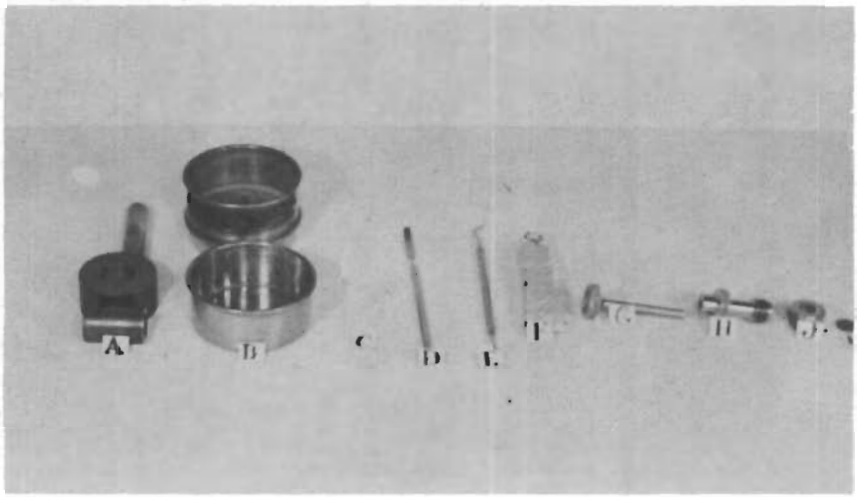

Figure 7. X-ray specimen preparation equipment - disassembled.

A. Mortar, collar and pestle.
B. Seive.
C. Glass slide.
D. Spatula
E. Scraper
F. Glue
G. Plunger
H. Body
J. Cap.
K. Spinnerette

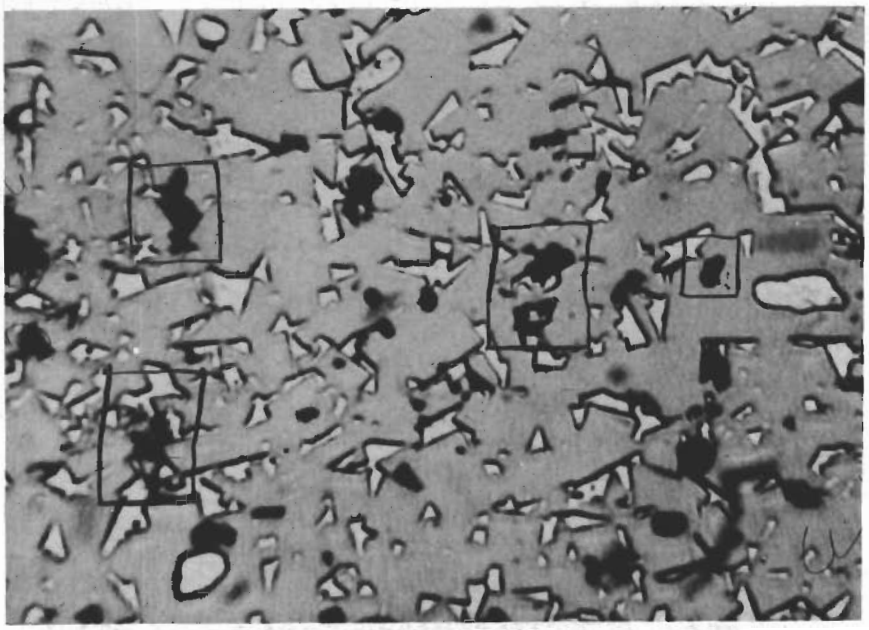

Figure 8. K-151-A. As-sintered. Unetched. 1500X.

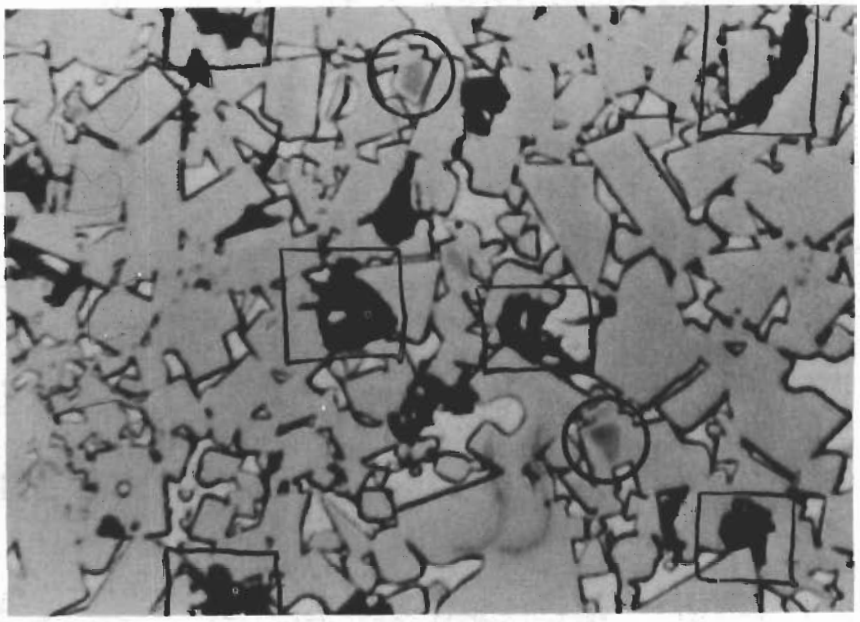

Figure 9. K-152-B. As-sintered. Unetched. 1500X.

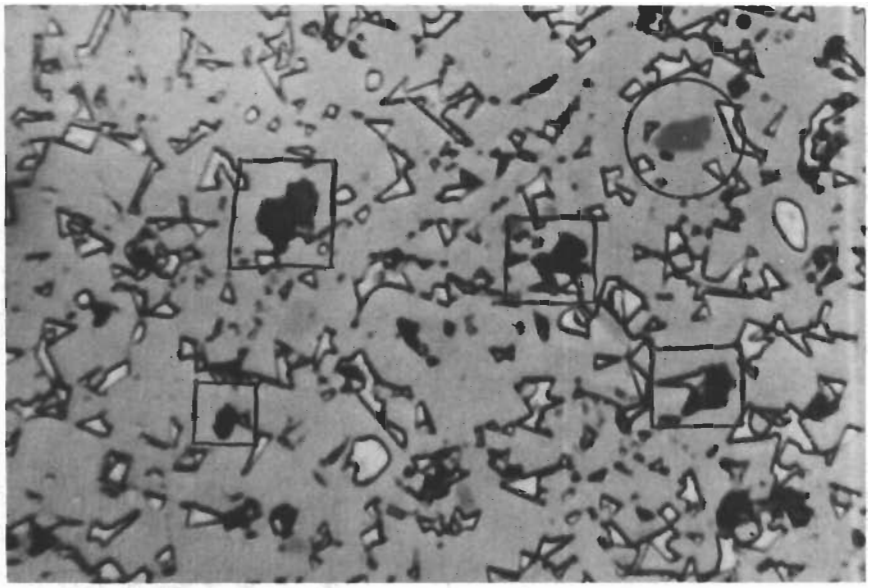

Figure 10. K-151-A after heating at 2000°F for 100 hours in a helium atmosphere. Quenched in oil. Unetched. 1500X.

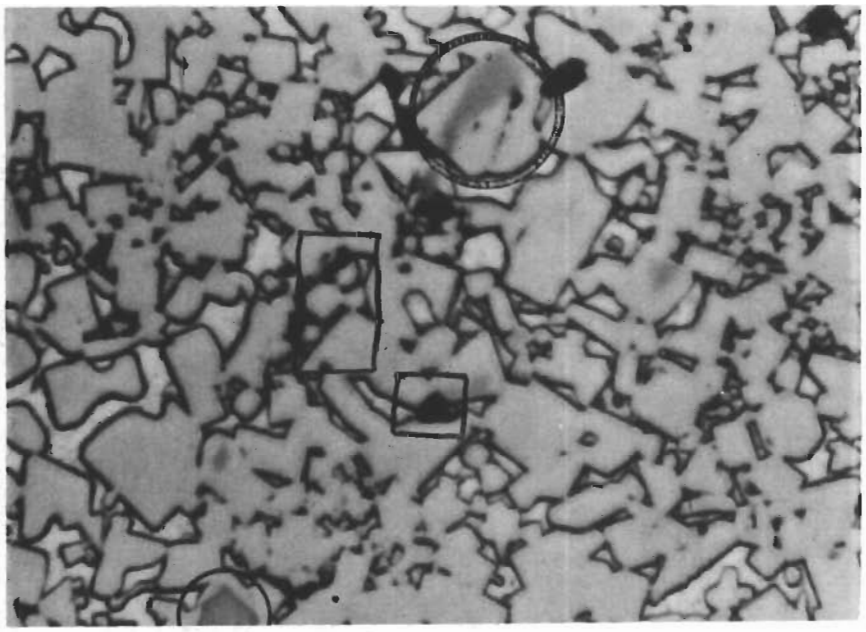

Figure 11. K-152-B after heating at 2000°F for 100 hours in a helium atmosphere. Quenched in oil. Unetched. 1500X.

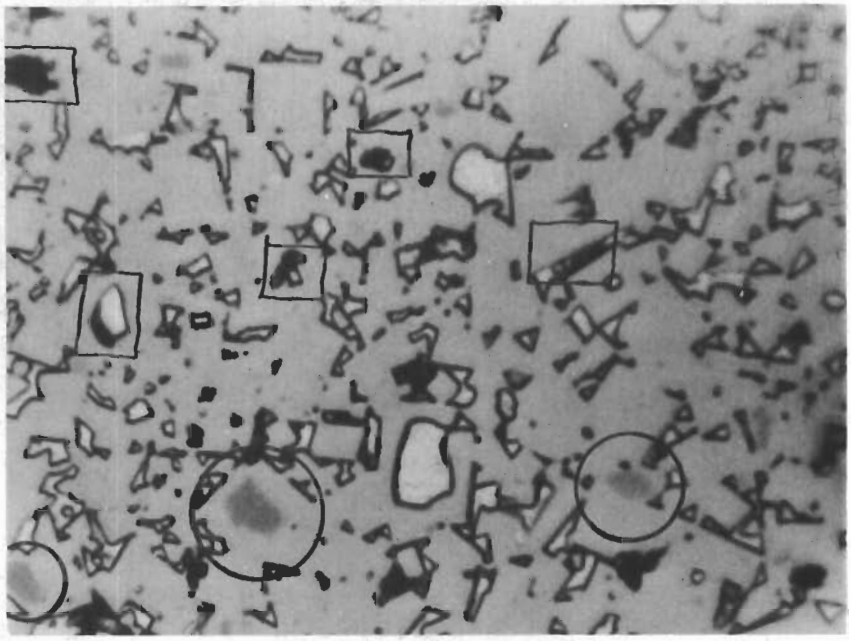

Figure 12. K-151-A after heating at 2000°F for 200 hours in a helium atmosphere. Quenched in oil. Unetched. 1500X.

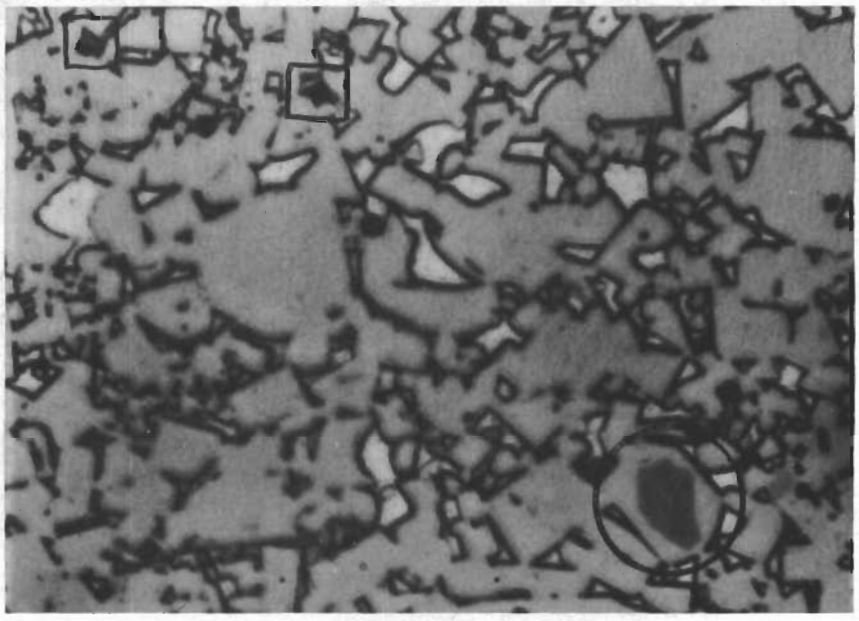

Figure 13. K-152-B after heating at 2000°F. for 200 hours in a helium atmosphere. Quenched in oil. Unetched. 1500X

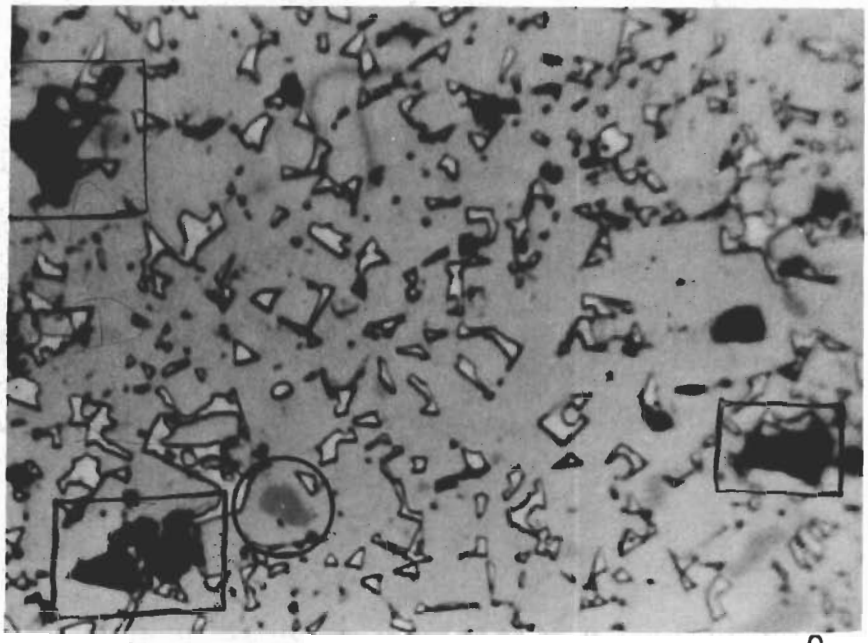

Figure 14. K-151-A after heating at 2000°F for 300 hours in a helium atmosphere. Quenched in oil. Unetched. 1500X

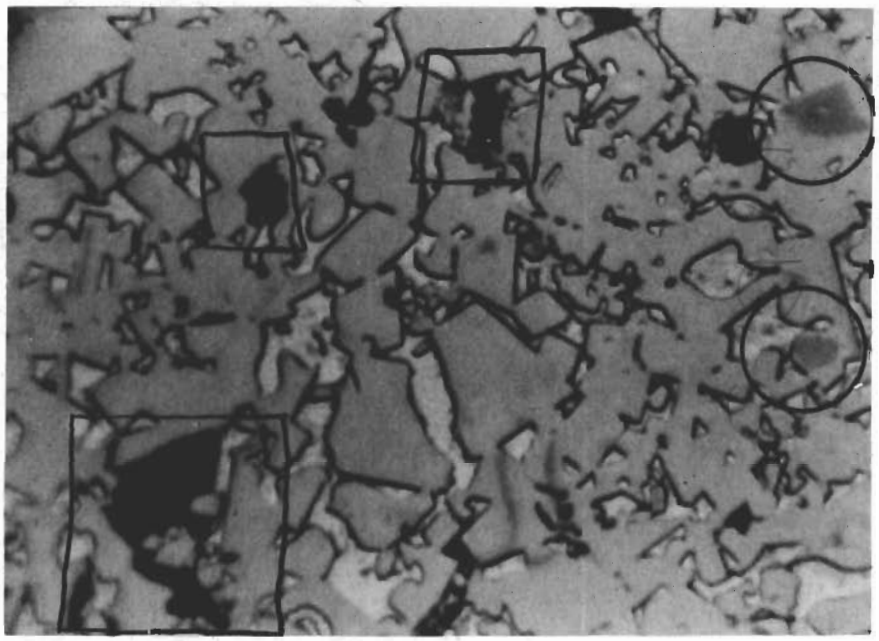

Figure 15. K-152-B after heating at 2000°F for 300 hours in a helium atmosphere. Quenched in oil. Unetched. 1500X.

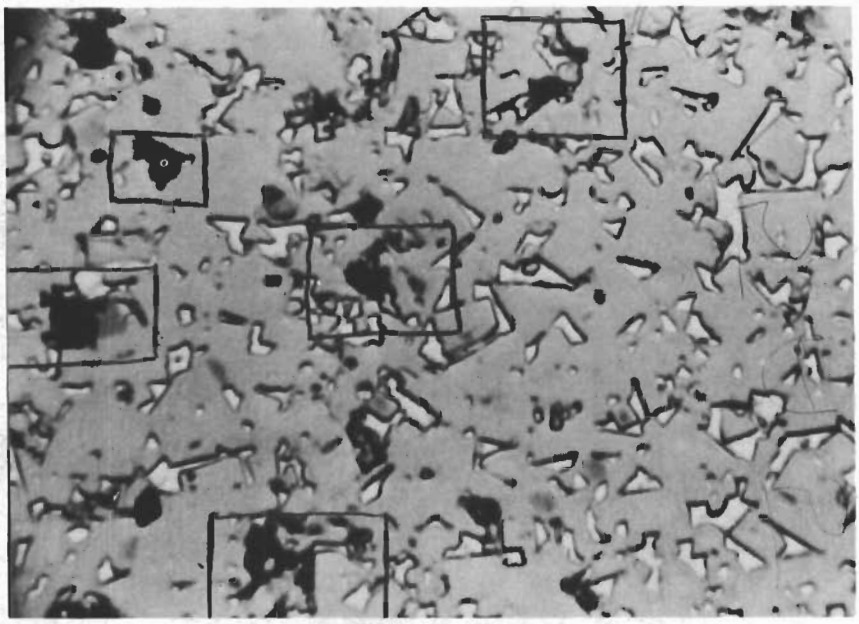

Figure 16. K-151-A after heating at 2000°F for 500 hours in a helium atmosphere. Quenched in oil. Unetched. 1500X.

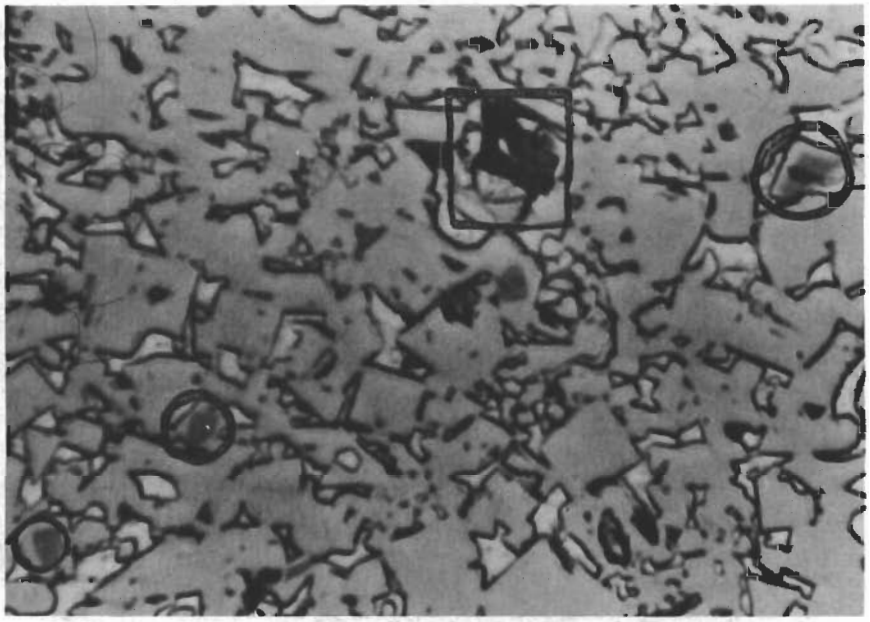

Figure 17. K-152-B after heating at 2000°F for 500 hours in a helium atmosphere. Quenched in oil. Unetched. 1500X.

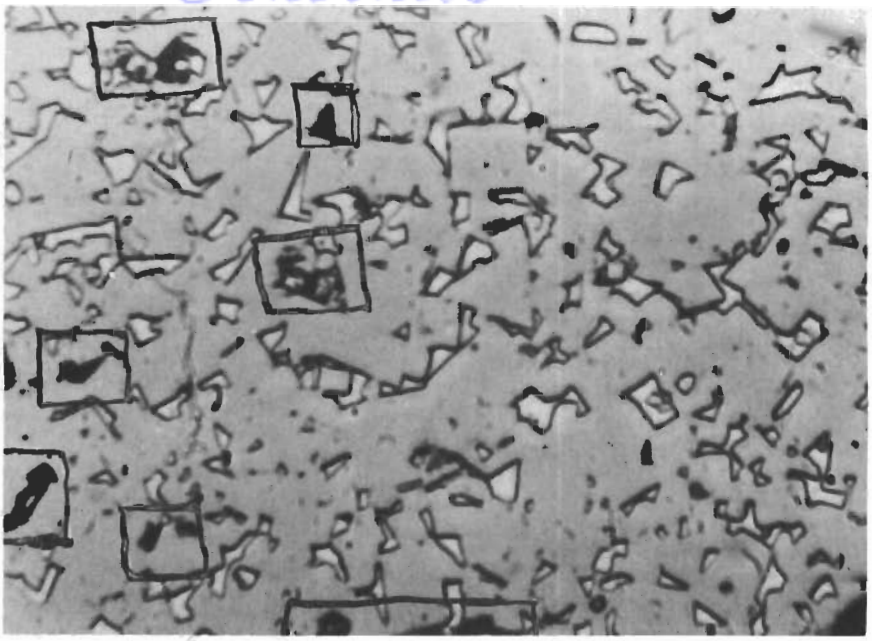

Figure 18. K-151-A after heating at 2000°F for 700 hours in a helium atmosphere. Quenched in oil. Unetched. 1500X.

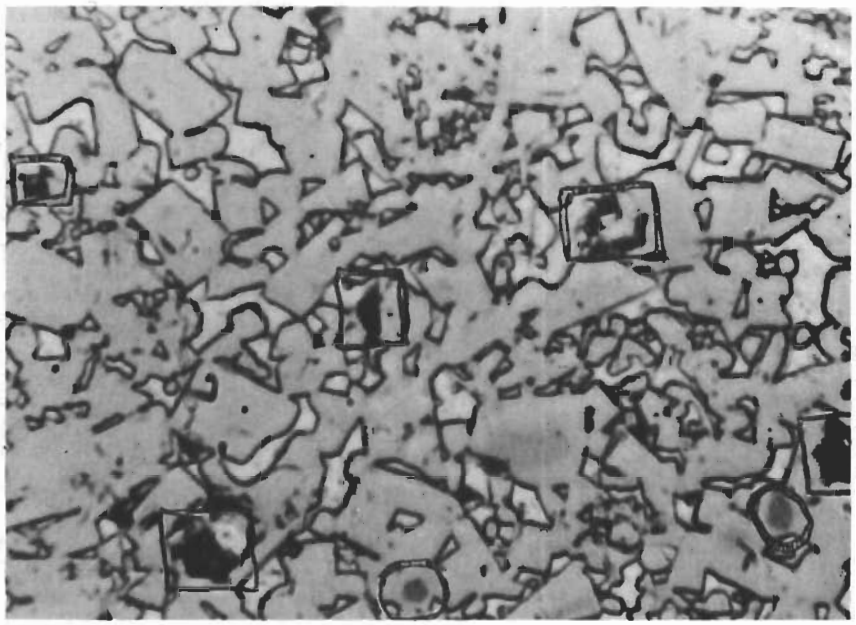

Figure 19. K-152-B after heating at 2000°F for 700 hours in a helium atmosphere. Quenched in oil. Unetched. 1500X.

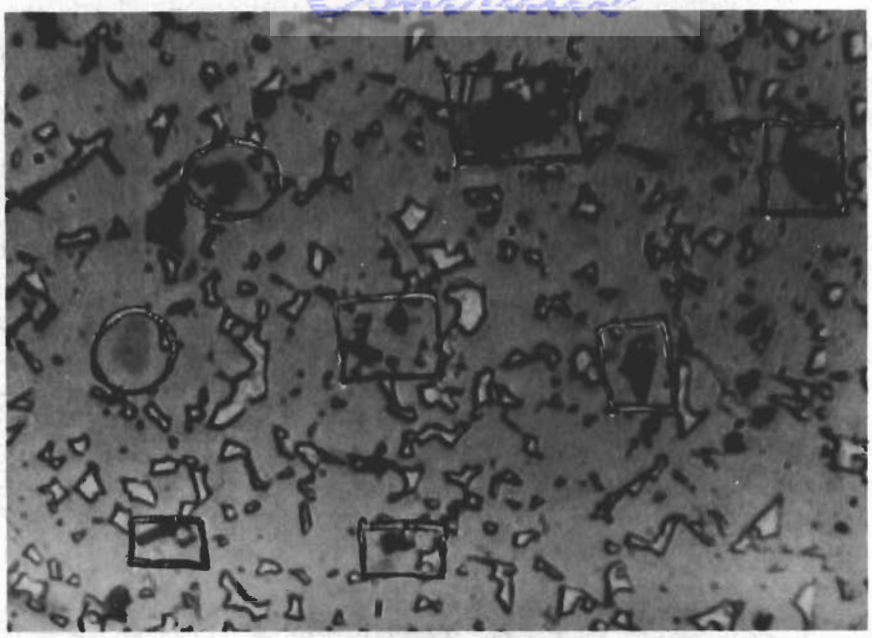

Figure 20. K-151-A after heating at 2000°F for 1000 hours in a helium atmosphere. Quenched in oil. Unetched. 1500X.

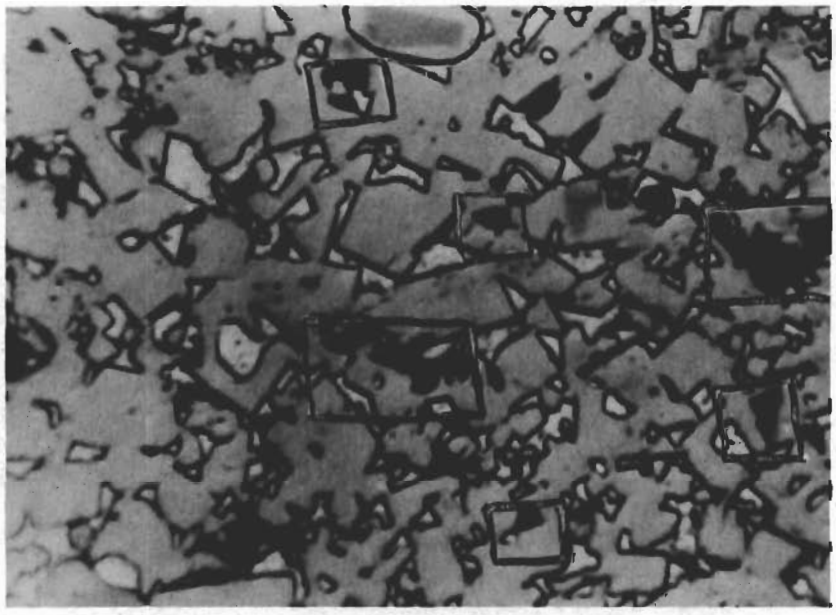

Figure 21. K-152-B after heating at 2000°F for 1000 hours in a helium atmosphere. Quenched in oil. Unetched. 1500X.

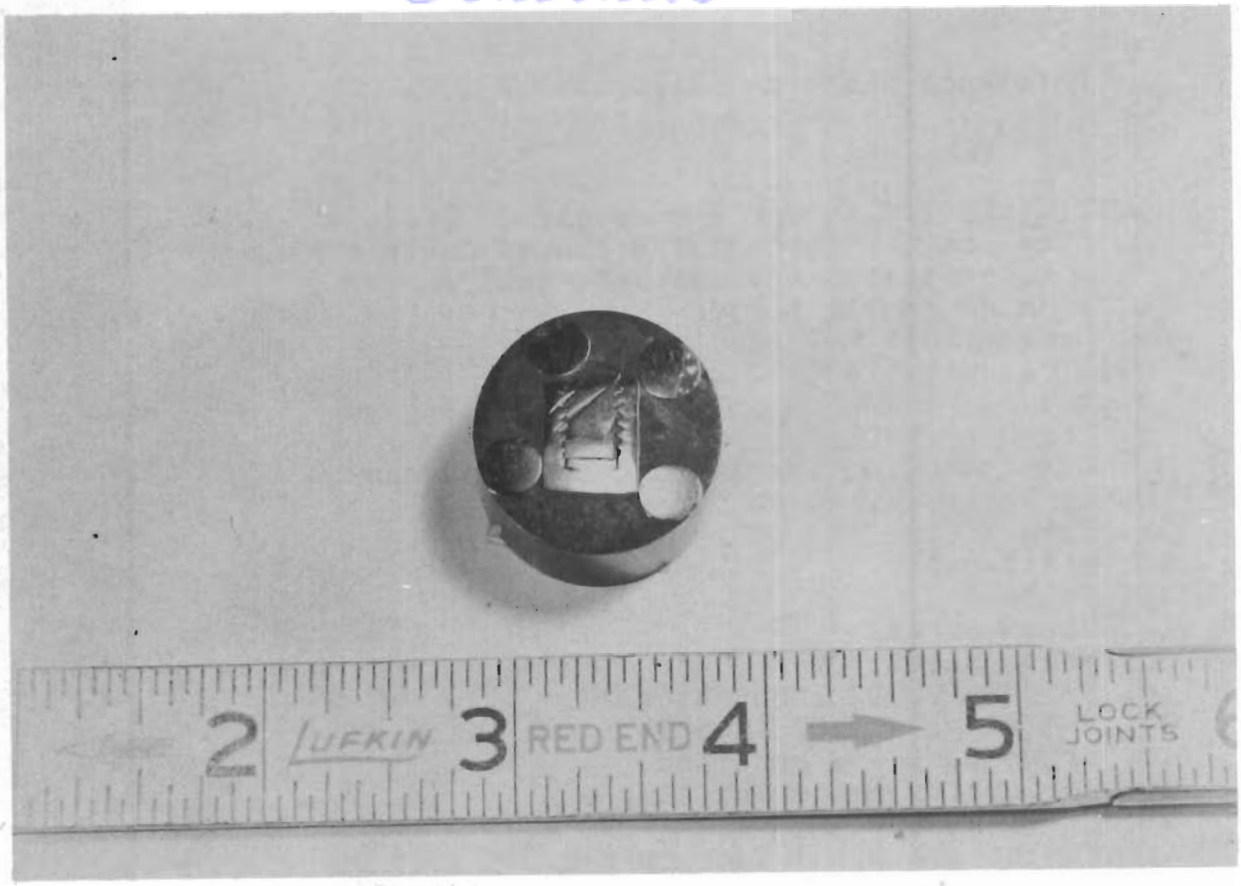

Figure 22. Sectioned Ni crucible mounted in Bakelite.

Reference Numbers - Figures 23, 24, 26, 28 and 31.

1. Stupakoff fittings - 6 required
2. Steel holder for alumina thermocouple tubing
3. 2 hole alumina thermocouple tubing
4. Alumina sample holder
5. Brass plate - 2 required
6. Alumina tubing - 2 required
7. Alumina rod
8. Thumb screw
9. Brass bushing for Garlock seal and shaft
10. Pt wire-resistance furnace
11. Film holder
12. Black paper
13. Film
14. Brass sheet
15. Brass sheet
16. Be foil 0.012 inch thick
17. "O" rings - 4.00 inch ID x 4.25 inch OD
18. Brass post - 2 required
19. Holder for centering sample
20. Steel shaft
21. "O" Ring - 0.500 inch ID x 0.625 inch OD
22. Garlock Klozure, Model 51, Part #51X3863
23. Pulley
24. Washer
25. Brass plate
26. Brass ring
27. Brass shell
28. X-ray beam-trap assembly
29. Collimator assembly
30. Base support--beam-trap end
31. Base support--collimator end
32. Thumb screws - 2 required
33. Steel springs - 2 required
34. Pt, Pt-10% Rh thermocouple

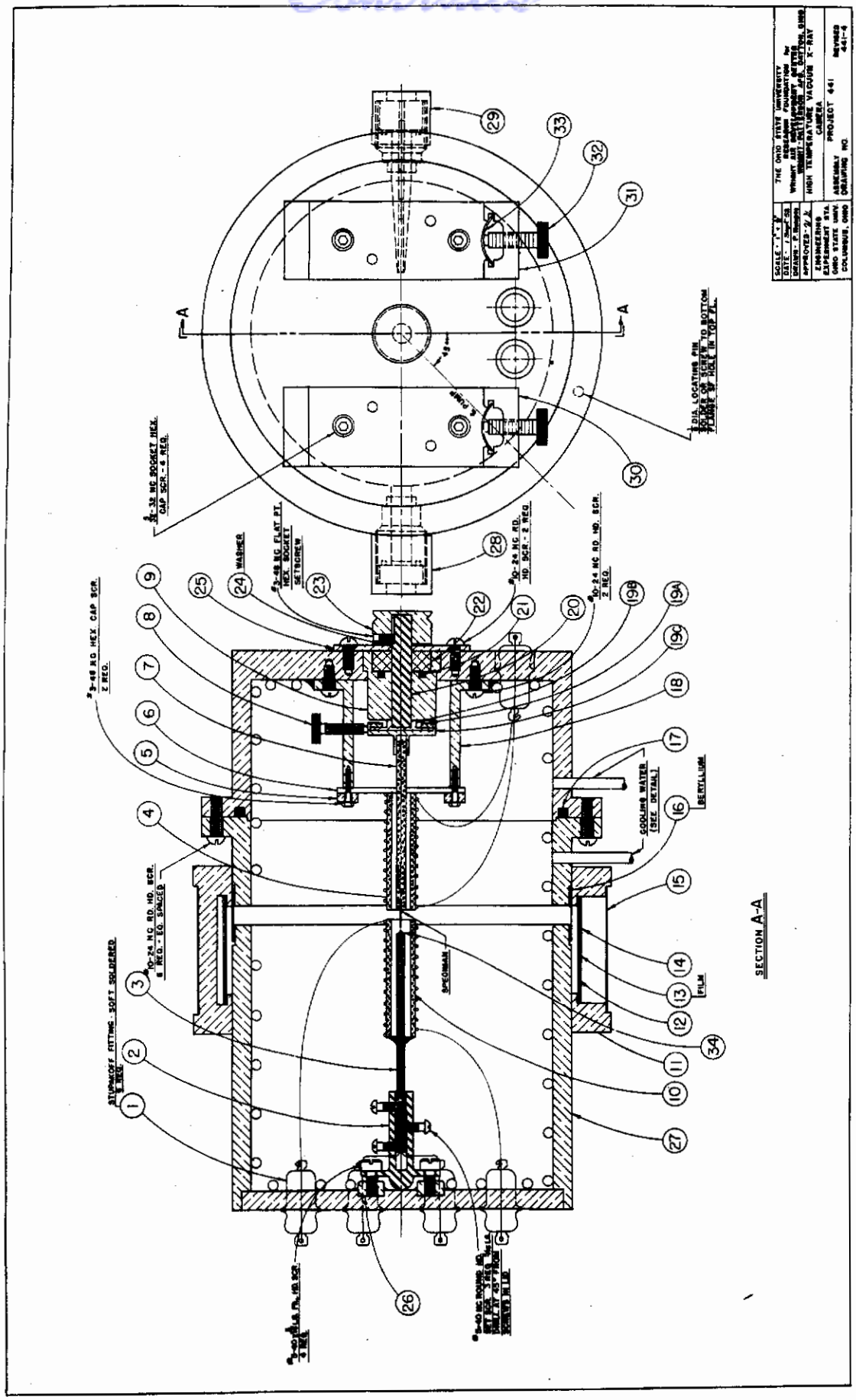

Figure 23. Assembly drawing of high temperature X-ray camera.

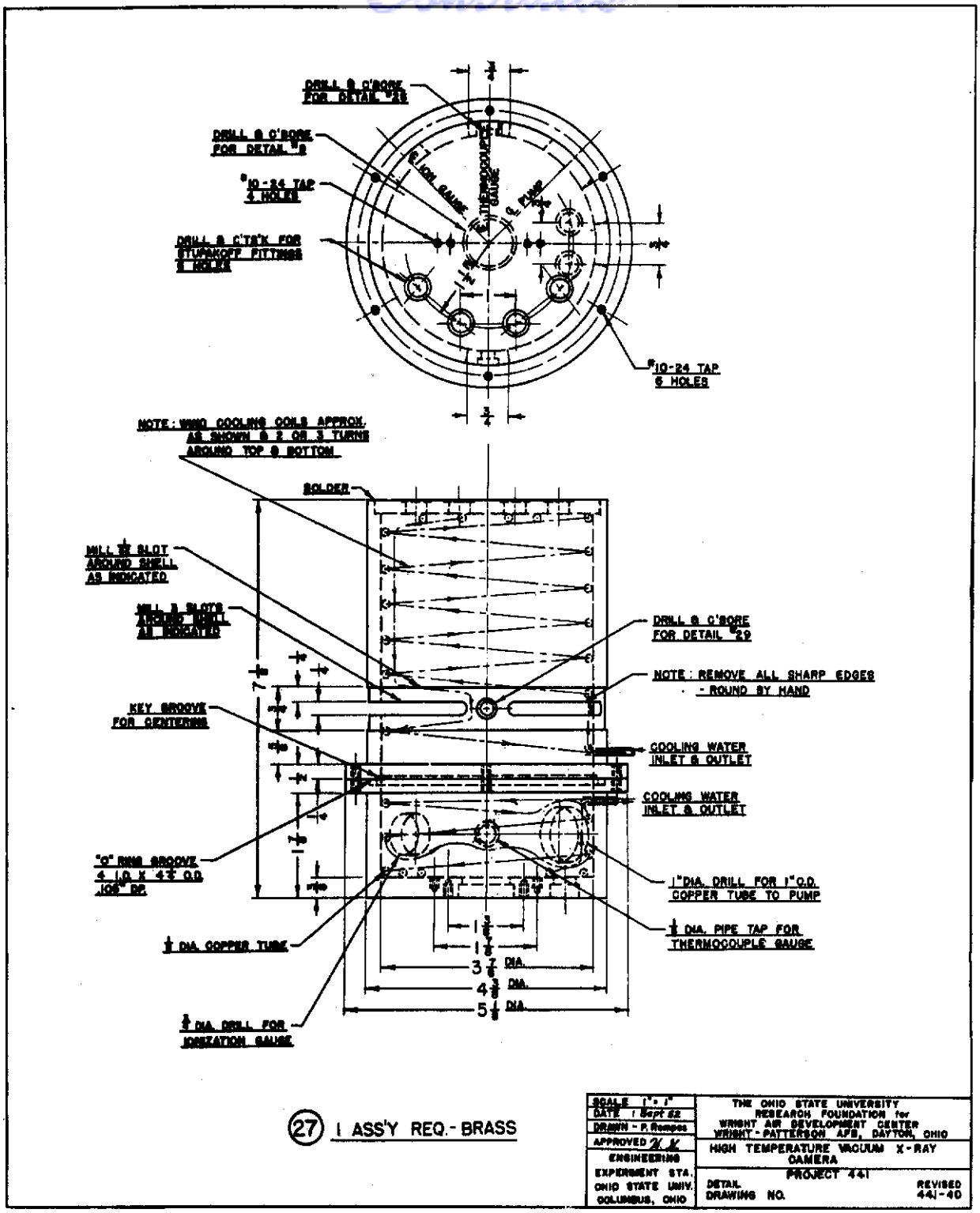

Figure 24. Assembled brass shell of high temperature x-ray camera.

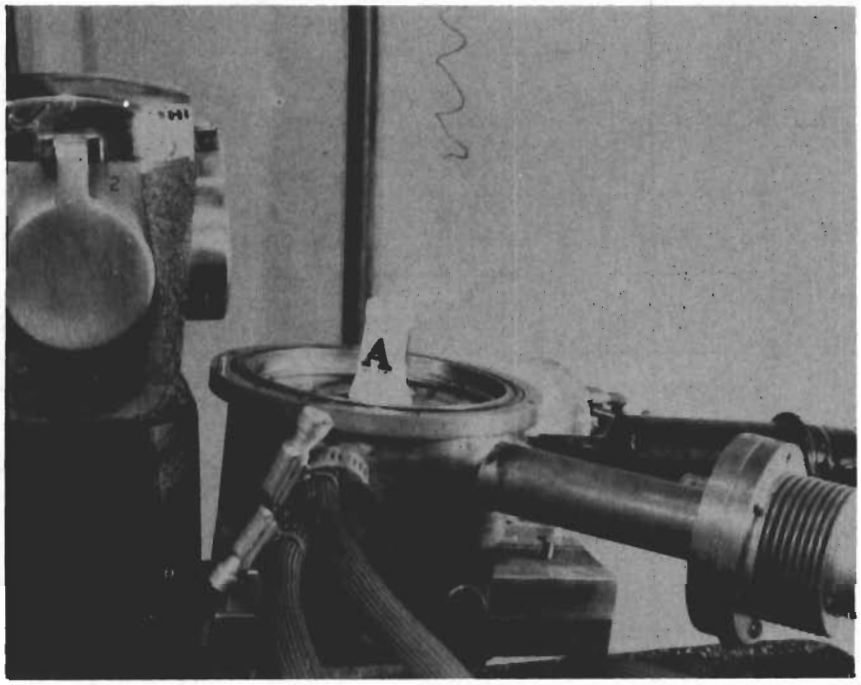

Figure 25. Body of high temperature x-ray camera.

A. Lower half of Pt-20% Rh wound x-ray furnace.

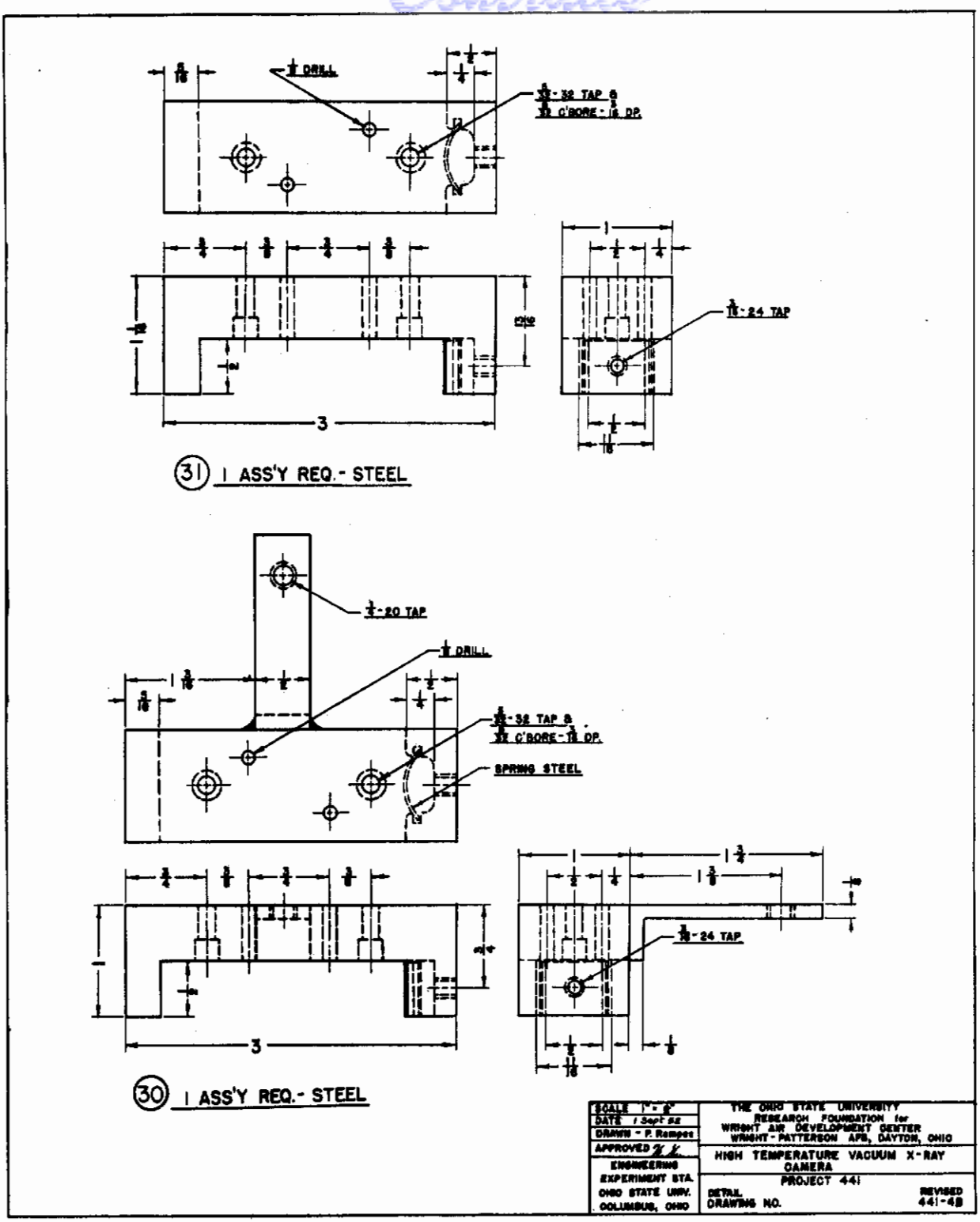

Figure 26. Base assembly of high temperature x-ray camera.

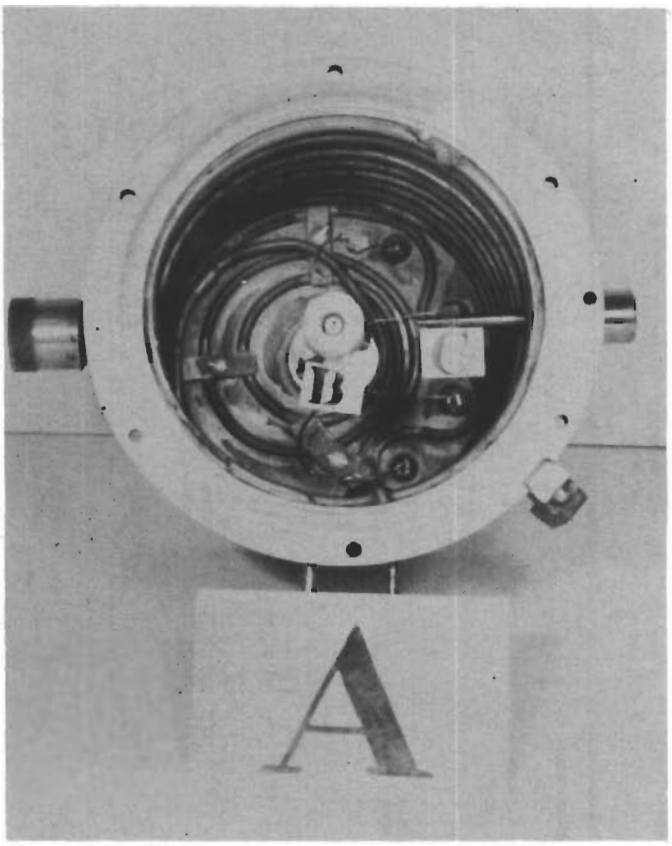

Figure 27. Top cover of high temperature x-ray camera.

A. Top cover.
B. Upper half of Pt-20% Rh wound x-ray furnace.
Note thermocouple in center of furnace.
C. Collimator.

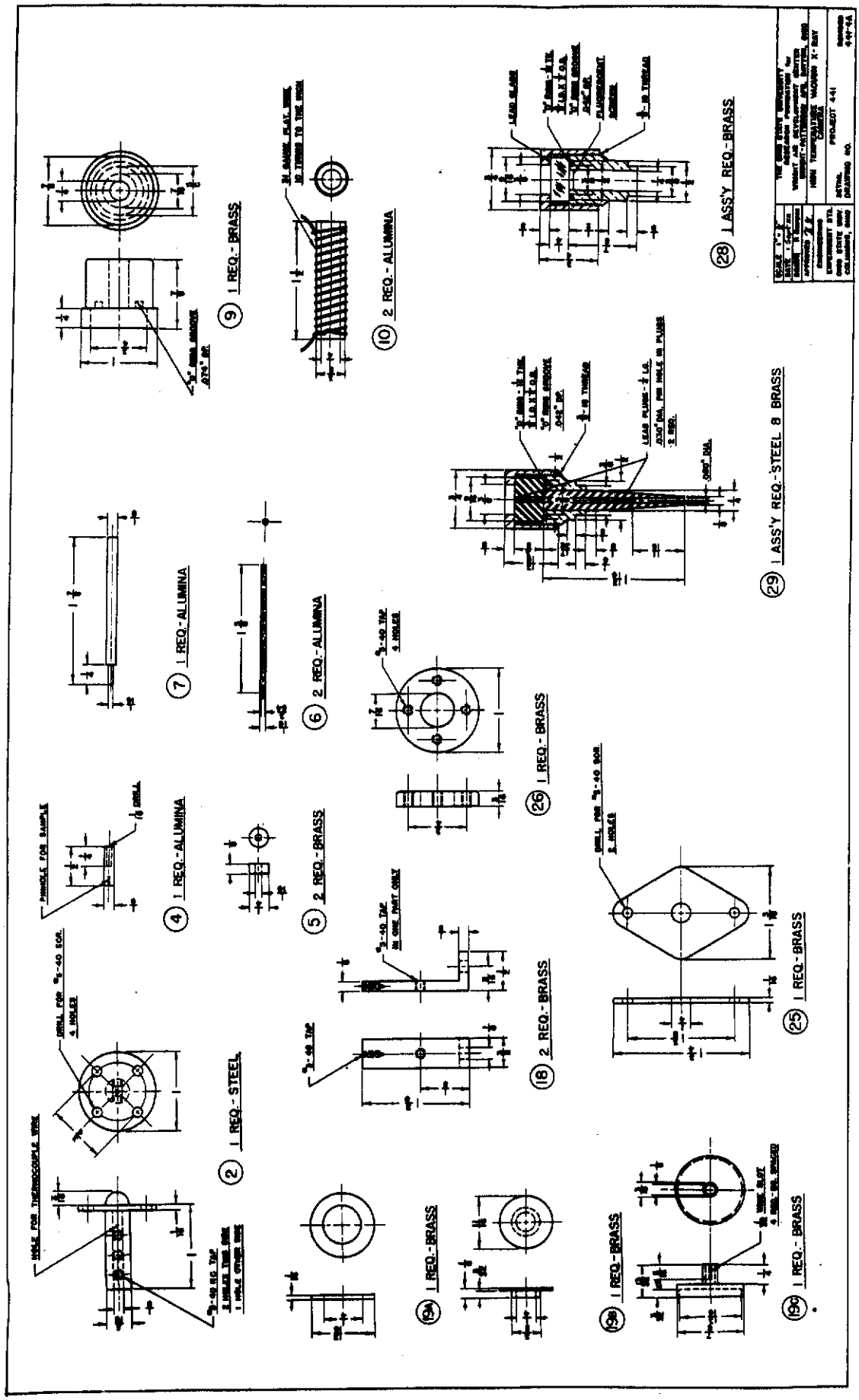

Figure 28. Detail drawing of high temperature x-ray camera.

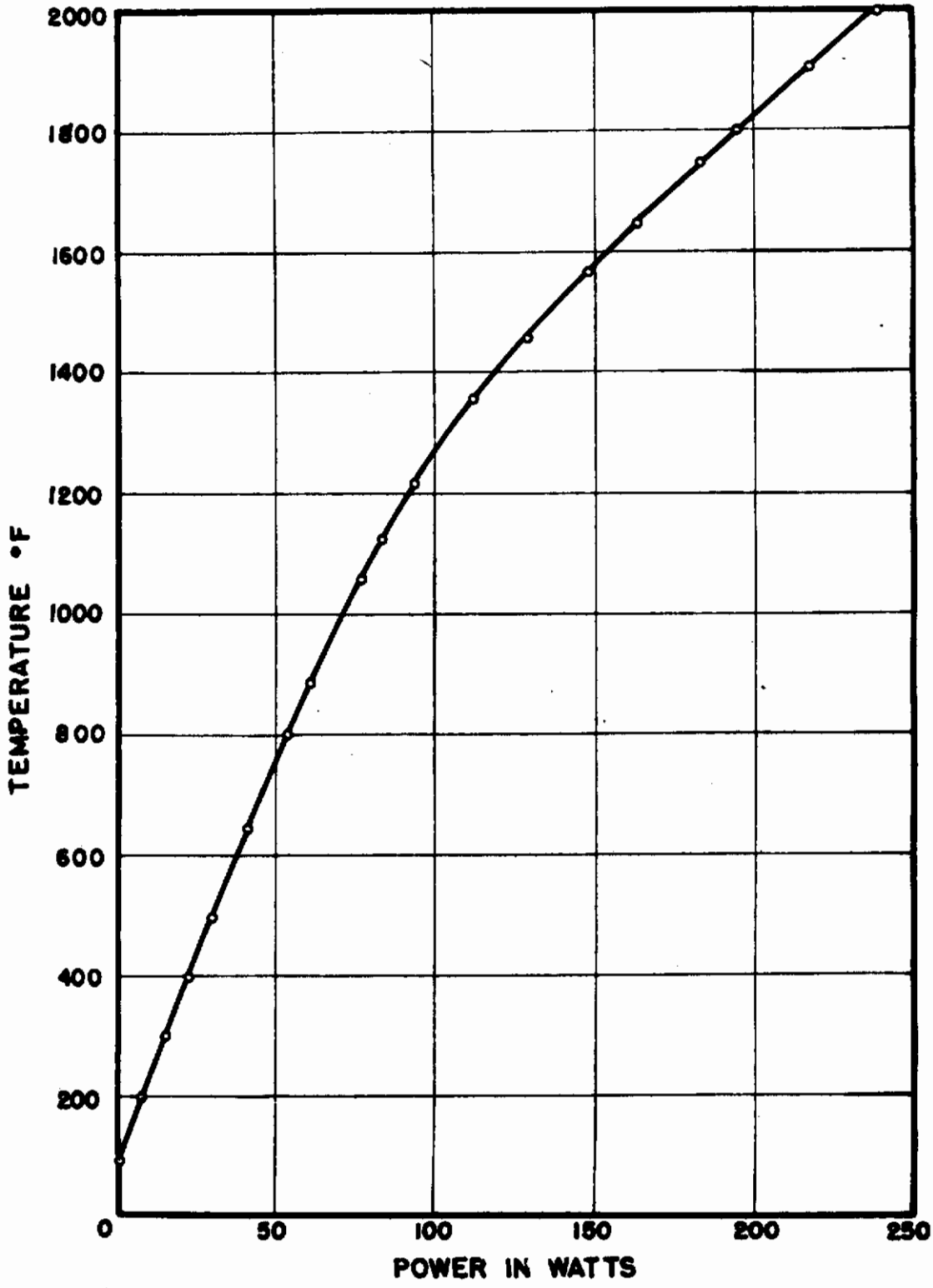

Figure 29. Heating curve for x-ray furnace.

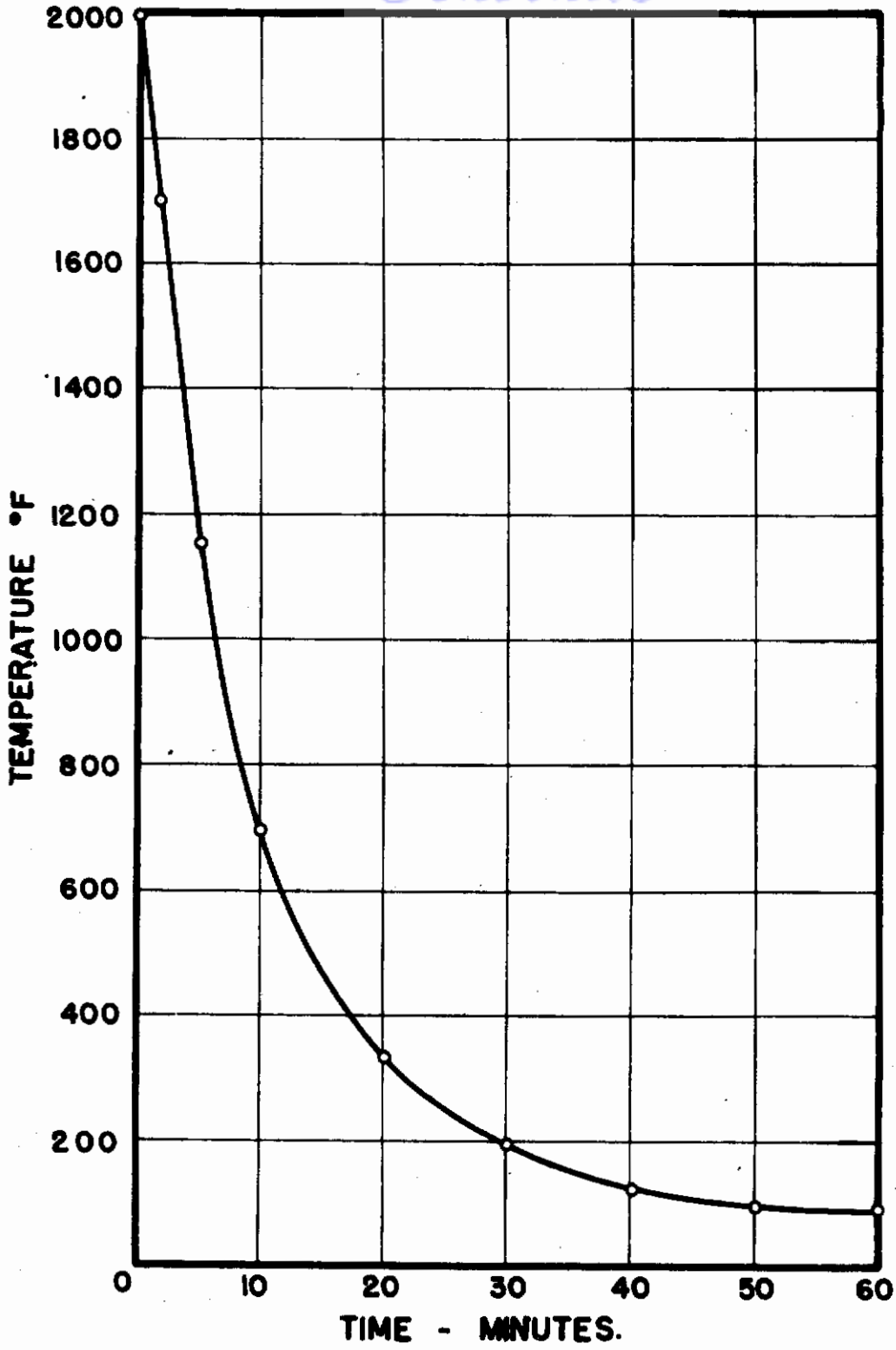

Figure 30. Cooling curve for x-ray furnace.

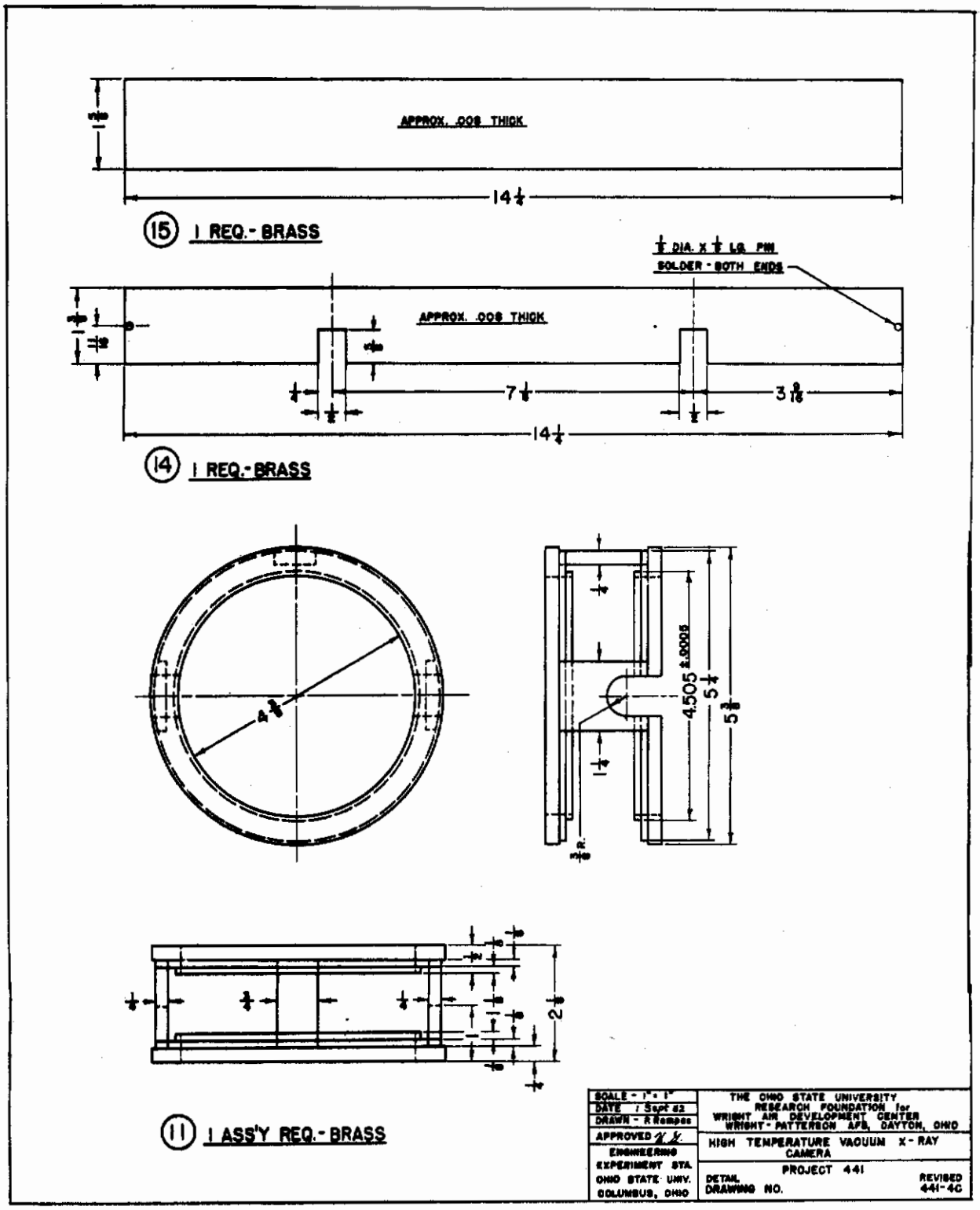

Figure 31. Detail drawing of disassembled film cassette.

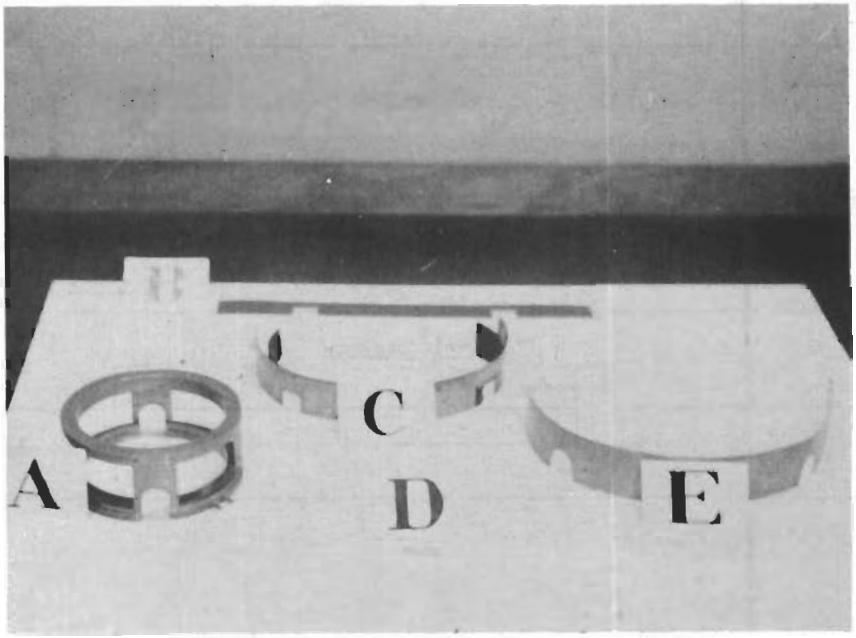

Figure 32. Disassembled film cassette.

A. Cassette frame.
B. Film template.
C. Brass and film holder.
D. Wire clamp.
E. Brass band stray light shield.

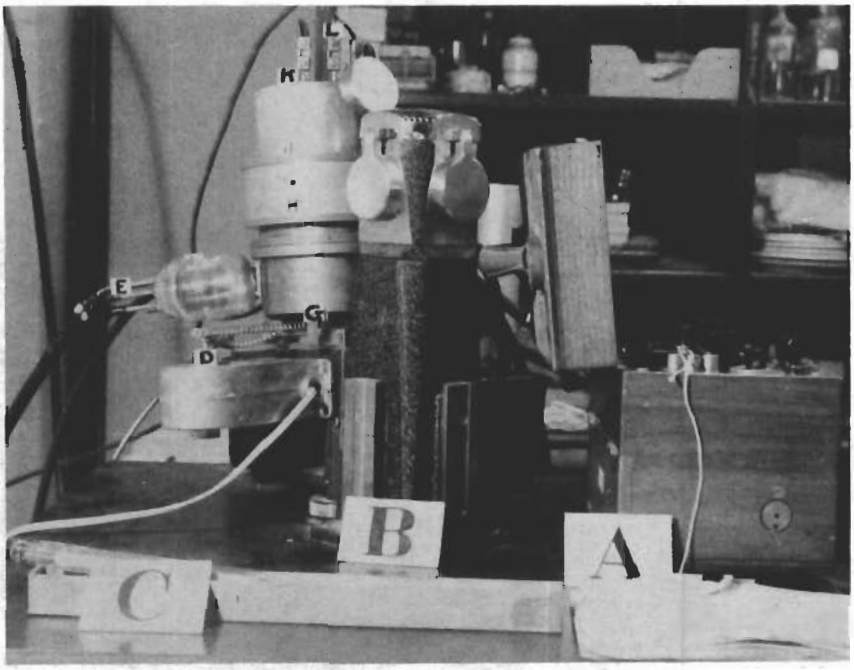

Figure 33. High temperature x-ray camera in operation.

A. Variable potentiometer.
B. X-ray tube housing.
C. Thermometer.
D. Gear and chain sample rotating device.
E. Ionization gauge.
F. Thermocouple gauge.
G. Camera body.
H. Film cassette.
J. Top cover.
K. Power leads connected to glass-metal fittings.
L. Thermocouple leads connected to glass-metal fittings.

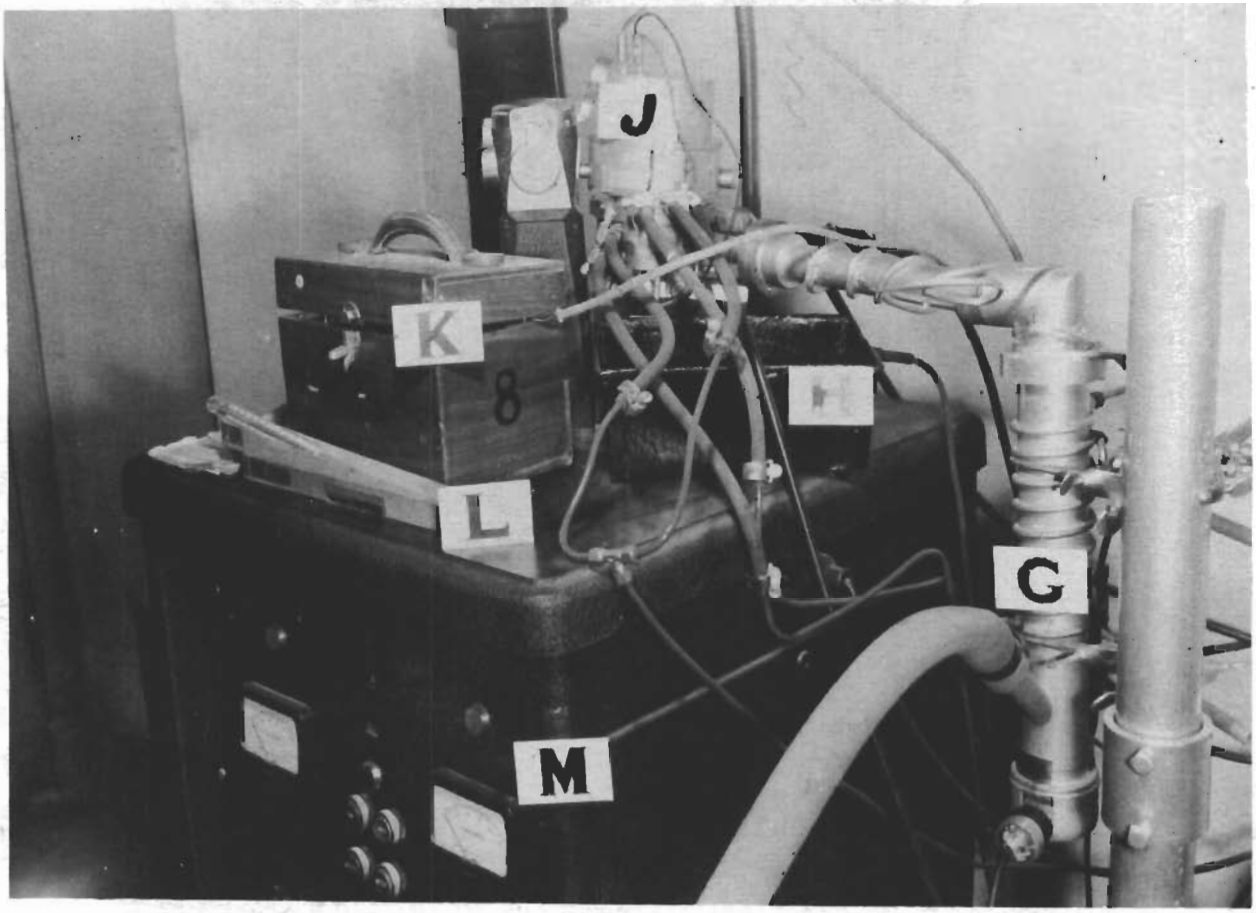

Figure 34. **High temperature x-ray camera in operation.**

G. Diffusion pump.
H. Safety water bucket.
J. High temperature x-ray camera.
K. Variable potentiometer.
L. Thermometer.
M. Philips x-ray diffraction unit.

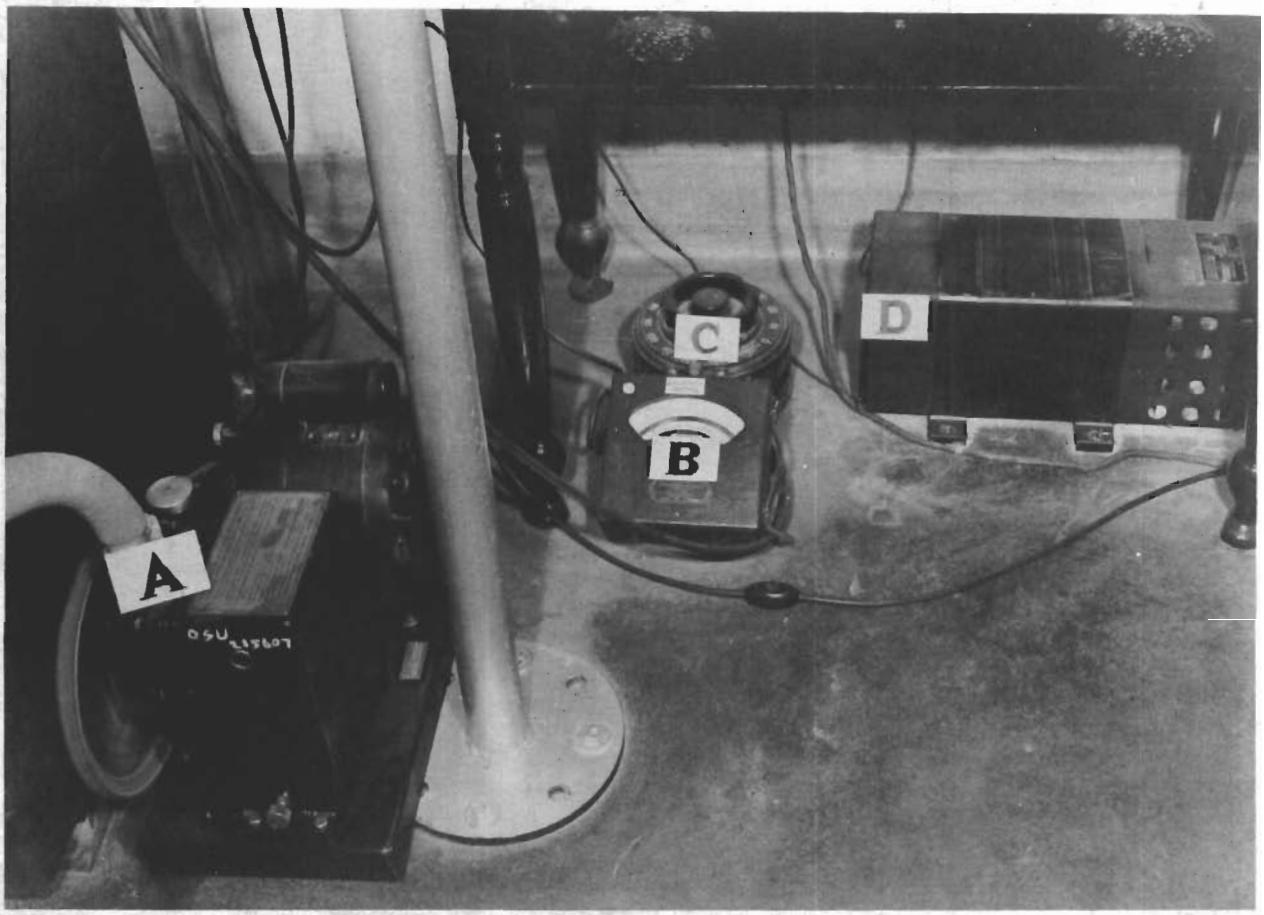

Figure 35. Electrical and vacuum equipment for high temperature x-ray camera.

A. Welch mechanical pump.
B. Ammeter.
C. Variac.
D. Sola constant voltage transformer.

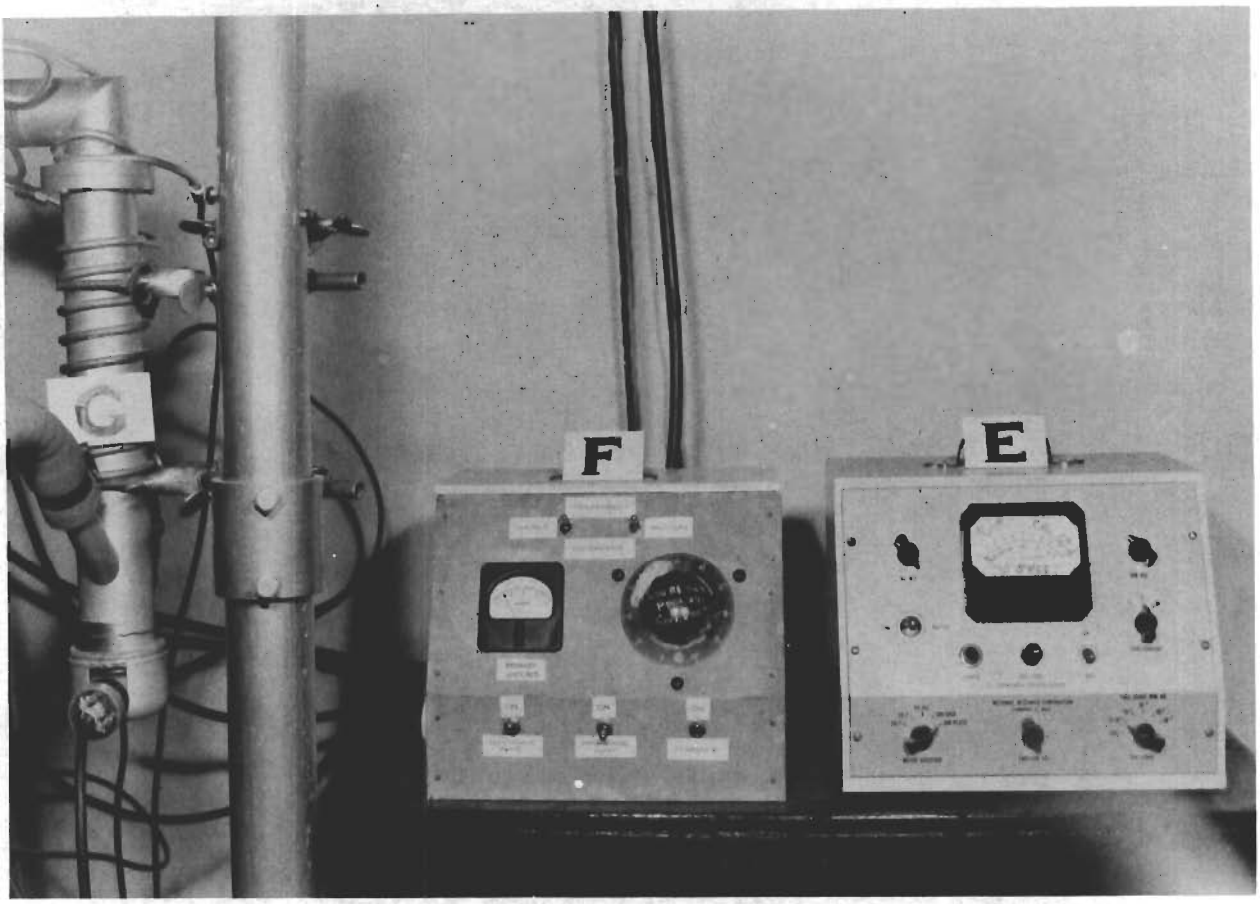

Figure 36. Control panels and vacuum equipment for high temperature x-ray camera.

E. NRC combination thermocouple and ionization gauge control panel.
F. Main control panel.
G. Diffusion pump.

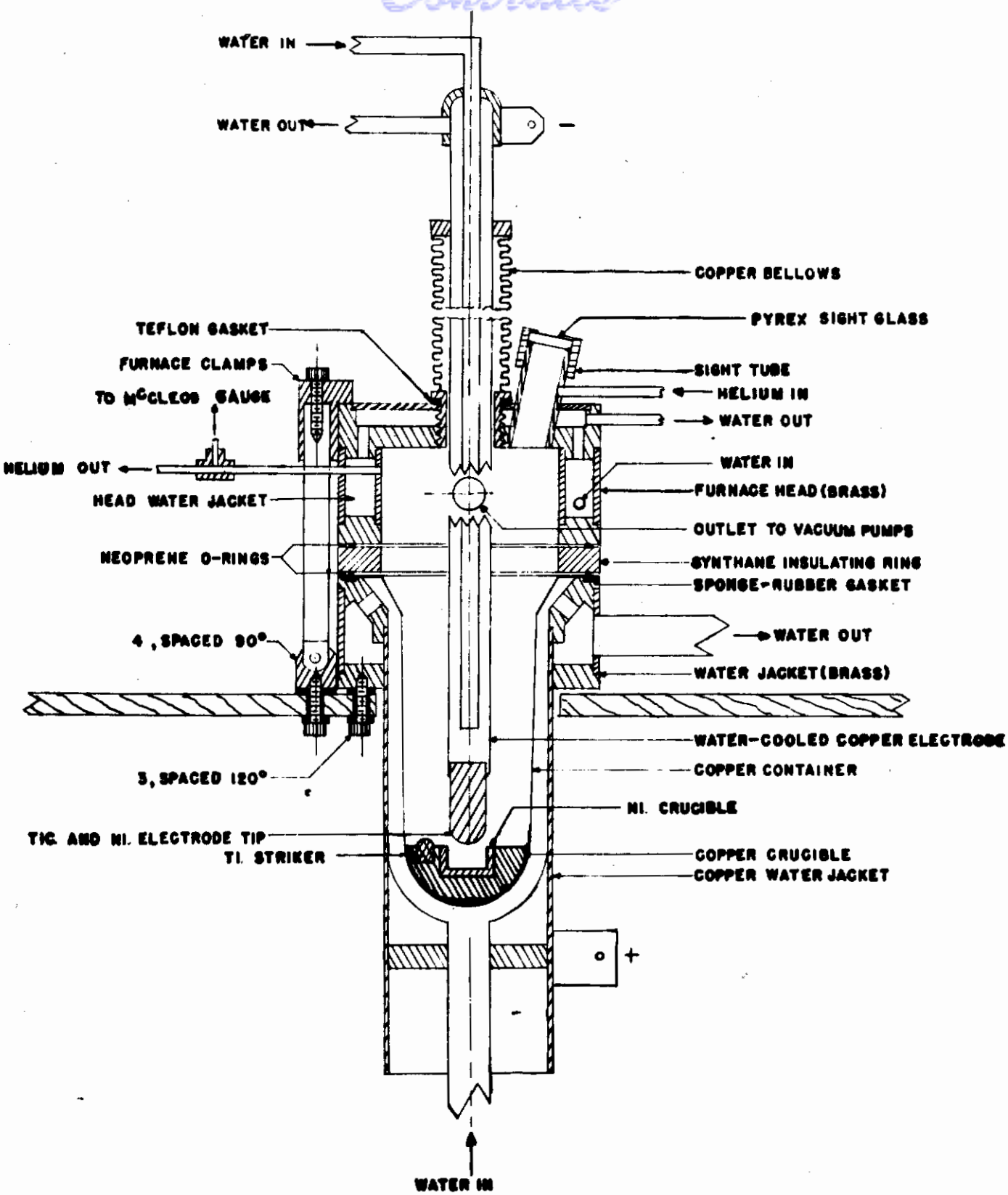

Figure 37. Drawing of arc furnace.

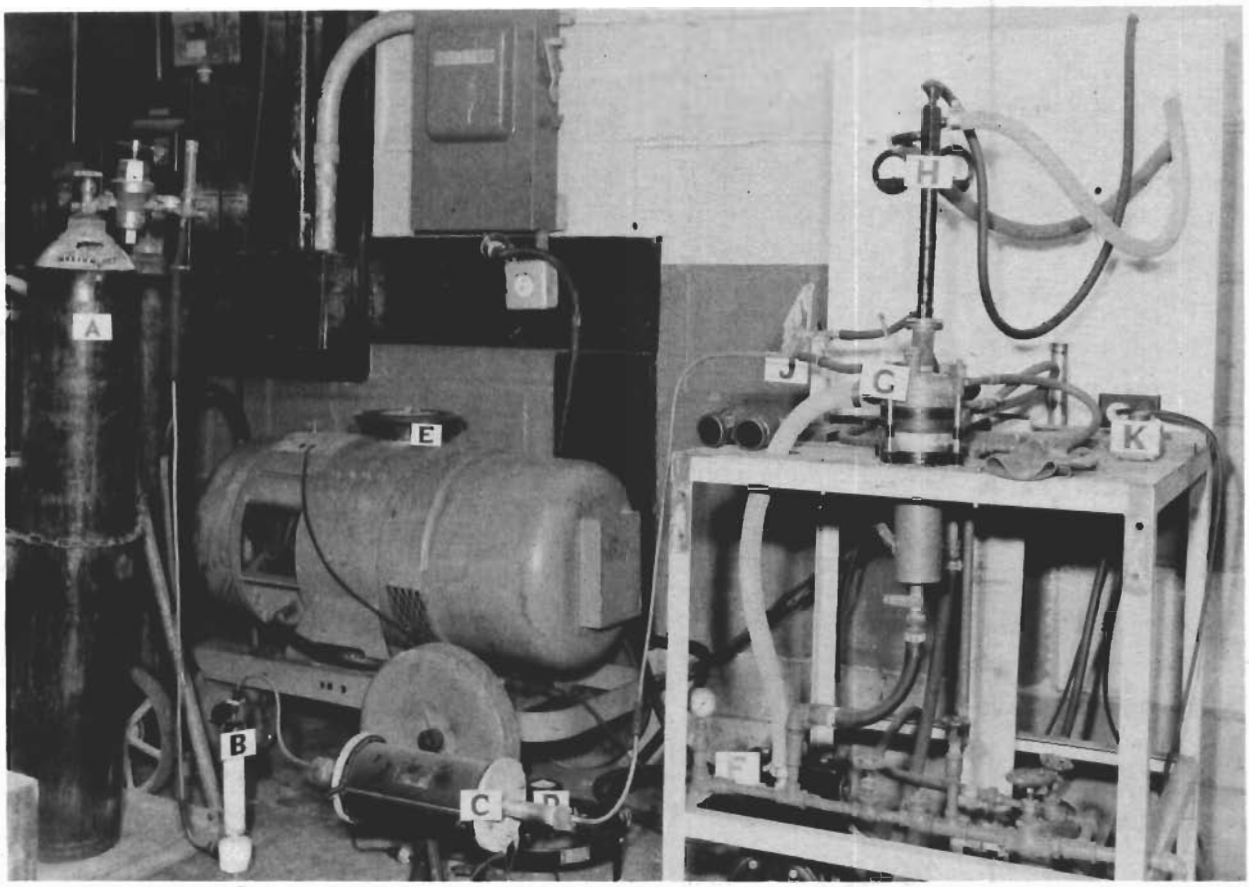

Figure 38. Arc furnace in operation.

A. He tank mounted on portable cart.
B. Tower filled with alumina.
C. Hevi-Duty electric furnace containing monel tube filled with Ti chips.
D. Variable rheostat for controlling power to furnace.
E. Wilson Hornet motor - generator power supply.
F. Welch Duo - Seal mechanical pump.
G. Furnace head.
H. Water cooled electrode shaft.
J. McLeod gauge.
K. Stop - start control switch.

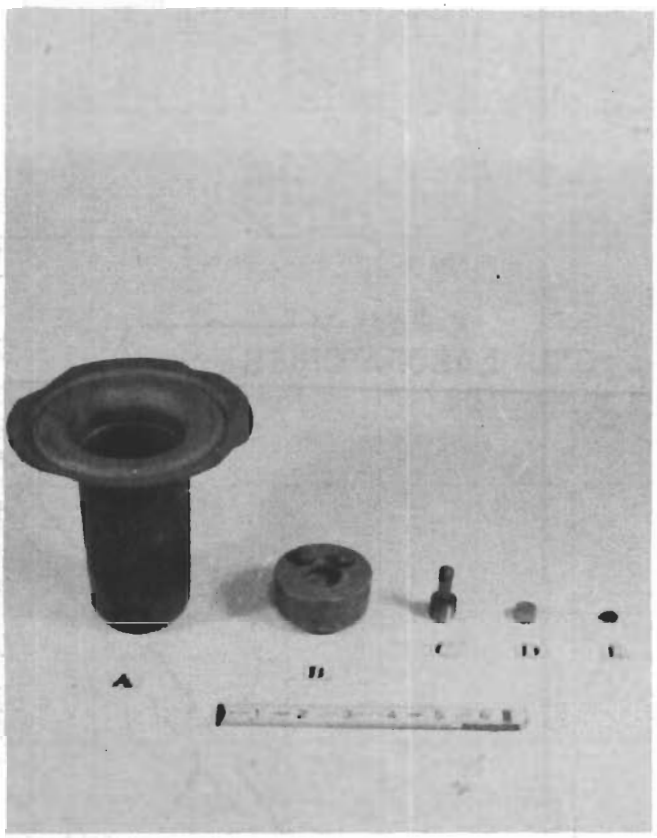

Figure 39. **Arc furnace crucible and samples.**

A. Cu container.
B. Cu crucible containing smaller Ni crucible and Ti strikers.
C. Ni + TiC electrode tip mounted in a threaded Cu holder.
D. Sample before arc melting.
E. Sample after arc melting.

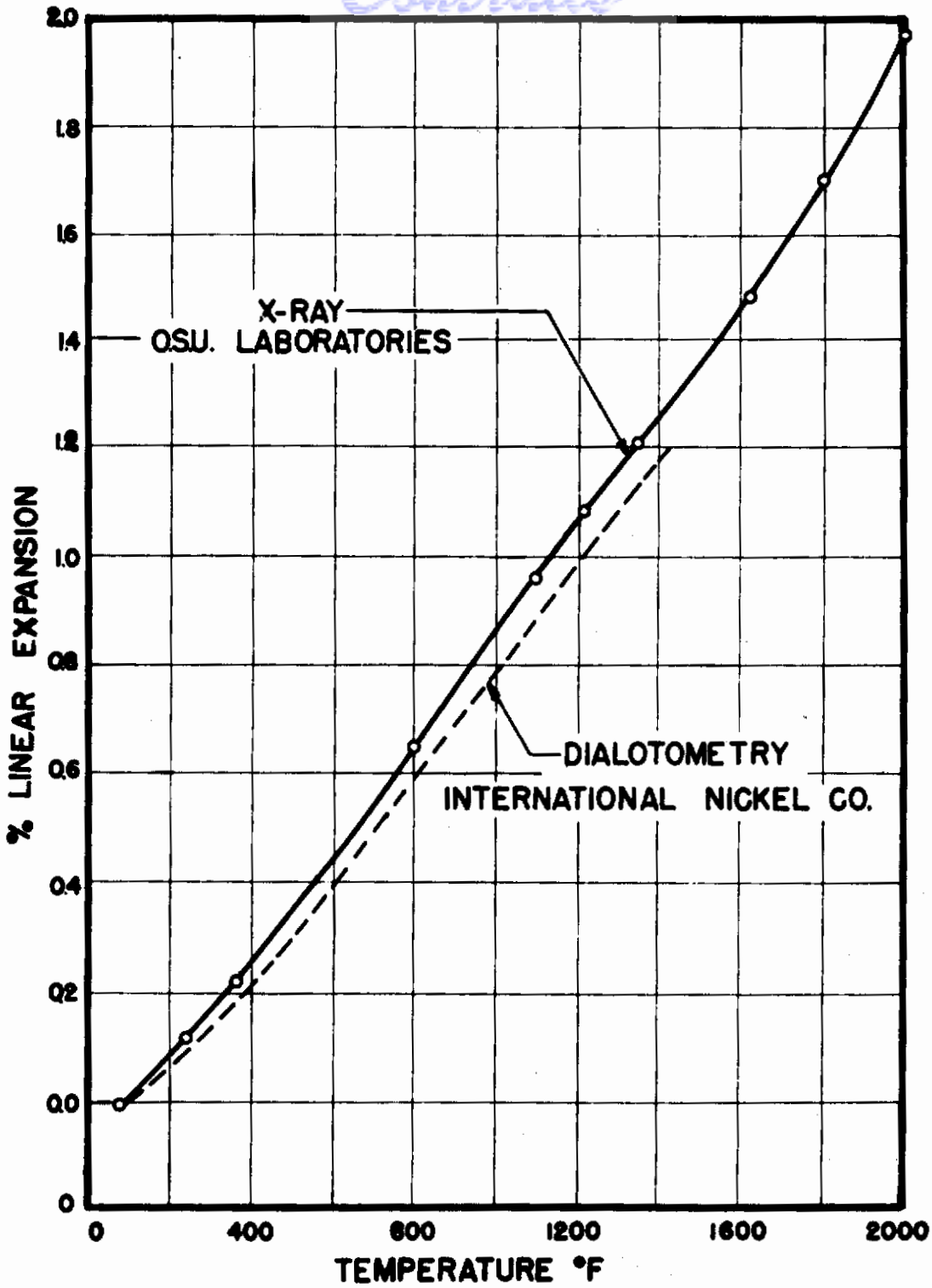

Figure 40.0 Thermal expansion of Ni.

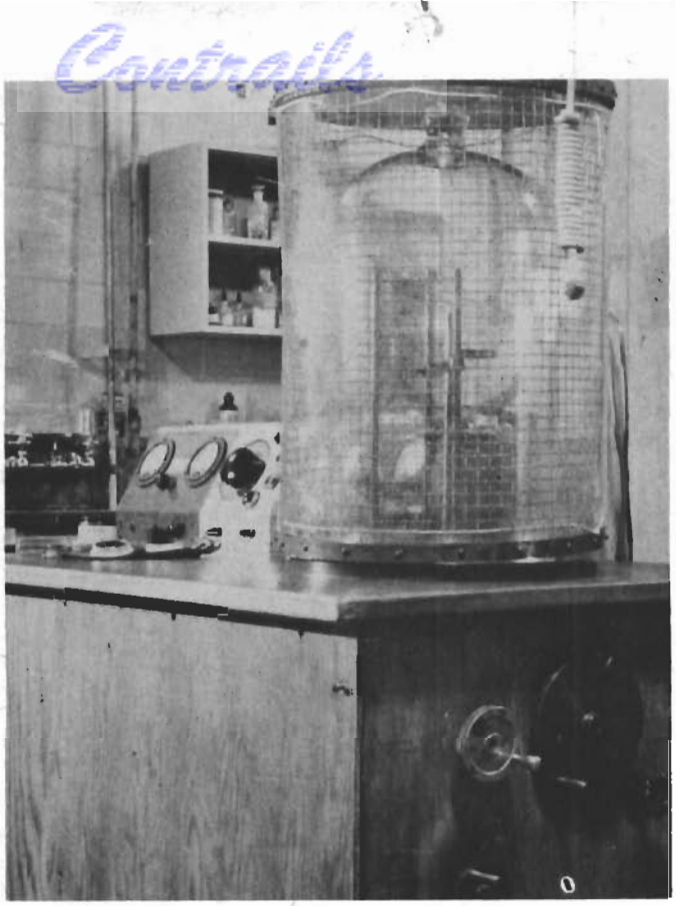

Figure 41. Evaporation unit - assembled.

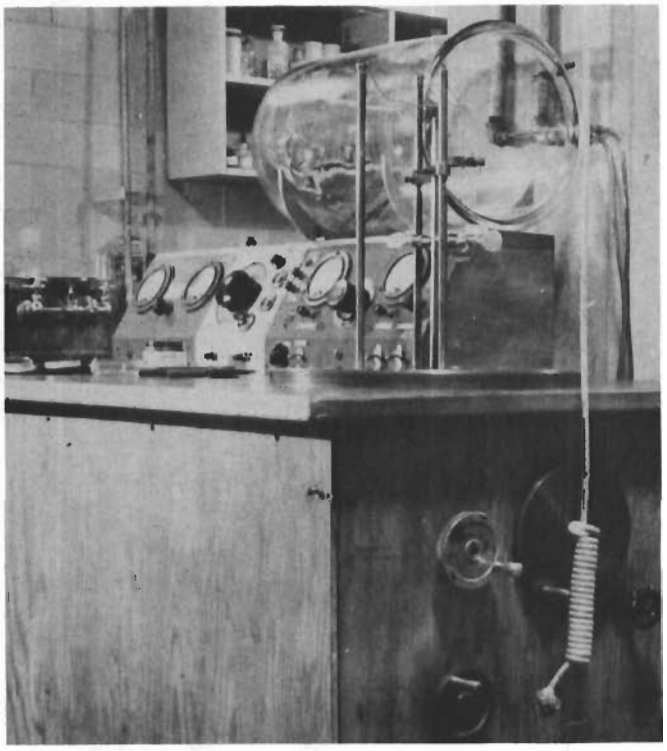

Figure 42. Evaporation unit - disassembled.

Figures 43 to 54. K-152-B As-sintered.

PREPARATION

Mechanically polished.
Unetched.
Electron microscope photograph -6,500 x direct.
Photographically enlarged to 13,000 x.
Fine particles of TiC in Ni phase are circled.

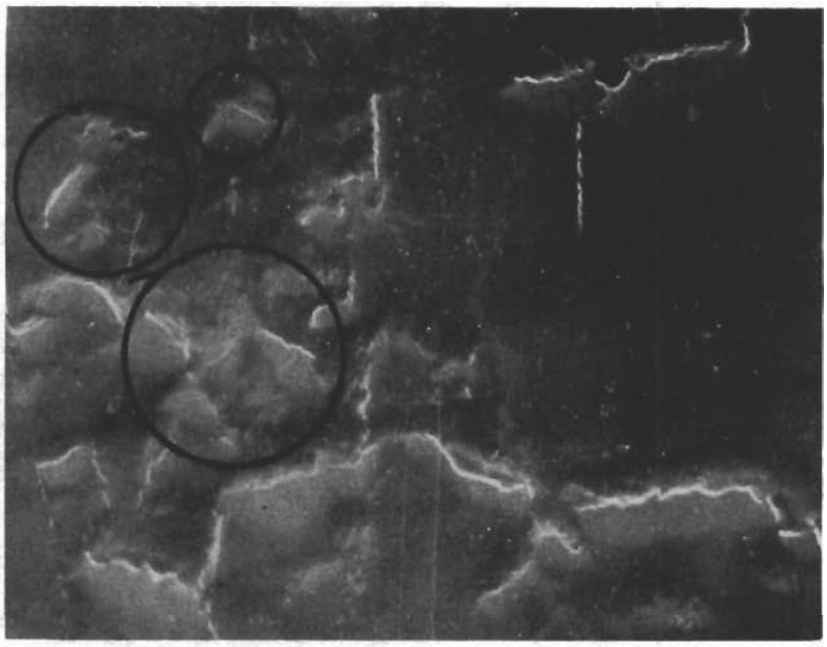

Figure 43.
K-152-B As-sintered. Fine particles of TiC in Ni phase are circled.

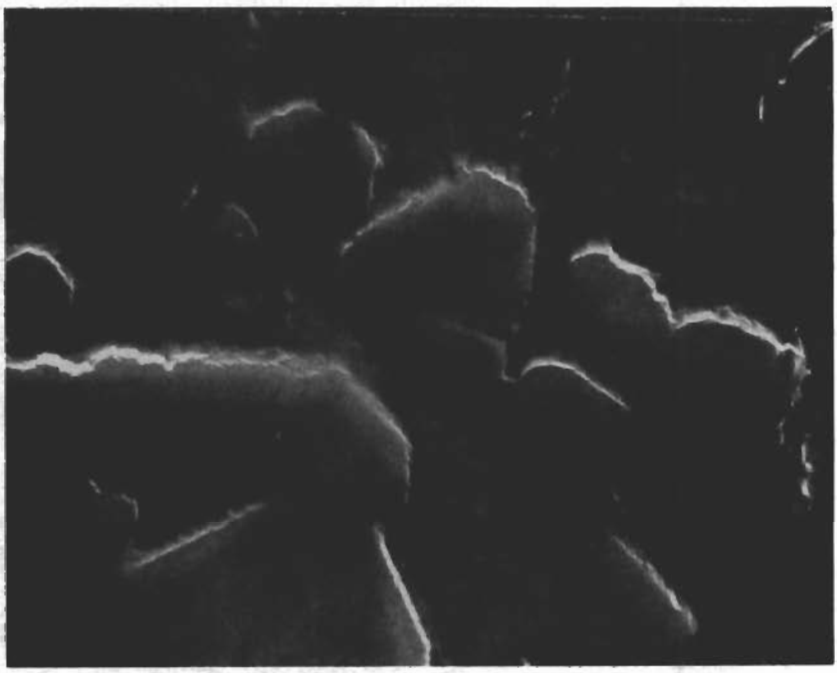

Figure 44.
K-152-B As-sintered. Fine particles of TiC in Ni phase are circled.

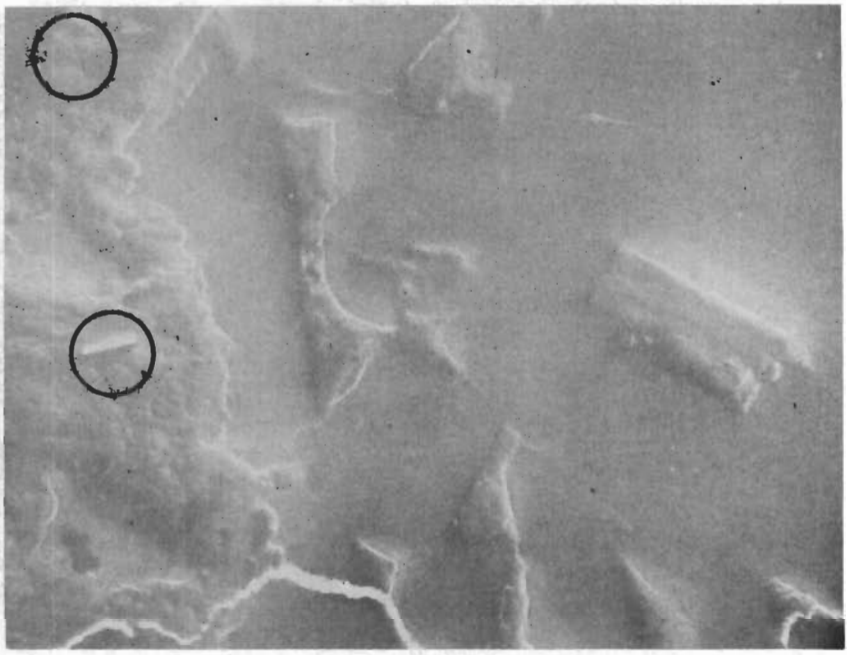

Figure 45
K-152-B As-sintered. Fine particles of TiC in Ni phase are circled.

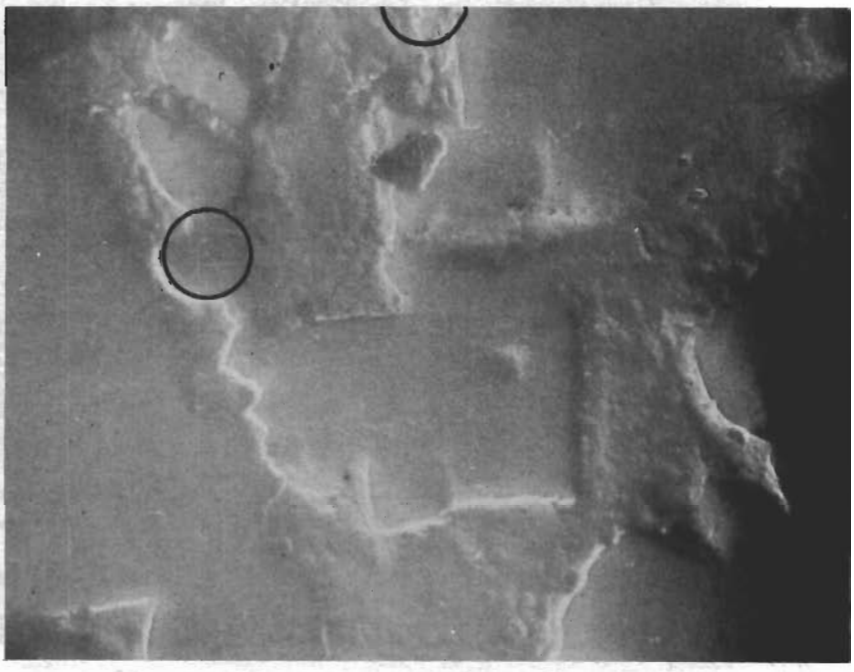

Figure 46
K-152-B As-sintered. Fine particles of TiC in Ni phase are circled.

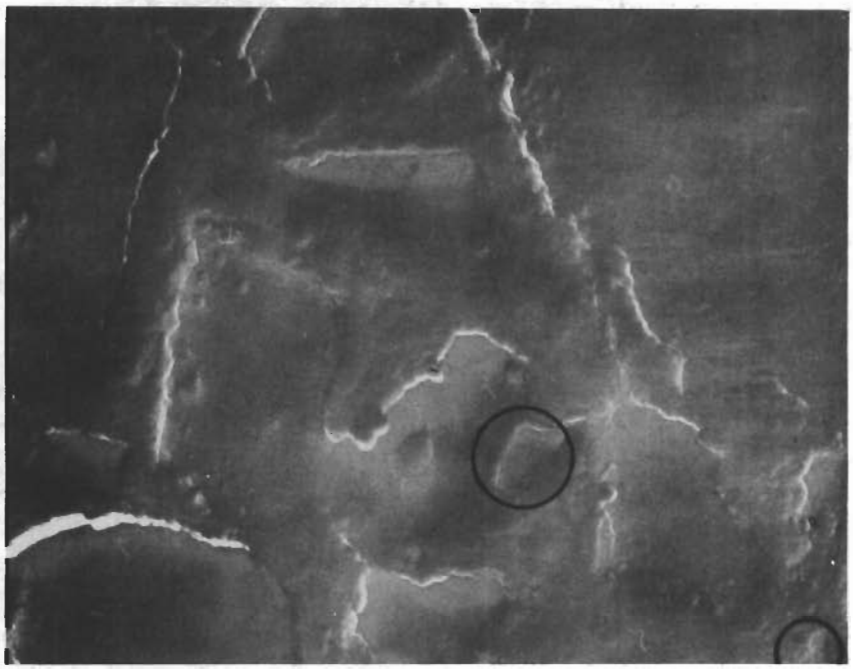

Figure 47.
K-152-B As-sintered. Fine particles of TiC in Ni phase are circled.

Figure 48.
K-152-B As-sintered. Fine particles of TiC in Ni phase are circled.

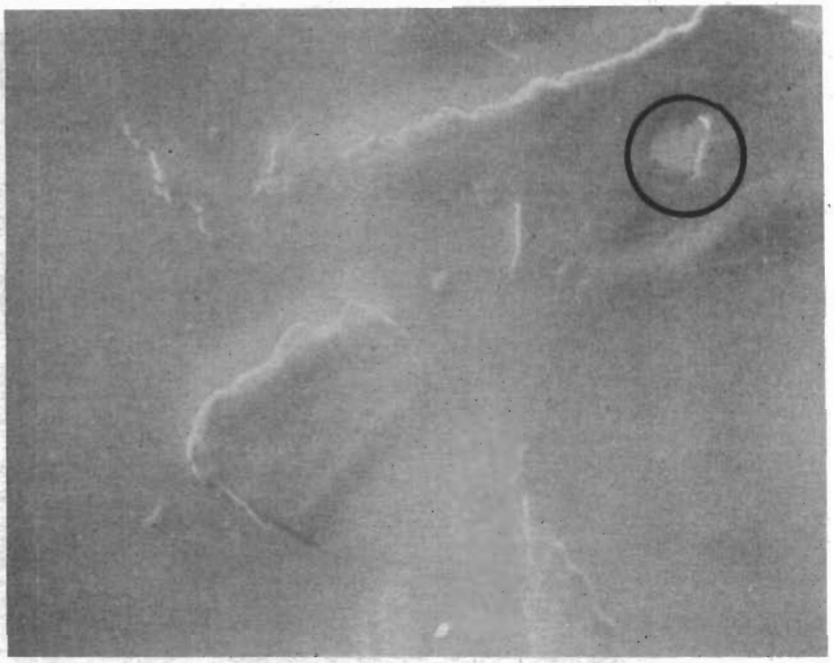

Figure 49.
K-152-B As-sintered. Fine particles of TiC in Ni phase are circled.

Figure 50
K-152-B As-sintered. Fine particles of TiC in Ni phase are circled.

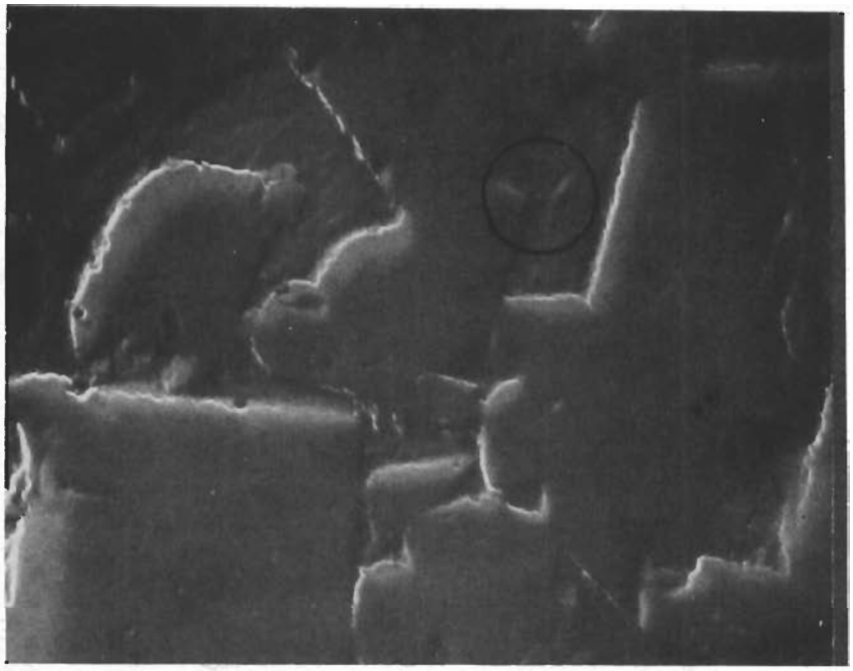

Figure 51
K-152-B As-sintered. Fine particles of TiC in Ni phase are circled.

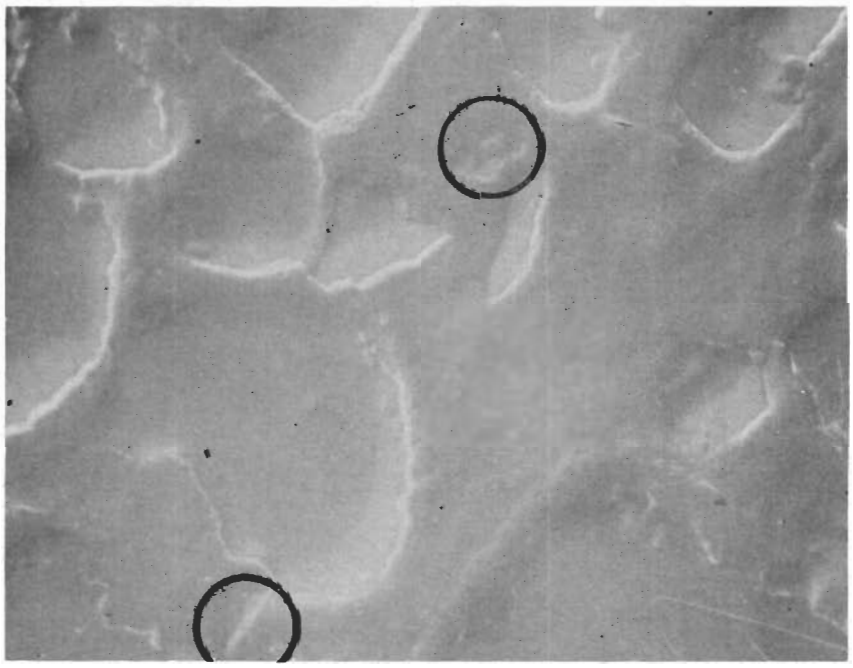

Figure 52
K-152-B As-sintered. Fine particles of TiC in Ni phase are circled.

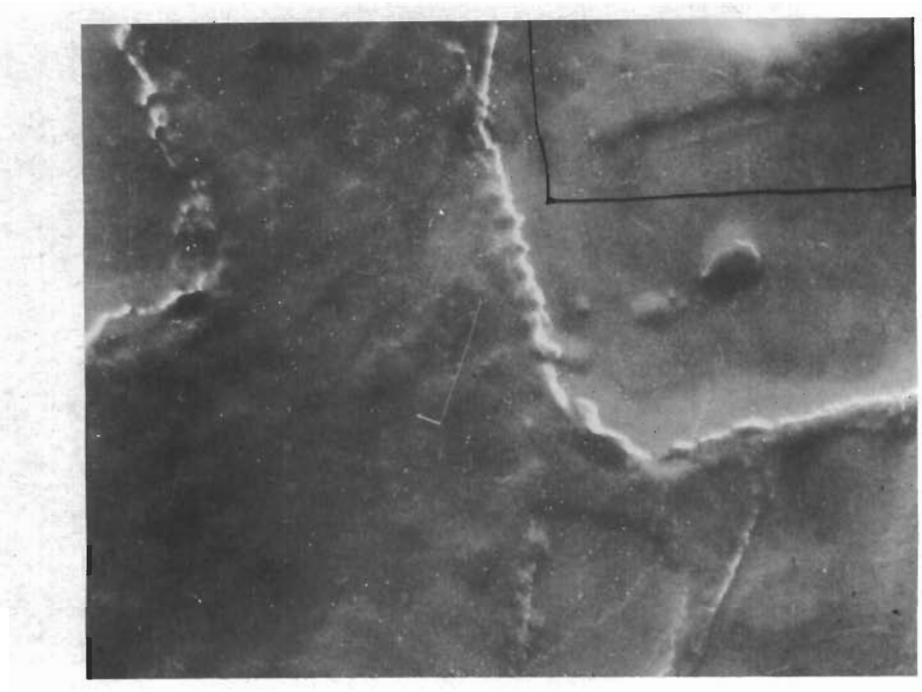

Figure 53
K-152-B As-sintered. Fine particles of TiC in Ni phase are circled.

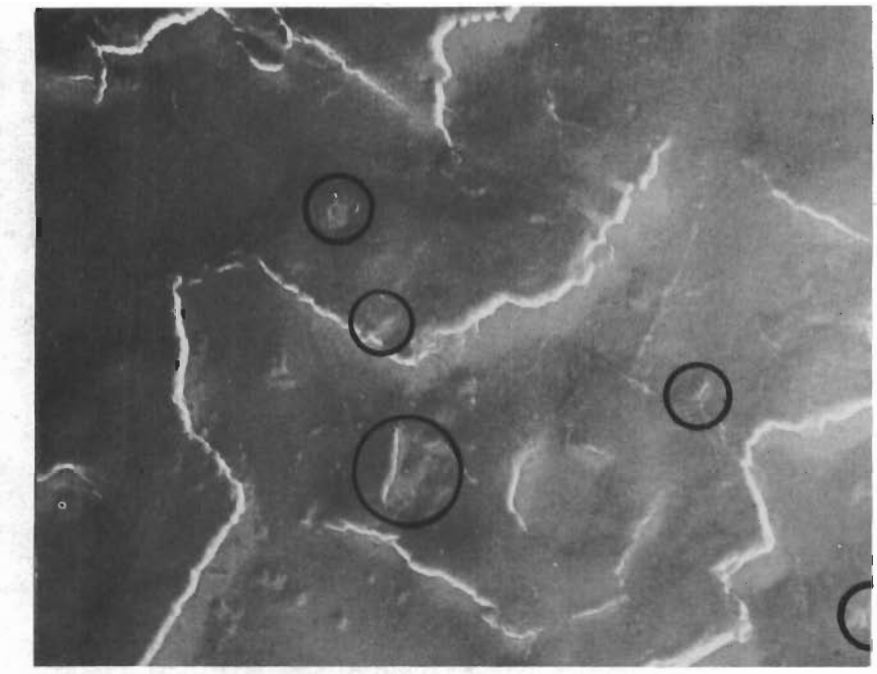

Figure 54
K-152-B As-sintered. Fine particles of TiC in Ni phase are circled.

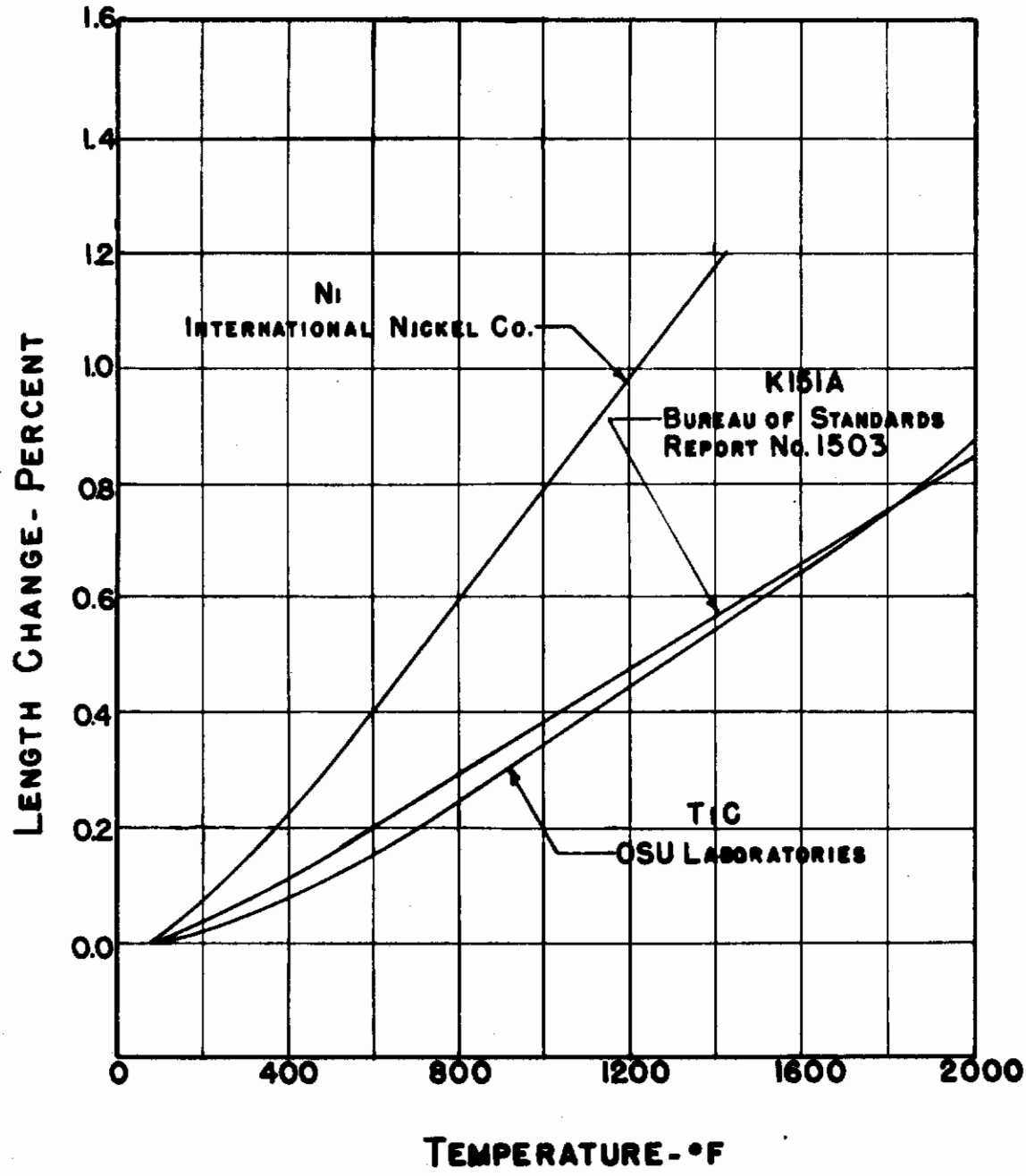

Figure 55. Thermal expansion of Ni, TiC and K-151-A.

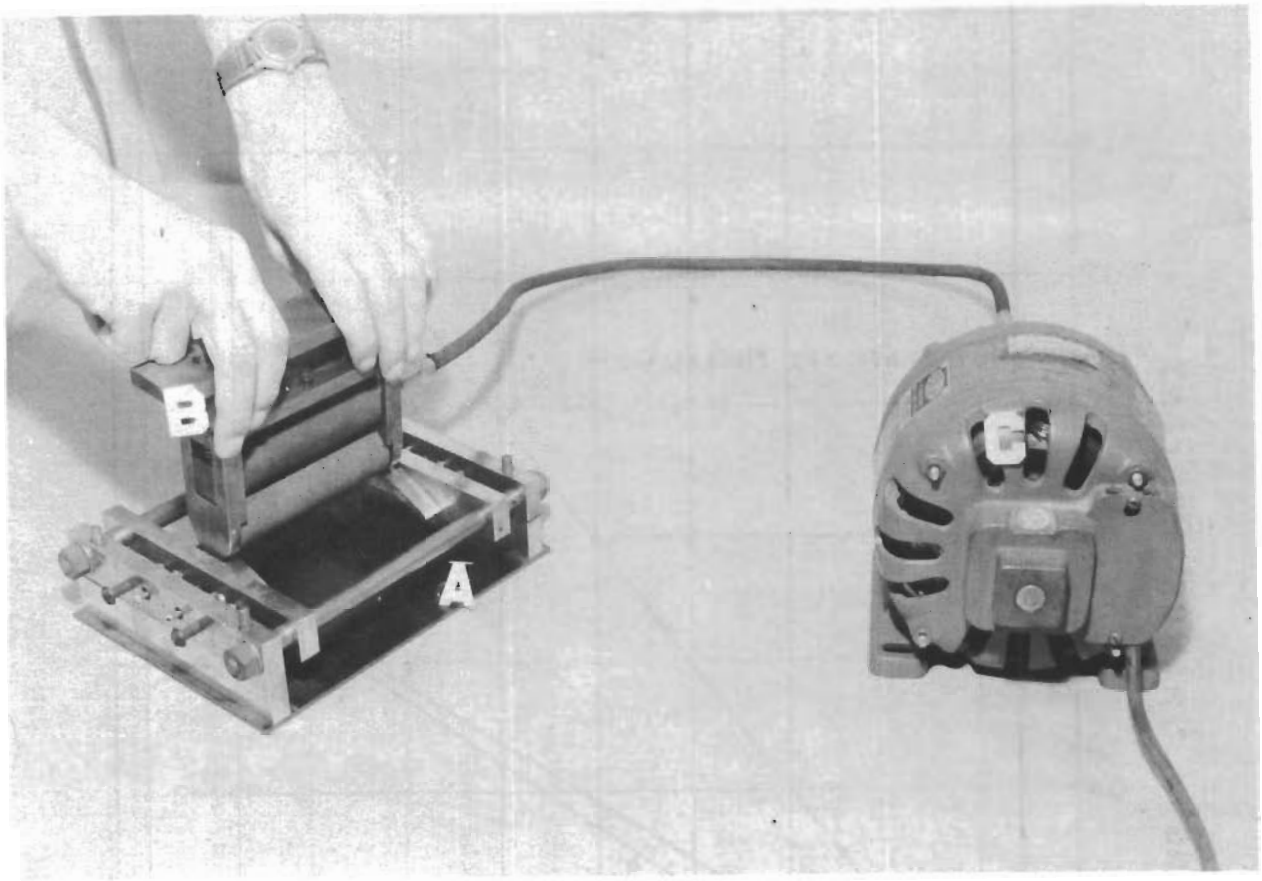

Figure 56. Blade forming equipment - after hydrostatic pressing.

A. Blade holding fixture.
B. Sanding drum assembly, fixture.
C. Sanding drum assembly, motor.

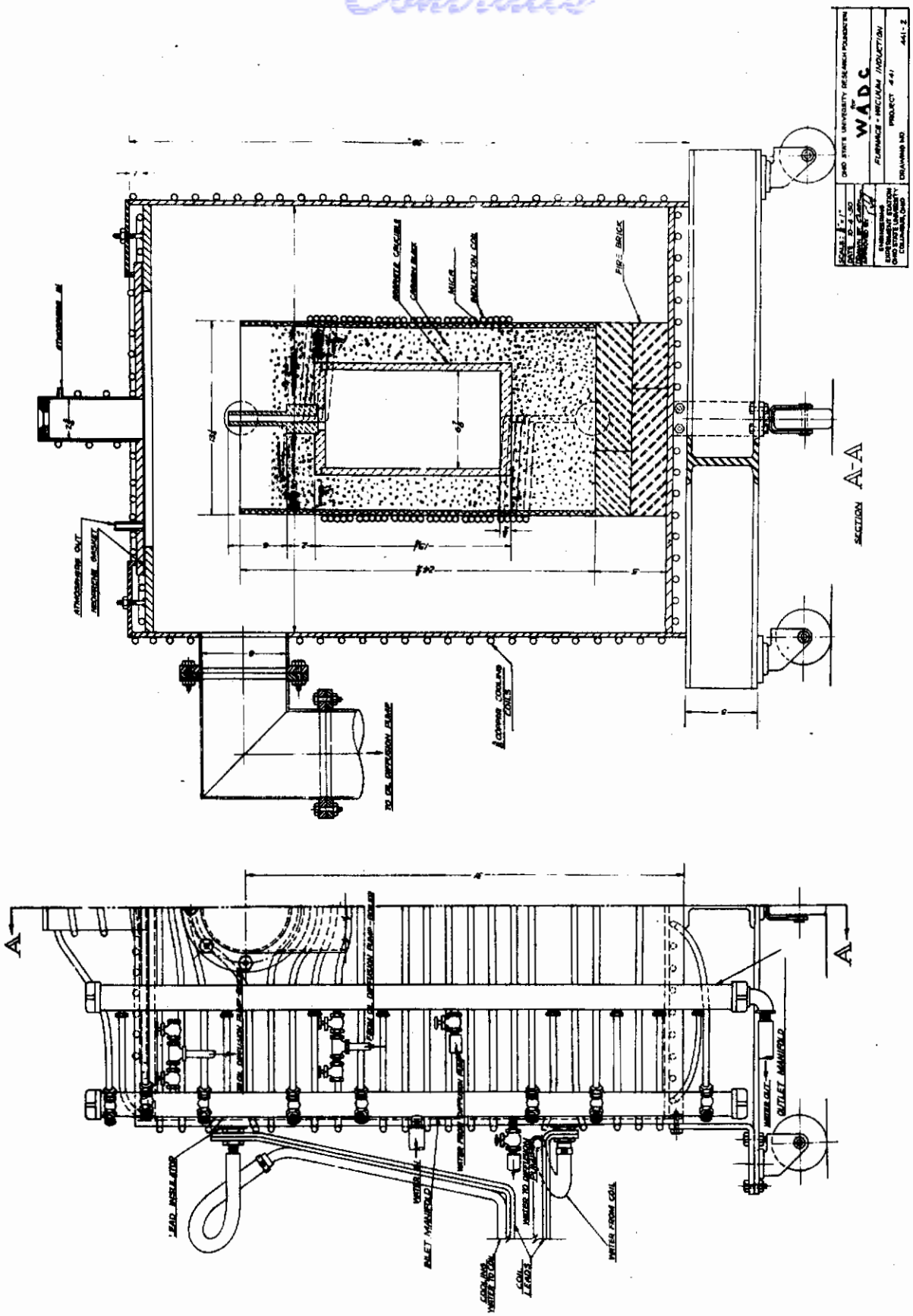

Figure 57. Induction furnace.

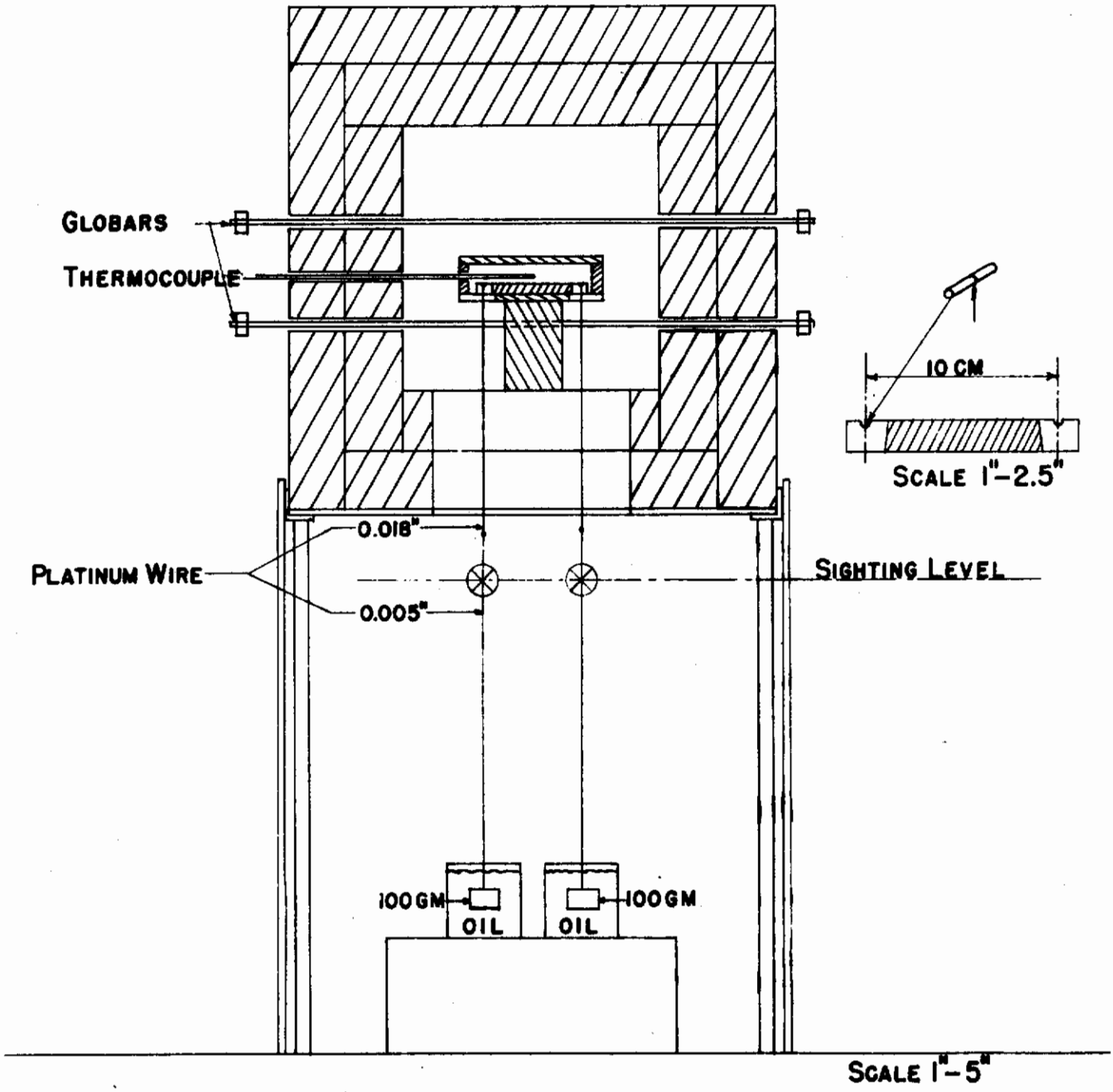

Figure 58. Thermal expansion furnace.

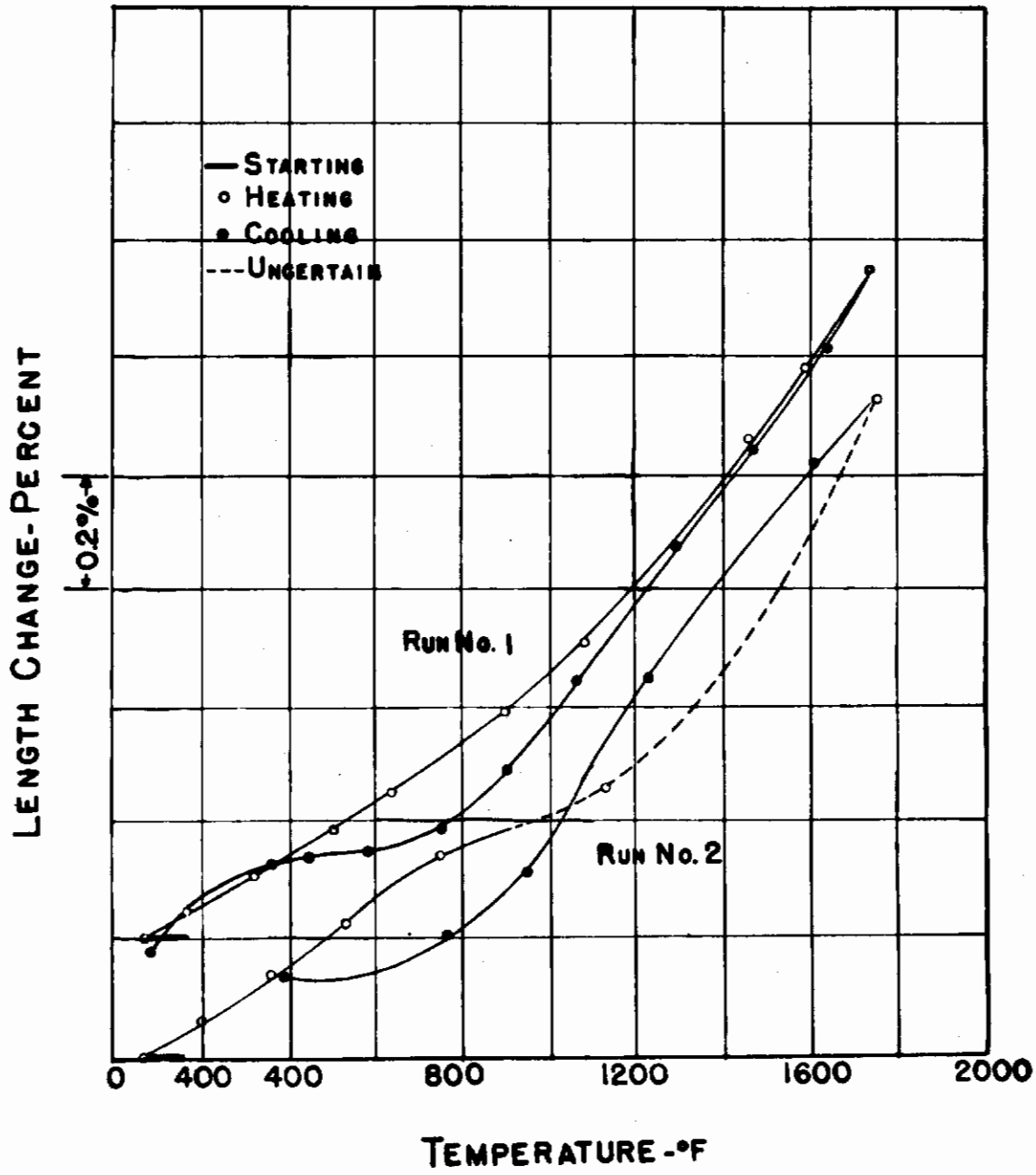

Figure 59. Thermal expansion of Fernico alloy.

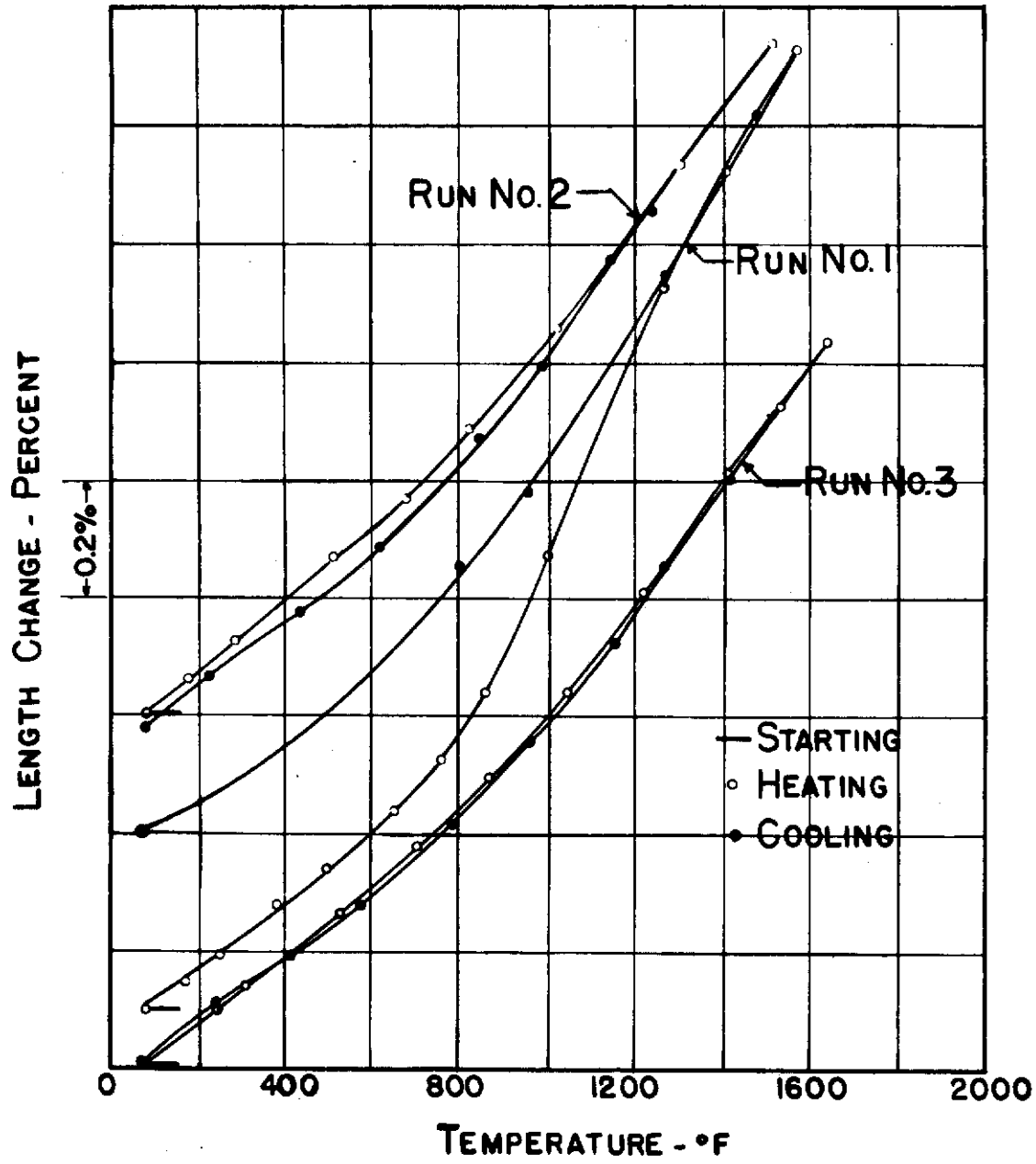

Figure 60. Thermal expansion of Fernichrome alloy.

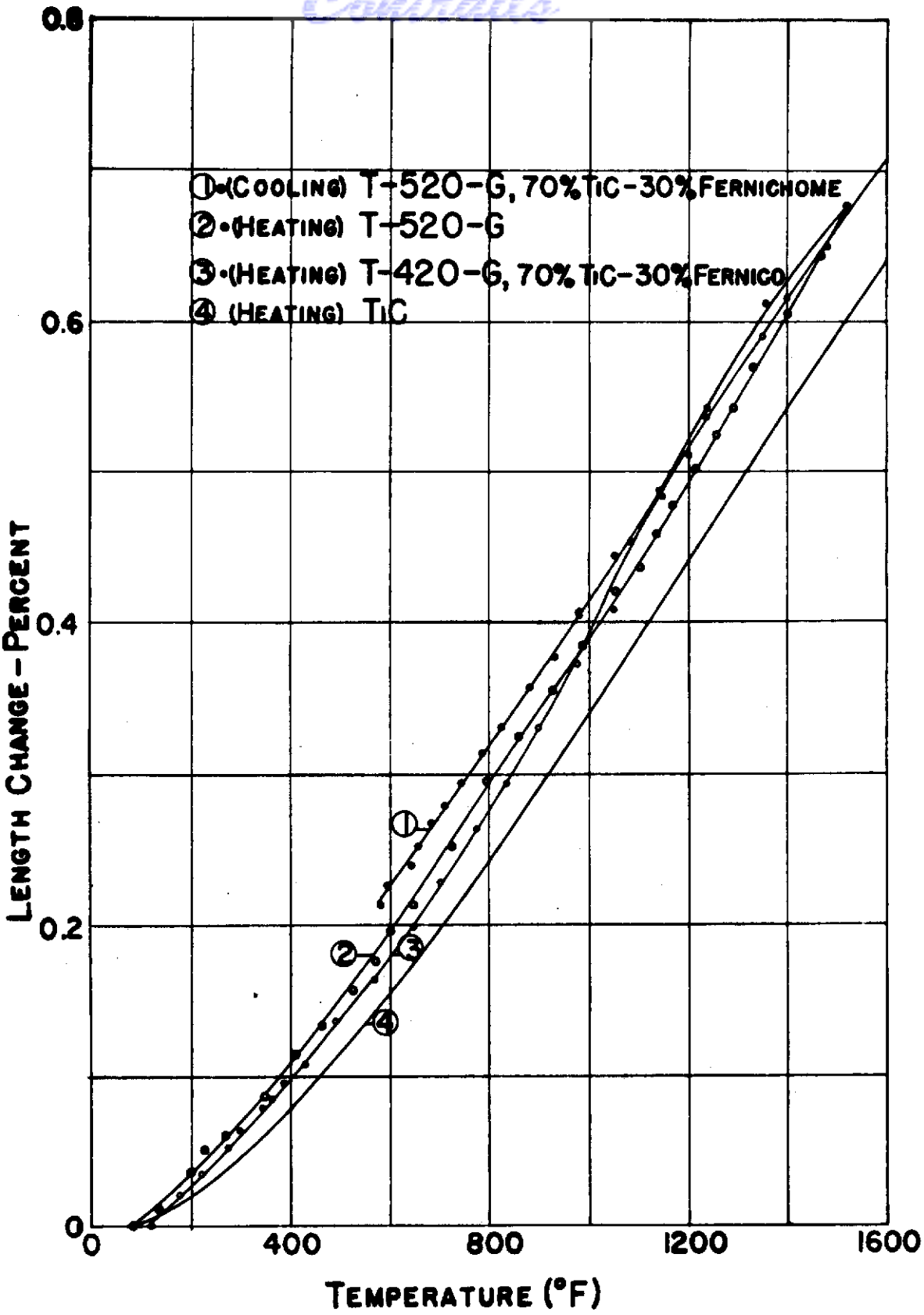

Figure 61. Thermal expansion of T-420-G, T-520-G and TiC.

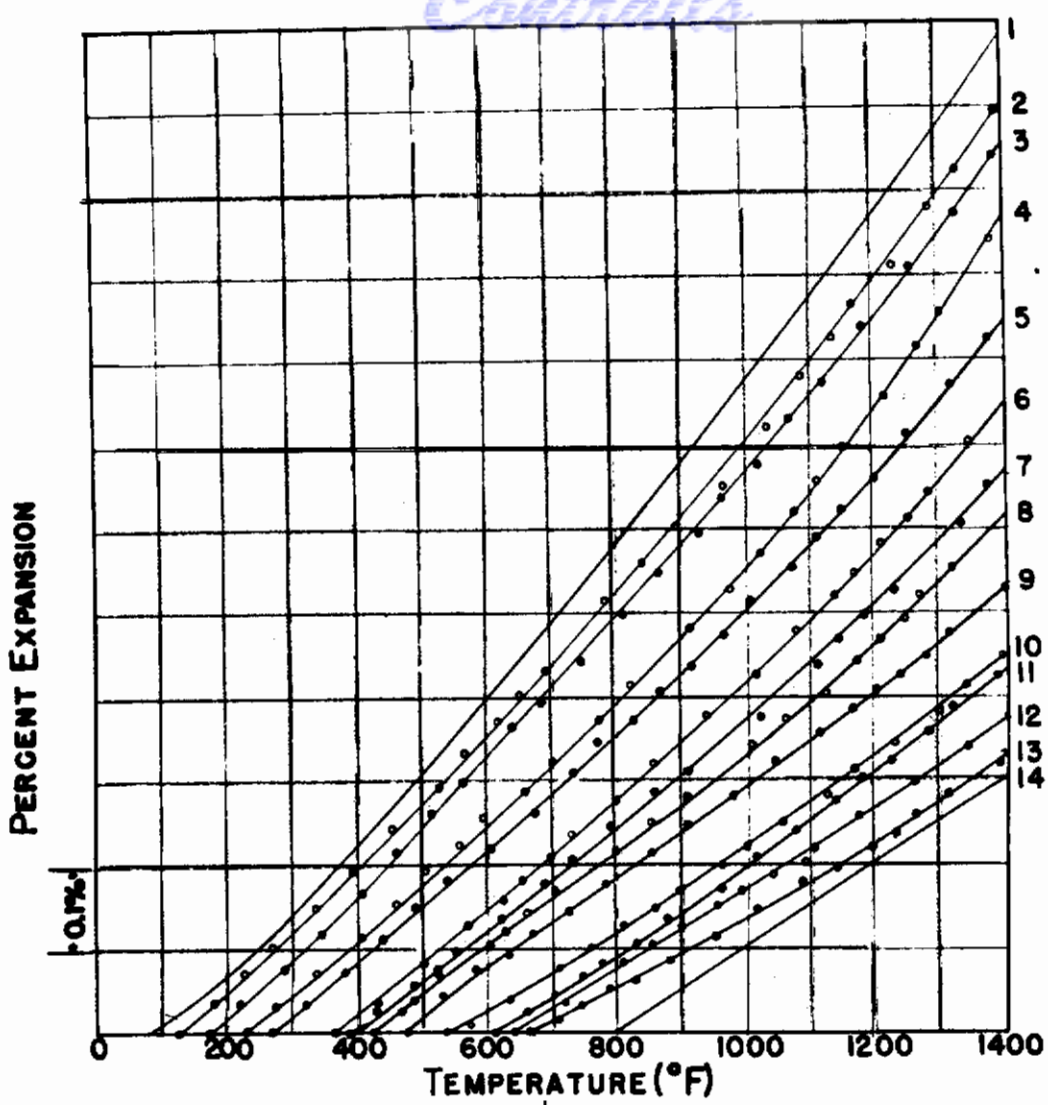

1 - Ni	8 - 25% Cr 25% Ni 50% Mo
2 - 50% Ni 50% Cr	9 - 75% Cr 25% Mo
3 - 75% Ni 25% Cr	10 - 50% Ni 50% Mo
4 - 50% Ni 25% Cr 25% Mo	11 - 50% Cr 50% Mo
5 - 75% Ni 25% Mo	12 - 25% Ni 75% Mo
6 - 75% Cr 25% Ni	13 - 25% Cr 75% Mo
7 - 25% Ni 25% Mo 50% Cr	14 - TiC

Figure 62. Thermal expansion of Ni-Cr-Mo alloys and TiC.

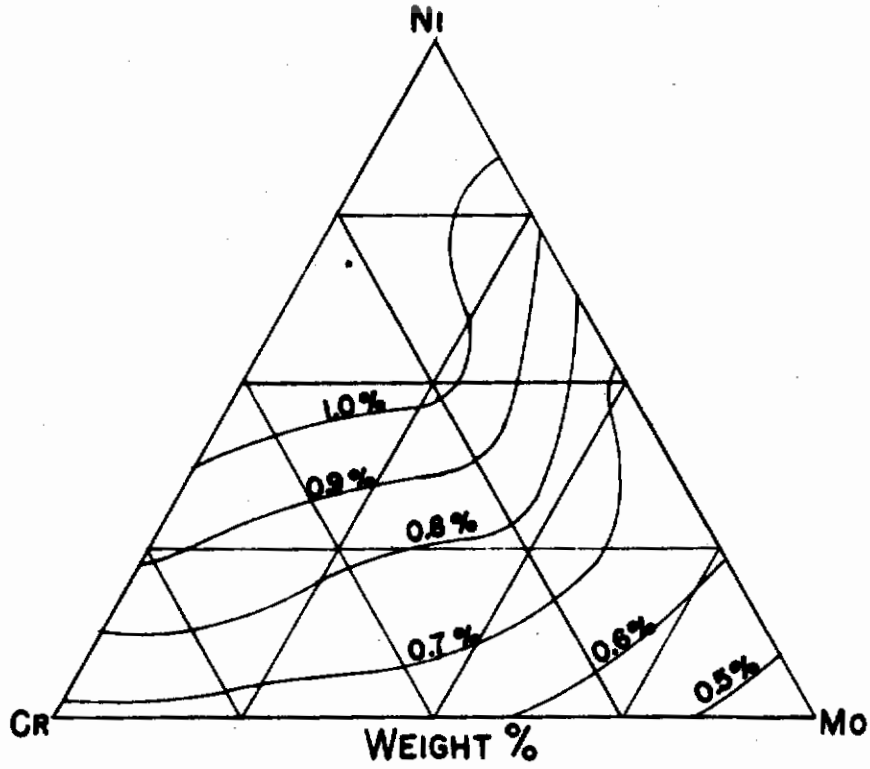

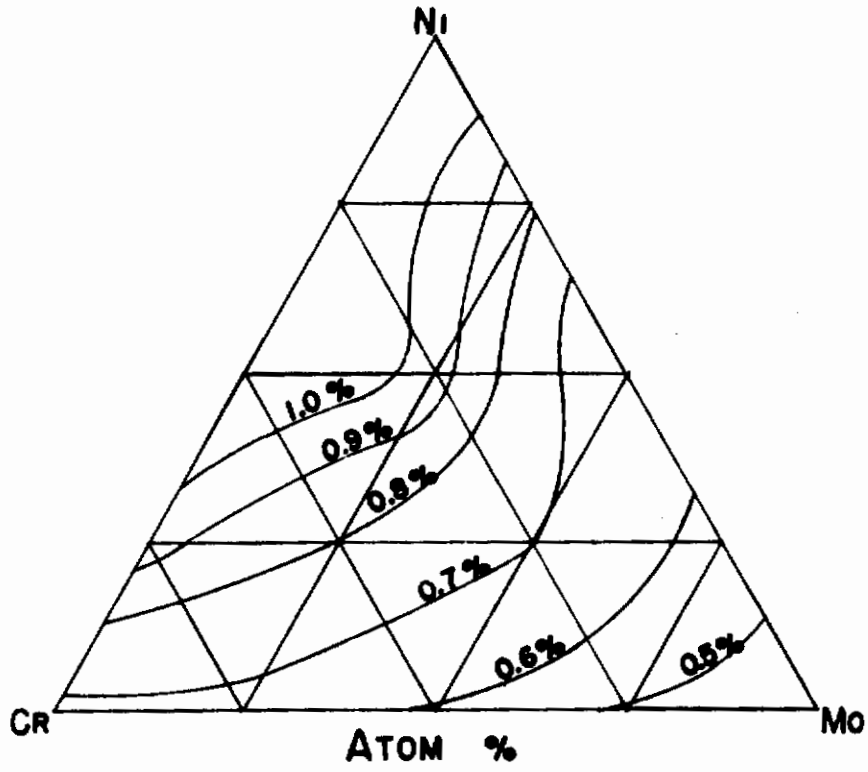

Figure 63. Thermal expansion at 1400°F of Ni-Cr-Mo alloys.

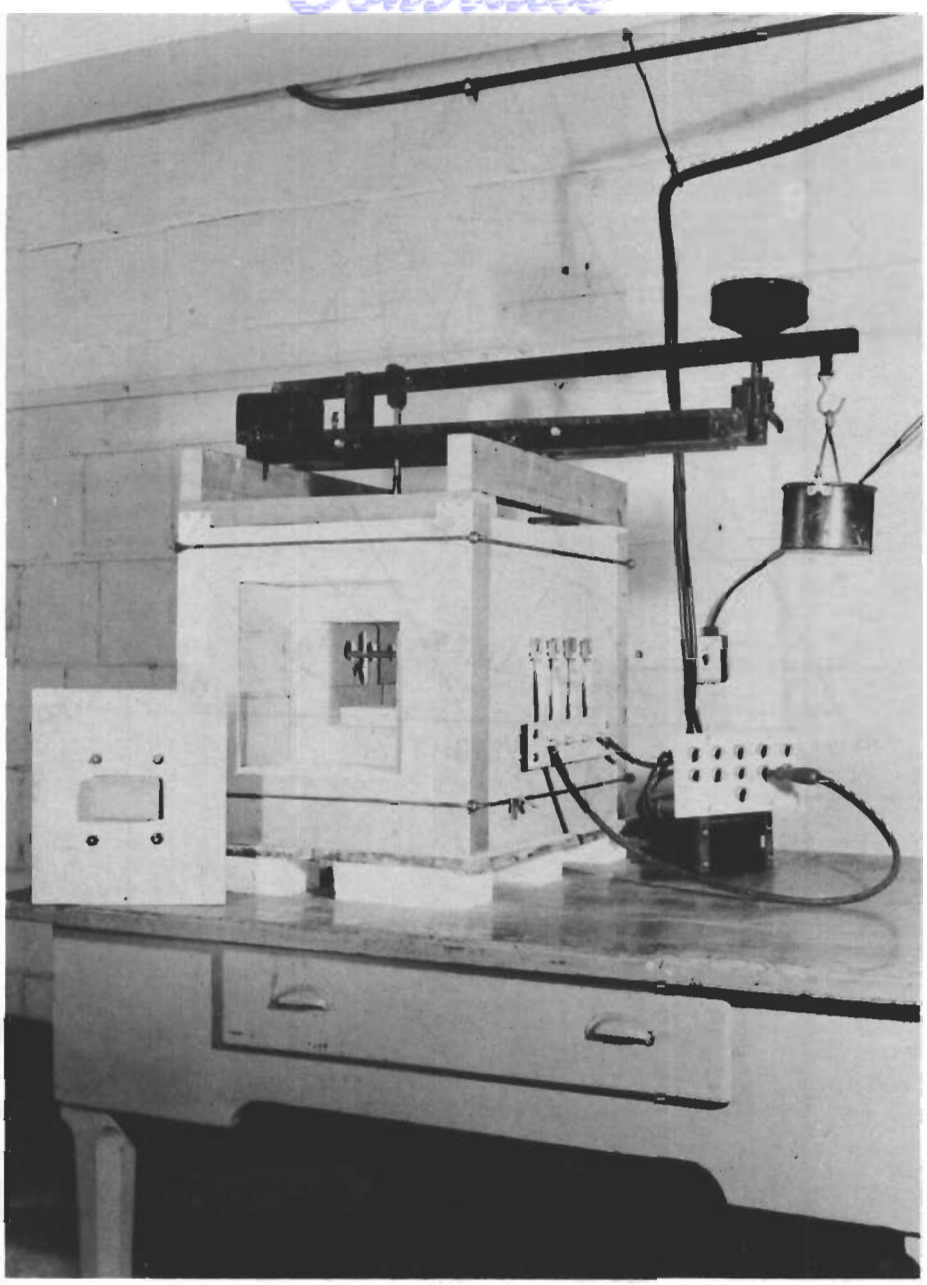

Figure 64. Modulus of rupture furnace.

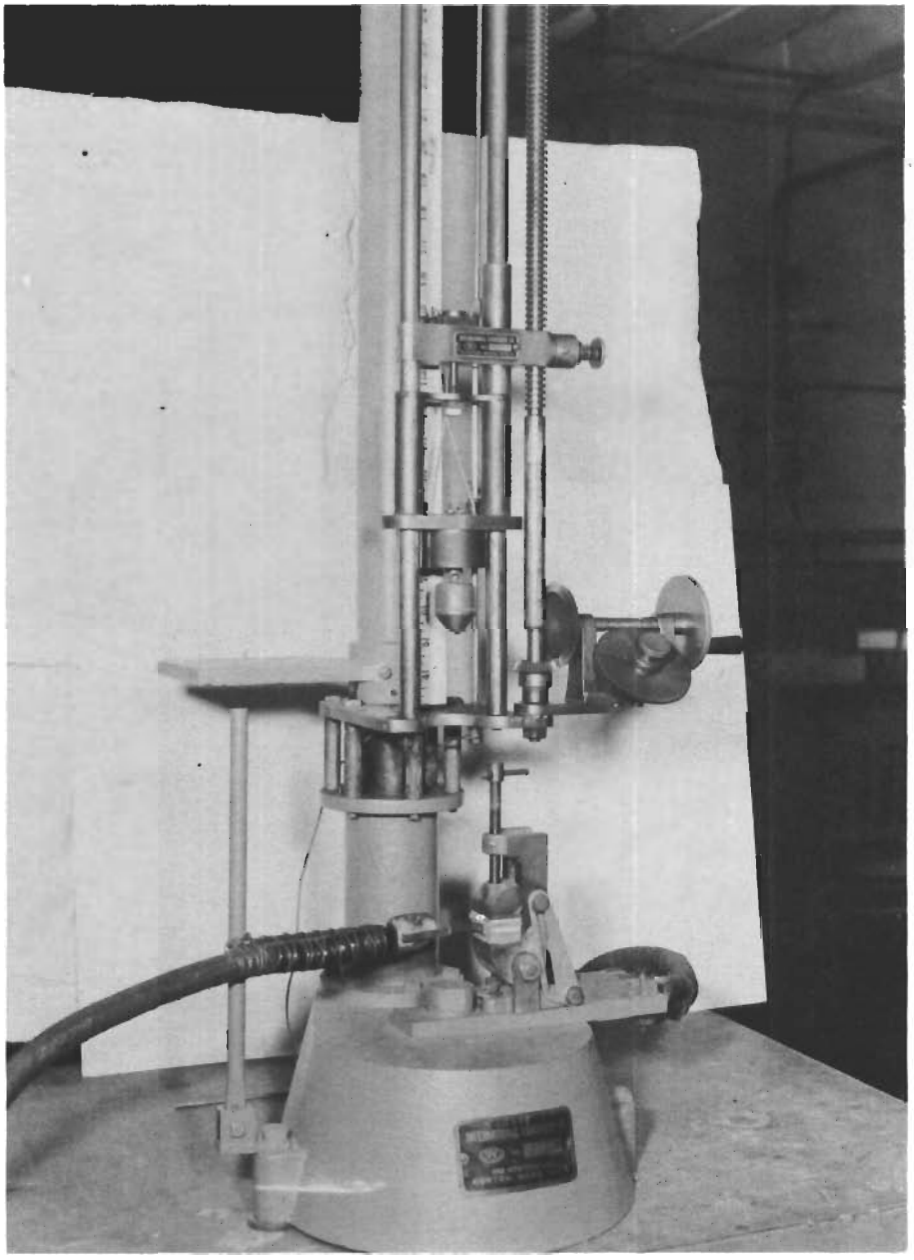

Figure 65. Impact testing apparatus.